Online ISSN : 2249-4596
Print ISSN : 0975-5861
DOI : 10.17406/GJRE

# Global Journal of Researches in Engineering: F

## Electrical and Electronic Engineering

Highlights

- Low Frequency Oscillations
- Analysis of Electrical Characteristics
- Single Switch Power Factor
- Reduction by Revolutionary Algorithm

**Discovering Thoughts, Inventing Future**

VOLUME 17 ISSUE 5 VERSION 1.0

Global Journal of Researches in Engineering: F
Electrical and Electronics Engineering

Global Journal of Researches in Engineering: F
Electrical and Electronics Engineering

Volume 17 Issue 5 (Ver. 1.0)

Open Association of Research Society

**Incorporation No.: 0423089**
**License No.: 42125/022010/1186**
**Registration No.: 430374**
**Import-Export Code: 1109007027**
**Employer Identification Number (EIN):**
**USA Tax ID: 98-0673427**

## Global Journals Inc.

*(A Delaware USA Incorporation with "Good Standing"; **Reg. Number: 0423089**)*

*Sponsors: Open Association of Research Society*
*Open Scientific Standards*

### *Publisher's Headquarters office*

Global Journals® Headquarters
945th Concord Streets,
Framingham Massachusetts Pin: 01701,
United States of America
*USA Toll Free: +001-888-839-7392*
*USA Toll Free Fax: +001-888-839-7392*

### *Offset Typesetting*

Global Journals Incorporated
2nd, Lansdowne, Lansdowne Rd., Croydon-Surrey,
Pin: CR9 2ER, United Kingdom

### *Packaging & Continental Dispatching*

Global Journals Pvt. Ltd.
E-3130 Sudama Nagar, Near Gopur Square,
Indore, M.P., Pin:452009, India

### *Find a correspondence nodal officer near you*

To find nodal officer of your country, please email us at *local@globaljournals.org*

### *eContacts*

Press Inquiries: *press@globaljournals.org*
Investor Inquiries: *investors@globaljournals.org*
Technical Support: *technology@globaljournals.org*
Media & Releases: *media@globaljournals.org*

### *Pricing (Including by Air Parcel Charges):*

*For Authors:*
22 USD (B/W) & 50 USD (Color)
*Yearly Subscription (Personal & Institutional):*
200 USD (B/W) & 250 USD (Color)

# Contents of the Issue


i. Copyright Notice
ii. Editorial Board Members
iii. Chief Author and Dean
iv. Contents of the Issue

1. Source Localization of Low Frequency Oscillations in Power Systems and Methods of Damping. *1-5*
2. Reduced Size Single Switch Power Factor Correction Circuit. *7-14*
3. Optimal Power Flow using a Hybrid Particle Swarm Optimizer with Moth Flame Optimizer. *15-32*
4. Detecting Defective Bypass Diodes in Photovoltaic Modules using Mamdani Fuzzy Logic System. *33-44*
5. Review-Reservoir Computing Trend on Software and Hardware Implementation. *45-49*
6. Numerical Analysis of Electrical Characteristics in a Squared Channel EHD Gas Pump. *51-56*
7. Real Power Loss Reduction by Revolutionary Algorithm. *57-61*

v. Fellows
vi. Auxiliary Memberships
vii. Process of Submission of Research Paper
viii. Preferred Author Guidelines
ix. Index

Global Journal of Researches in Engineering: F
Electrical and Electronics Engineering
Volume 17 Issue 5 Version 1.0 Year 2017
Type: Double Blind Peer Reviewed International Research Journal
Publisher: Global Journals Inc. (USA)
Online ISSN: 2249-4596 & Print ISSN: 0975-5861

# Source Localization of Low Frequency Oscillations in Power Systems and Methods of Damping

By T. G. Klimova & M.V. Savvatin
*National Research University*

*Abstract-* One of the urgent problems of modern power system are low frequency oscillations (hereinafter LFO) as they reduce the static and dynamic stability of power systems. Today the important task is to detection and localization of sources of LFO and means of effectively damping such vibrations.

The basic characteristics of oscillation frequency and amplitude of voltage at station buses obtained using devices phazor measurement units (hereinafter, PMU). In the software-hardware complex Real-Time Digital Simulation (RTDS) the study method for the determination sources of perturbations that give rise to low-frequency oscillations and suppression of low-frequency oscillations.

*Keywords:* *low-frequency oscillations, periodic perturbations, phazor measurement units, automatic regulator of excitation, methods of damping.*

*GJRE-F Classification:* *FOR Code: 090607*

SOURCELOCALIZATIONOFLOWFREQUENCYOSCILLATIONSINPOWERSYSTEMSANDMETHODSOFDAMPING

*Strictly as per the compliance and regulations of:*

# Source Localization of Low Frequency Oscillations in Power Systems and Methods of Damping

T. G. Klimova [α] & M.V. Savvatin [σ]

*Abstract-* One of the urgent problems of modern power system are low frequency oscillations (hereinafter LFO) as they reduce the static and dynamic stability of power systems. Today the important task is to detection and localization of sources of LFO and means of effectively damping such vibrations.

The basic characteristics of oscillation frequency and amplitude of voltage at station buses obtained using devices phazor measurement units (hereinafter, PMU). In the software-hardware complex Real-Time Digital Simulation (RTDS) the study method for the determination sources of perturbations that give rise to low-frequency oscillations and suppression of low-frequency oscillations.

On the basis of measurements obtained using the established in different parts of the power system, PMU for different types of periodic perturbations defined characteristics of oscillations, indicating the location of source of low frequency oscillations. Reviewed and verified way of reducing the influence of LFO on operation of generator. This regularity allows to obtain information about the location of source periodic perturbation, leading to the emergence of LFO on the grid. Further work aimed at creation of algorithm fast detection source LFO based on vector measurements, and research methods reduce the influence of LFO on synchronous generator will help determine the optimal setting of the automatic regulator of excitation for maximum damping occurs in the LFO power system.

*Keywords: low-frequency oscillations, periodic perturbations, phazor measurement units, automatic regulator of excitation, methods of damping.*

## I. Introduction

Currently, the issue LFO is given attention throughout the progressive world. Already significant progress has been made in identifying the reasons for LFO. The analysis of the influence of periodic disturbances on occurrence of low frequency oscillations in power system, which proves the existence of direct relationship between the periodic variations of load and periodic fluctuations in operating parameters in the power system, as well as strengthening the existing fluctuations in system at resonance with oscillation of load.

Today, an important challenge remains determination location source of the perturbations that give rise to LFO in the power system, and developing effective ways of minimizing the impact of LFO on the work of rotating machines [1].

Also one of the main causes of low-frequency oscillation is inefficient excitation systems and automatic regulators of excitation. Therefore, an important task is to study the influence of the structure and parameters of automatic excitation controllers on oscillatory processes arising due to disturbances of different kinds.

In modern conditions in the systems collecting and information transfer widespread digital technology based on the synchronized vector measurements, which allow to obtain high accuracy and measurement stability, the lowest latency of the measured variables and increase reliability of the measuring system as a whole [2]. Phasor measurement unit (hereinafter, PMU) – a device (or software-implemented function) that measures complex values of current and voltage. Measurement from a PMU is synchronized in time based on the signals of GLONASS or GPS, which are transmitted to determine the exact location and time synchronization accuracy is ± 0.2 microseconds. PMU are located in the nodes of the grid form a wide area measurement system (WAMS) [3].

## II. Identification of Dangerous Resonant Frequencies

In the software-hardware complex real-time digital simulator (hereinafter, RTDS) studies have been conducted method of determining the points application of the perturbations that give rise to LFO. RTDS allows to set model PMU in any given test points diagrams energy district and to sync them according to signals a single time.

As one of the perturbation is used periodically varying load, mounted at various points on the system. This external perturbation for all synchronous generators of the power system. Another type of perturbation – mechanical moment on a shaft of one of the generators. It will be an internal perturbation for generator, and for the rest–external [2–3].

Disturbance of any kind cause fluctuations in the frequency and amplitude of voltage at all points of the system. In the network map was implemented the point of application of a periodic load Pn1, Pn2 = var, and changes in the moment generator shaft is Tm =

*Author α σ: National Research University "Moscow Power Engineering Institute", Moscow, Russian Federation. e-mail: KlimovaTG@mpei.ru*

var. The place of installation, PMU designated in figures 1–13 in Fig. 1

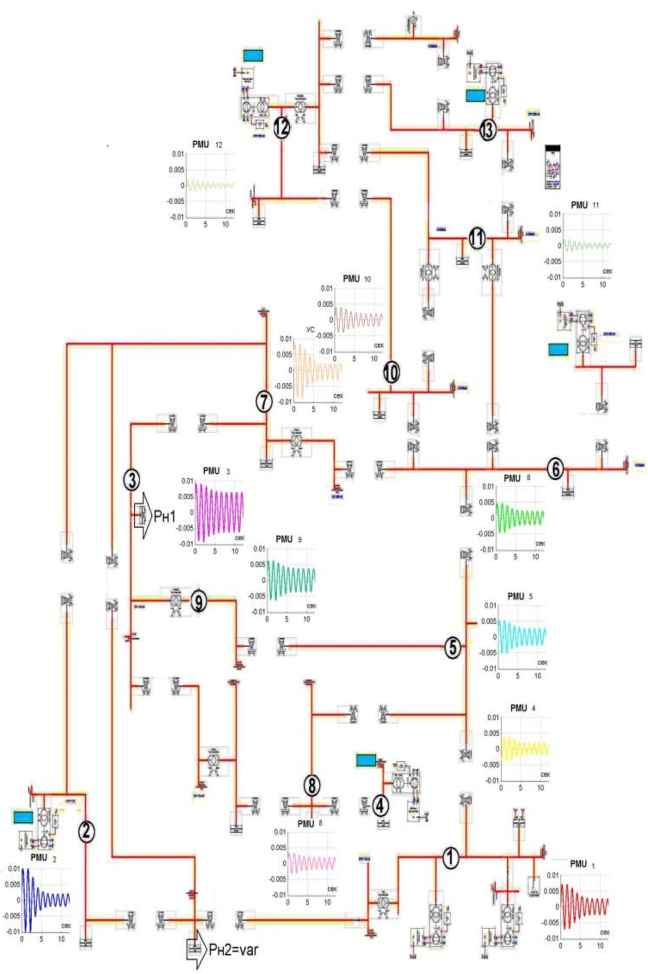


*Fig. 1:* The test grid and oscilloscope record frequency variations in the place of installation PMU (the model created in RTDS)

By studying the spectral composition and operating parameters have been selected the two most pronounced dangerous (resonant) frequency of oscillations periodic disturbances [4], which correspond to values of 0.47 Hz and 0.74 Hz, which is almost the same for all operating parameters.

## III. The Construction Vector Diagrams of Fluctuations in the Operating Parameters when the External Periodic Perturbation Load

Study of the effect periodic load was carried out with the change in oscillation frequency of load in the range 0.4–0.9, is necessarily encompassing both resonant frequencies. For periodic load change dPn1 in the most typical (close to resonance) frequencies of 0.7 Hz and 0.4 Hz in different parts of the system (for a frequency of 0.7 Hz the results are shown in Fig. 2) the obtained waveforms show that the phase shift and the amplitude of the oscillation frequency voltage (Fig. 2, a) and voltage amplitude (Fig. 2, c) depends on the measurement points the modal parameters (the place of installation, PMU)

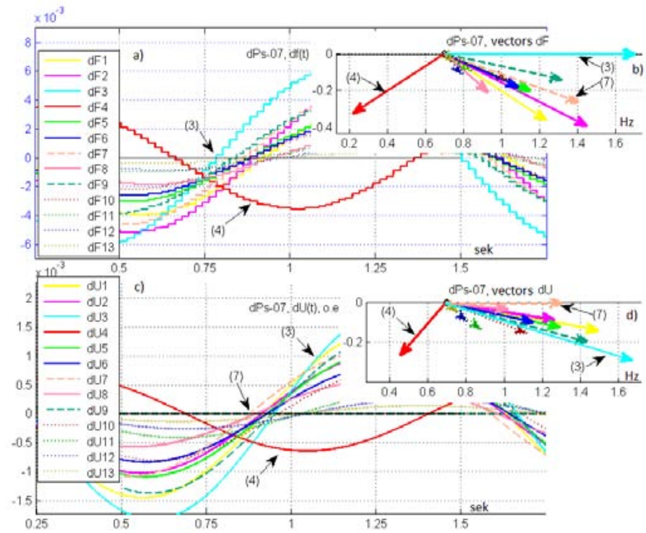


*Fig. 2:* Waveforms of the oscillation frequency (a) and amplitude (c) voltage, and the vectors of the oscillation frequency (b) and amplitude (d) the voltage at points 1–13 installation PMU

When using a visual geometric method of representation harmonic oscillations, namely, their image as vectors in the complex plane [5], are shown the vector fluctuations of operating parameters at different points installation, PMU. The horizontal axis represents the frequency of oscillation settings and the vertical attenuation constant (parameters of roots of the equation of free motion). The length of vector is proportional to amplitude of the corresponding modal parameters, and its phase equal to the phase oscillations relative to signal sync. Each vector (Fig. 2, b, d) starts at the point of 0.7 Hz, a value of zero damping constant, since the amplitude of sine wave oscillations operating parameters constant.

Device, PMU 3 is set almost at the point of disturbance. In this case, the phase of the oscillation frequency at point 3 the minimum relative to reference point (1PPS signal), and its amplitude is maximum . The vector of this oscillation (see Fig. 2, b) – basic, next to it the vectors, shown as a dotted line, is built on the basis of measurements in area closest to point of application perturbation. Among the vectors oscillation amplitude of the voltage (see Fig. 2, d), the oscillation amplitude, measured at the point 3, is maximum, but the phase of this vector is significantly different from minimum.

Therefore, only the phase vectors of the oscillation frequency of the voltage measured at different points power system, uniquely identifies a source location LFO. Phase vectors of the oscillation frequency of voltage measured, PMU, are minimum

Global Journal of Researches in Engineering ( F ) Volume XVII Issue V Version I Year 2017

where the measurements were performed close to source of perturbation. The module vector of oscillation frequency depends on the degree of coincidence of frequencies LFO and the resonance frequency in the considered point of grid and shows the sensitivity of object to fluctuations considered frequency.

## IV. Study of the Ways to Minimize Impact of LFO in Power System on Synchronous Generator

Identified in the previous Chapter the pattern allows through synchronized vector measurements to obtain information about location of source periodic perturbation, leading to the emergence of LFO in grid. Considering all the operating parameters of low-frequency fluctuations and fine tuning of automatic excitation regulators (AEC) generators at stations located near the source of the LFO, which would improve the damping performance of AECs and reduce the probability of violations parallel operation of power plants and grids, the occurrence of asynchronous mode and cascade development process disturbances [6].

In a hardware-software complex of RTDS were studied and proven method of reducing the effects of the various LFO on the performance of synchronous generator.

The first method is the change in the prescribed setpoint voltage of the AEC on the generators of the power plant, located closest to the source of the LFO. To study the simulated real network with multiple parallel links. PMU were placed. Fig.3 shows part of the studied schemes. Shows diagrams that contain PMU caught in this part, provided their numbers.

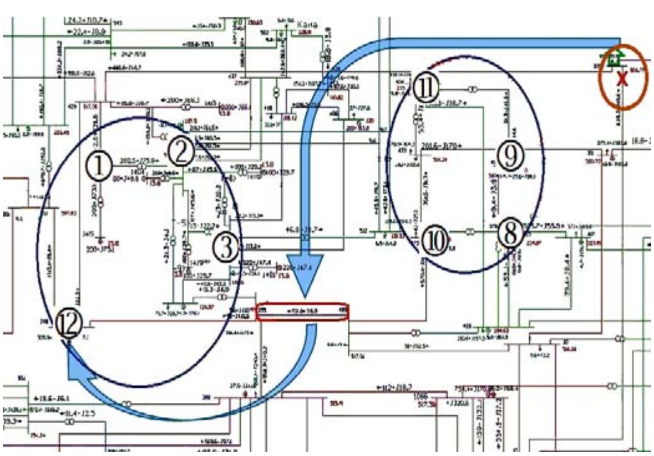


*Fig. 3:* Part of the scheme of the studied network

After an outage of line (X marks in Fig. 3), is an increase in flow in said line, until it exceeds the maximum value.

Using the identified patterns, and analysing data with PMU determined that PMU installed at the point 12 (Fig.3) shows the minimum phase of the oscillation frequency of the voltage (Fig.4), which indicates a location closest to the source of the disturbance.

Fig.4 shows the transition of the local fluctuations (Fig.4,b) arising out of the disconnection of the line, zonal continuous. Fig.3 ovals marked stations having the same type of zonal oscillation that is manifested in the waveform in Fig.4,a.

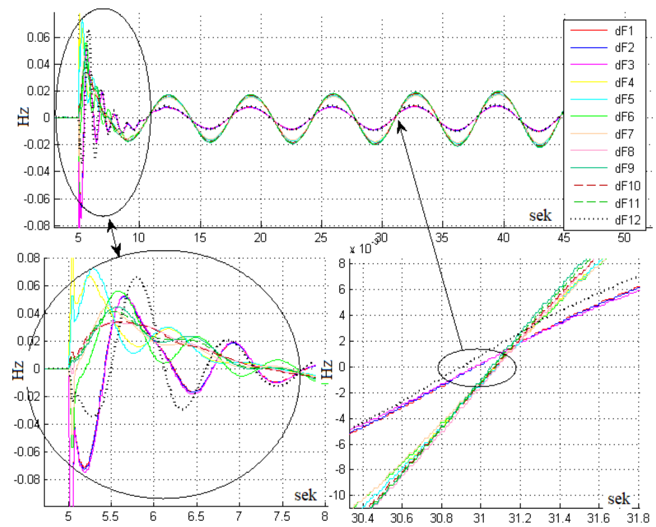


*Fig. 4:* Waveforms of the oscillation frequency at the installation location PMU

Changes prescribed setpoint voltage of AEC 10% of the station at point 12 leads to a decrease of the amplitude of the oscillations not only on the tires of the considered stations, but throughout the grid (fig.5).

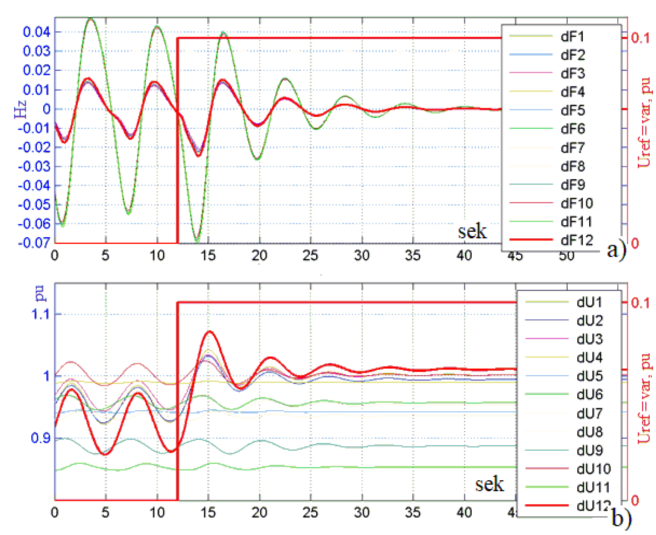


*Fig. 5:* Waveforms of the oscillation frequency and the amplitude of the voltage at the installation site PMU after a change in the prescribed setpoint voltage AECs

Thus, the change in the prescribed set point voltage of AECs improves damping of low frequency oscillations occurring in the power system.

The second way is to change the schema of the AEC. Analysis of oscillation in all nodes of the grid after setting the AEC, the station closest to the source of an LFO will allow for the synchronized vector measurement gauges to assess the impact of the settings of AES on fluctuations in the working parameters of all the given points of the power system

Change the structure and parameters of AEC, located near a permanent source of vibrations. The scheme upgraded the device ARV is shown in Fig. 6. Overbuild the part is highlighted and presented on the same figure. 6.

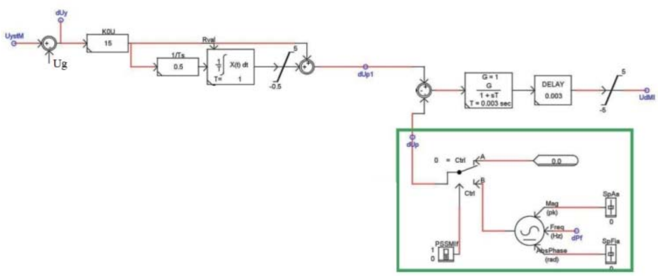

*Fig. 6:* The scheme of the studied device AEC (the model created in RTDS)

The main design feature of this AEC is the summation of the output signal dUp1 with amplitude-modulated and frequency of voltage signal dUp, the main amplitude and frequency of which correspond to parameters of low-frequency oscillations. In addition, the frequency of the b phase modulated oscillations are so chosen that they are the opposite of own oscillations of the generator.

Fig. 7 shows the results of research work this AEC. The oscillograms are shown the measurements obtained in all the locations where the devices are synchronized vector measurements. The oscillograms clearly traced the decrease in the amplitude of oscillation frequency, which proves the efficiency AEC.

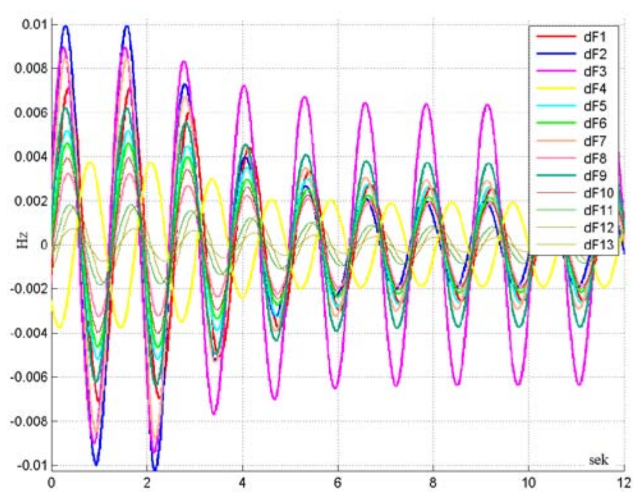


*Fig. 7:* Diagram of the test network and waveforms of the oscillation frequency in the place of installation PMU

It should be noted that implementation's AECs have been used only at node 2 (Fig. 1), the oscillation frequency at this point is a maximum.

When comparing the waveforms of oscillation frequency in Fig. 7 observed in different points, you can see that the modified AECs has a positive effect on damping of oscillations not only at the station but in whole energy area.

## V. Conclusion

This regularity allows to obtain information about location of source periodic perturbation, leading to the emergence of LFO on the grid. Further work are aimed at creation of algorithm of fast detection source of LFO on the basis of vector measurement.

Research methods reduce the influence of LFO on synchronous generator will help determine the optimal setting automatic regulator of excitation for maximum damping LFO has occuring in the power system. Also it is possible to develop adaptive-customizable automatic excitation regulators depending on the parameters of low frequency oscillations in power system.

## References Références Referencias


1. Sorokin D.V. *Vybor nastroek ARV generatorov slozhnoj jenergosistemy na osnove primenenija geneticheskogo algoritma i metodov modal'nogo analiza*. [The choice of settings ARV generators of complex energy systems based on the use of genetic algorithm and modal analysis methods], Dis.kand. tehn. nauk: 05.14.02.D.V. Sorokin; SPbGPU; Nauch.ruk. S.V.Smolovik– Sankt-Peterburg, 2009.
2. J. Xiao, J. Han, J. Wu, Dynamic *Tracking of Low-frequency Oscillations with Improved Prony Method in Wide-Area Measurement System*. IEEE Power Meeting 2004. Denver.
3. Task Force on Identification of Electromechanical Modes, *Identification of Electromechanical Modes in Power Systems*, IEEE Task Force Report, 2012.
4. Klimova T.G.,Savvatin M.V. *Analiz vlijanija periodicheski menjajushhejsja nagruzki na vozniknovenie nizkochastotnyh kolebanij* [The analysis estimates periodically changing load on the occurrence of low-frequency oscillations] in Sbornik dokladov Mezhdunarodnoy nauchno-tehnicheskoy konferencii SIGRE "Sovremennye napravleniya razvitiya system releynoy zaschity i avtomatiki energosisem", Sochi, 2015.
5. Arcishevkij Ja.L., Klimova T.G., Rasshhepljaev A.I. Predstavlenie perehodnyh processov jelektrojenergeticheskih sistem na giperploskosti s dvumja sistemami koordinat // Jelektrichestvo. 2011. № 4.

Venikov V.A. *Perehodnye jelektromehanicheskie processy v jelektricheskih sistemah: Ucheb. dlja jelektrojenerget. spec. vuzov* [Transient Electro-mechanical processes in electrical systems: Textbook. for electroenergy. spec. universities]. 4-e izd. pererab. i dop. –M.-Vyssh. shk, 1985.-536s..

Global Journal of Researches in Engineering ( F ) Volume XVII Issue V Version I Year 2017



This page is intentionally left blank

Global Journal of Researches in Engineering: F
Electrical and Electronics Engineering
Volume 17 Issue 5 Version 1.0 Year 2017
Type: Double Blind Peer Reviewed International Research Journal
Publisher: Global Journals Inc. (USA)
Online ISSN: 2249-4596 & Print ISSN: 0975-5861

# Reduced Size Single Switch Power Factor Correction Circuit

By Hussein al-bayaty, Ali Hussein Al-Omari, Marcel Ambroze & Mohammed Zaki Ahmed

*Plymouth University, United Kingdom*

*Abstract-* This article presents a new design of active power factor correction (APFC) circuit that can be used in single phase rectifiers. The proposed circuit provides almost a unity input power factor (PF) which contributes significantly in reduction of the total current harmonic distortion (THDI) as it eliminates the third harmonic component effectively from the input current.

The most important attribute of this circuit is the small size and numbers of components (one switch, small size (L & C) and a diode), which have been designed to get a unity PF at the AC source side. Therefore, the new circuit is cheaper, smaller size and lighter than other conventional PFC circuits.

In addition, the new proposed circuit is a snubber-less and uses reasonably low switching frequency which reduces switching losses and increases efficiency. The circuit has been designed and simulated using Lt-spice simulink program.

*Keywords:* *active power factor correction (APFC), AC - DC converter, total harmonic distortion (THD).*

*GJRE-F Classification:* *FOR Code: 090607*

REDUCEDSIZESINGLESWITCHPOWERFACTORCORRECTIONCIRCUIT

*Strictly as per the compliance and regulations of:*

# Reduced Size Single Switch Power Factor Correction Circuit

Hussein al-bayaty α, Ali Hussein Al-Omari σ, Marcel Ambroze ρ & Mohammed Zaki Ahmed ω

*Abstract-* This article presents a new design of active power factor correction (APFC) circuit that can be used in single phase rectifiers. The proposed circuit provides almost a unity input power factor (PF) which contributes significantly in reduction of the total current harmonic distortion (THDI) as it eliminates the third harmonic component effectively from the input current.

The most important attribute of this circuit is the small size and numbers of components (one switch, small size (L & C) and a diode), which have been designed to get a unity PF at the AC source side. Therefore, the new circuit is cheaper, smaller size and lighter than other conventional PFC circuits.

In addition, the new proposed circuit is a snubber-less and uses reasonably low switching frequency which reduces switching losses and increases efficiency. The circuit has been designed and simulated using Lt-spice simulink program.

*Keywords: active power factor correction (APFC), AC - DC converter, total harmonic distortion (THD).*

## I. Introduction

Single phase AC/DC rectifiers with a large electrolytic capacitor are commonly used for manufacturer and business issues. The main purpose to use diode rectifiers is to operate the switching power supply in data processing apparatus and to operate low power motor drive systems [1].

The large capacitor draws current in short pulses, which brings in a lot of problems including decreasing in the available power, increasing losses and reduction of the efficiency. In the conventional way of design, the capacitor voltage preserves the peak voltage of the input sine wave until the next peak comes along to recharge it [2].

The only way to recharge the capacitor is drawing the current from the input source at the peaks of the source waveform as a long pulse which includes an adequate amount of energy to nourish the load until the next peak. This is happens when the capacitor draws a large charge during short time, after the slowly discharge of the capacitor into the load. Therefore, the capacitor's current draws 5 to 10 times of the average current in 10% or 20% of the cycle period. Consequently, the source current has narrow and long pulses and the effective (r.m.s.) value increases [3], [4].

Customers with a large number of nonlinear loads also have large neutral current rich in third harmonics current. In order to increase the PF, decrease the losses and save the energy, then the input current harmonics (specially the third order harmonic) have to be eliminated. Several methods and techniques have been proposed to solve the problem of a poor power factor, which can be classified as active and passive methods [5].

Passive PFC circuits are generally simple, fewer components, smaller size and easy to design for small rating power (less than 200 watt). However, its bulky and not economical for large power ratings and the input power factor is (0.6 - 0.7) and THD = 150% in best conditions without using big size elements [6].

Active PFC circuits, can considerably diminish losses and costs associated with the generation and distribution of the electric power and significantly improved power quality. Therefore, APFC circuits are receiving more and more attention these days because of the widespread use of electrical appliances that draw non sinusoidal current from the electric power systems. However, PFC circuits require additional, more expensive and complex components [7]. The author in [8], designed a novel PFC circuit that depends on the principle of limiting the work of the main capacitor in a manner which can eliminate the third order harmonic and improve the input PF into 0.99. However, this design has been used two Mosfets and high switching frequency equal to 200 KHZ which may increase the switching losses and reduce the efficiency.

In this paper, a new design of PFC converter has been introduced and presented in figure (1). The new design is depending on the flexibility of the parameters' variation which produces low harmonics, high input PF and high efficiency.

The new proposed design, reduces the required number of components into one Mosfet switch with low switching frequency equal to 20 KHZ, and uses small value of inductor which is smaller more than 96% of the inductors used in conventional boost PFC circuits, because the new proposed design focuses on shifting the harmonics components to the high frequency region and consequently eliminating the third order harmonic current, therefore the cost, the weight and the size of the new circuit will be reduced hugely.

The description of the circuit, operation topology, control circuit and operation stages are all

*Author α σ ρ ω : School of Computing Electronics and Mathematics, Plymouth University, UK. e-mails: hussein.al-bayaty@plymouth.ac.uk, kabily30@gmail.com*

described in section (II). The details of system's parameters are described in section (III). The discussion of simulation results and assessment are presented in section (IV), followed by an overall conclusion in section (V).

## II. Operation Principles and Analysis of the New Proposed Circuit

### a) *Circuit's Description*

The schematic circuit of the new proposed PFC circuit is shown below in figure (1).

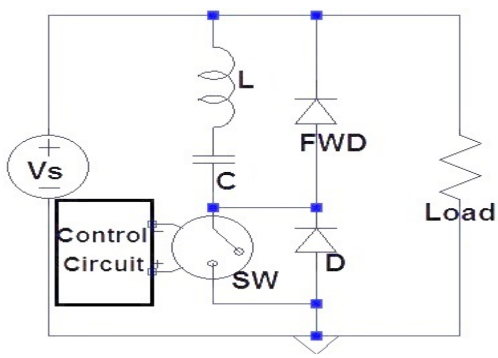


*Fig. 1:* New proposed APFC circuit

($V_S$) is the input DC source (represents AC single phase connected to full bridge rectifier), connected in parallel with LC resonant branch and MOSFET switch (SW) in parallel with the load. A control circuit has been designed in order to control the switching process.

### b) *Operation Topology*

The new proposed circuit has the ability to control the working period of the capacitor. Consequently, the value of the input power factor, $THD_I$ of the source current waveform and the value of the output ripple voltage can be controlled as well through using one switching devices.

The principle of this design is depending on the distributing of the working time intervals of the capacitor into two regions, at the beginning (0 - $t_1$) and at the end ($t_4$ $-\pi$) via using control circuit. This smart switching pattern would eliminates the third order harmonic component and improves the input PF as the third order harmonic is the most significant component in single phase systems.

This design uses a minimum number of components and minimum values of (L) & (C) a s capacitor turned off on the middle of each cycle, which shift the harmonics components to higher frequencies. consequently, reduces the size and the cost of the new proposed circuit.

This circuit is snubber-less circuit, because the freewheeling diode (FWD) presents an alternative path for the discharge current of inductor ($I_L$), so can the capacitor keep charged. Accordingly, (FWD) can avoids the negative part of $I_L$ and helps (C) to act as a snubber circuit in order to prevent the inductor's voltage ($V_L$) to increase more than rated value of the source voltage, in this way (C) will protect the MOSFET switch from being burned in the effect of the high voltage spikes which may happened without the FWD.

### c) *Control circuit*

A simple designed control circuit, as shown in figure (2) has been investigated in order to derive the MOSFET switch and control the switching frequency and duty cycle.

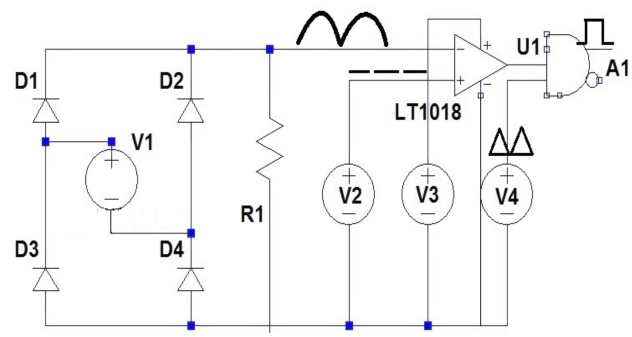


*Fig. 2:* Control circuit

Briefly, the circuit consists of a dual input comparator which compares two signals(the first signal is the output of full wave rectifier and the second is a dc voltage source). The output of the comparator, which is a square wave, would be combine in a logic (And gate) circuit with a triangular waveform in 20 KHz frequency. the output of and gate will go directly to the gate of the MOSFET switch.

### d) *Operation stages*

1) First mode: This mode describes the time period $0 \leq t < t_1$, when the capacitor voltage $V_C > V_S$. SW-ON/OFF, while $t_1$ is the moment when $V_S$ is equal or bigger than $V_C$. The circuit shown in figure (3-a), illustrates the path of the current at this mode:
In this period, (C & L) are discharging and feed the load.

$$I_C = C\frac{dV_C}{dt} = I_L = I_{Load} = \frac{V_{out}}{R}$$

because L, C and the load are series in this mode.

$$\therefore V_{Load} = V_{out} = V_C + V_L$$

$$\because V_L = L\frac{di_L}{dt}$$

then the value of $V_L$ is approximately zero because the value of $L_1$ is very small (few micro henres).

$$\therefore V_{out} \approx V_C$$

The full time period of the input source current waveform ($I_S$) is shown in figure (4) with the details of nine time modes.

2) Second mode: For the time period $t_1 \leq t < t_2$, when $V_S > V_{C1}$, and SW is ON. $t_2$, is the moment when the pulses turns off. The circuit shown above in figure (3-b), the bold line illustrates the active path at this mode.

In this mode, the load, C & L are all connected to the source and charging with frequency pulses (20 KHz), as a result, high values and short time current spikes appear on the input current waveform because of the capacitor current. $V_S = V_{Load} = V_{out}$

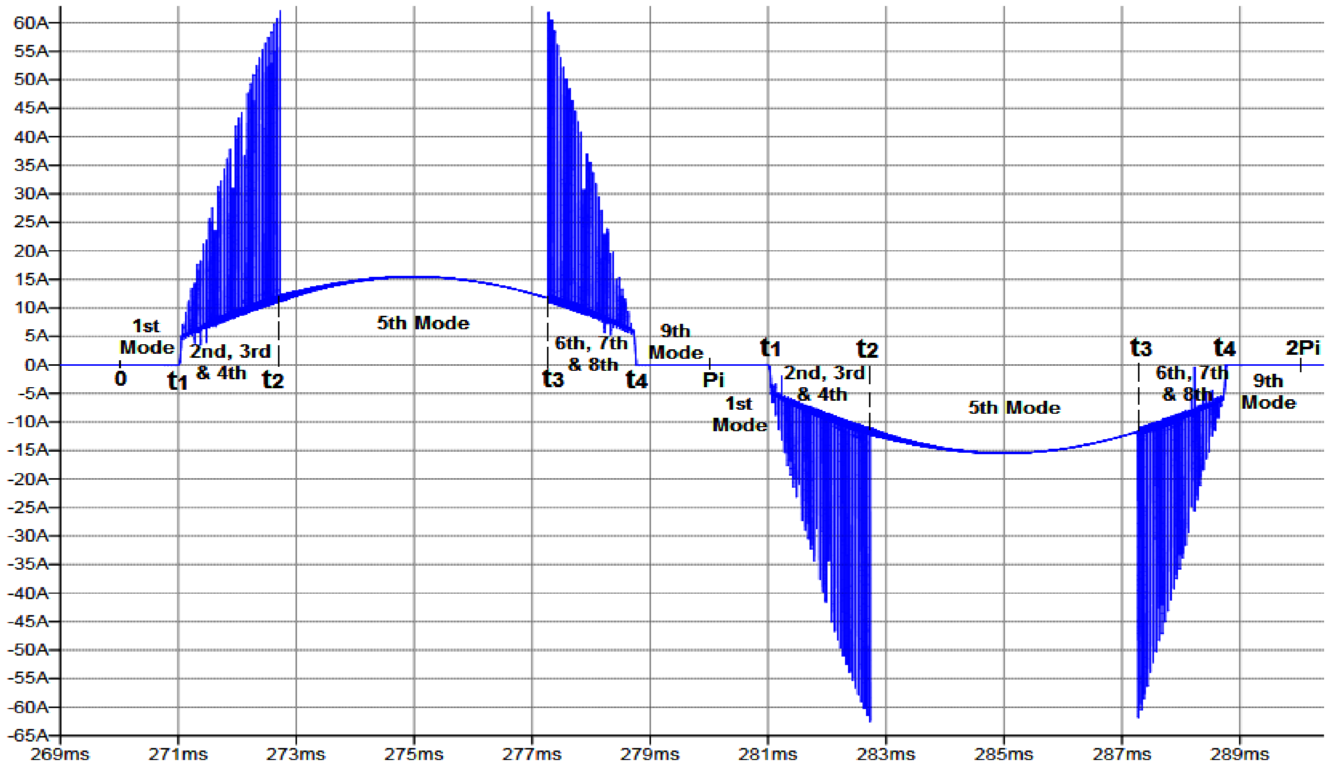


*Fig. 4:* The input source current

$V_S = V_C + V_L = V_C + L.\frac{di_L}{dt}$ $I_S = I_C + I_{Load} = C.\frac{dV_C}{dt} + I_{Load}$

3) Third mode: For the time period $t_1 \leq t < t_2$, when $V_S > V_{C1}$. This mode covers the interval time from switching OFF moment until ($t_d$) ms. $t_d$ is the moment when $I_L$ or $I_C$ discharge to zero ampere for each pulse. The circuit is shown above in figure (3-c).

At this mode, (L) discharges its current to (C) until being zero (at the $t_d$ moment), while the inductor voltage $V_L$ is equal to $V_C$ and remains charged. This topology dose not require a snubber circuit as $V_L$ has been prevented.

$$\because V_L = V_C \quad \& \quad I_L = I_C = C\frac{dV_C}{dt} \quad \therefore X_L = X_C$$

$$2\pi f L = \frac{1}{2\pi f C} \quad \therefore f_r = \frac{1}{2\pi\sqrt{LC}} = 1.59KHz$$

$f_r$ is the resonance frequency.

At this mode, the load is fed by the source.

$$V_L = L\frac{di_L}{dt} = V_C$$

$$I_S = I_{Load} = \frac{V_{out}}{R}$$

4) Fourth mode: For the time period $t_1 \leq t < t_2$, when $V_S > V_C$, SW is OFF (from ($t_d$) until the next ON-pulse). The bold line in the circuit shown above in figure (3-d), clarifies the source current's path.

At this mode, the inductor current ($I_L$) supposed to remain zero ampere. However, the internal capacitance of the diodes combines with stray inductance which form resonant circuit called parasitic resonant.

Due to this parasitic resonance, a sinusoidal current can flow into the inductor $L_1$ in a very high frequency (about 1.54 MHz) called self resonant (or parasitic) frequency ($f_p$).

At the same time, $V_L$ follows $I_L$ waveform and oscillate around zero. $I_L$ & $I_S$ values are variable and change in accordance to the values of L, C, $f_{sw2}$, $\frac{dv_c}{dt}$ and output load as it's clear from equations and shown in figures (4) and (5):

The capacitor voltage ($V_C$) remains charged and considered as a constant value due to the value of $I_C$ which is approximately zero, then the value of $\frac{dV_C}{dt}$ is very small value.

$$I_L = I_0.\cos(w_p.t)$$

$$w_p = 2\pi f_p \approx 9.5 \text{ M rad/sec.}$$

($I_0$) is approximately 0.5 Amp. For ideal conditions, the internal capacitance of diodes is zero, therefore the parasitic resonance and $I_0$ can considered as zero ampere.

Practically, a damper circuit (R=5 Ω & C=1 nF) can be connected in parallel with the freewheeling diode in order to eliminate the resonance current (I0) totally, however, 0.1 % of power losses can be increased in the circuit as a circuit of 3 kw output power, has only 3 watt losses in the damper circuit which is negligible. The modes (2,3,4) are repeating every ON/OFF switching pulse of SW.

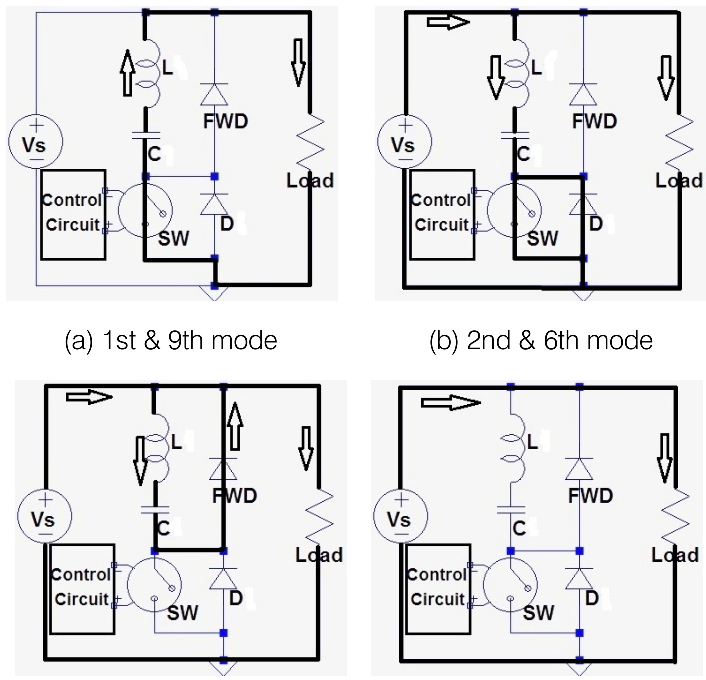


(a) 1st & 9th mode

(b) 2nd & 6th mode

(c) 3rd & 7th mode

(d) 4th, 5th & 8th mode

*Fig. 3:* Circuit diagram in different time modes

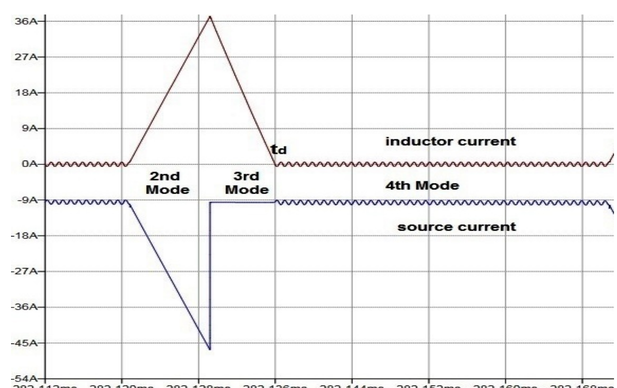


*Fig. 5:* IL & IS in the 2nd, 3rd & 4th modes

The figure (6), shows the full picture of $V_C$, $V_{out}$, $V_L$&$V_D$ waveforms. $V_C$ is in red color, $V_{out}$ is in brown color, $V_L$ is in green color, and $V_D$ is in blue color.

5) *Fifth mode:* For the time period $t_2 \leq t < t_3$, when pulses are ON/OFF. $t_3$ is the moment when SW turns OFF. The circuit shown in figure (3-d), illustrates the active path of current at this mode:

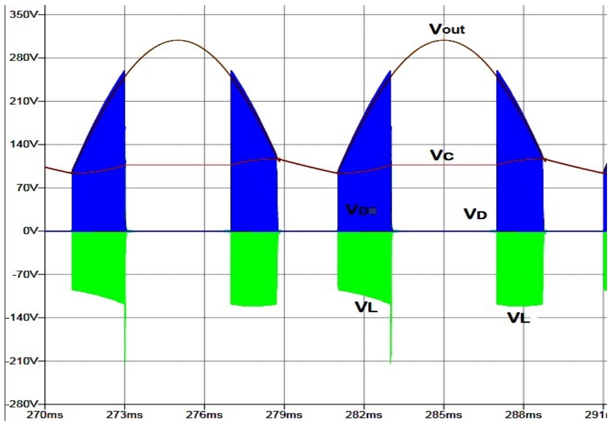


*Fig. 6:* $V_C$; $V_{out}$; $V_L$ & $V_D$ waveforms

Due to $V_S > V_C$, therefore $C$ and $L$ are considered as disconnected (open circuit), because they are reverse biased when SW is OFF and (FWD) is reverse biased.

Therefore, C and L are neither charging nor discharging, then $I_L = I_C =$ Zero, $V_L =$ Zero but $V_C$ is a constant value.

6) *Sixth mode:* For the time period $t_3 \leq t < t_4$, when $V_S > V_C$, SW is ON. $t_4$ is the moment when $V_C$ is greater than $V_S$. The circuit is shown in figure (3-b).
At this mode, C and L are charging and the load is fed by the source. All the derived equations in the 2nd mode are valid for this mode.

7) *Seventh mode:* For the time period $t_3 \leq t < t_4$, when $V_S > V_C$. The circuit is shown in figure (3-c).
At this mode, (C) is charging while $V_L$ is equal to $V_C$ until $L$ fully discharges its current into zero ampere at the time of ($t_d$).
All the derived equations in the 3rd mode are valid for this mode.

8) *Eighth mode:* For the time period $t_3 \leq t < t_4$, when $V_S > V_{C1}$, SW is OFF, for period ($t_d$) until the next ON-pulse for $SW_2$. The circuit is shown in figure (3-d).
$V_C$ still charged and slightly charging but approximately constant due to very small $\frac{dV_C}{dt}$.
$V_{C1}$ remains charged and considered as a constant value due to the value of $I_{C1}$ is approximately zero, then the value of dVC1 would be very small.

$$I_{L1} = I_0 . \cos(w_p.t)$$

$$w_p = 2\pi f_p \approx 9.5 \text{ M rad/sec.}$$

The modes (6,7,8) repeat themselves every ON/OFF switching of the MOSFET.

9) *Ninth mode:* For the time period $t_4 \leq t < 10$ ms., when $V_C > V_S$. SW-ON/OFF, the circuit is shown above in Fig. (3-a).
L & C are discharging while the R-load is fed by the main capacitor.

$$\therefore I_L = \frac{V_{out}}{R}$$

$$V_{Load} = V_{out} = V_C + V_L$$

All the derived equations in the first mode are valid for this mode.

## III. System Parameters

The proposed circuit has been simulated in LT-spice program and the parameters have been specified as the following table:

*Table I:* System Parameters

| | | |
|---|---|---|
| Inductor (L) | $R_{\text{Internal Ser.}} = 2.236$ m $\Omega$ | $R_{\text{Internal Par.}} = 1413\ \Omega$ |
| Capacitor (C) | ESR = 0.035 $\Omega$ | ESL = 0 $\Omega$ |
| MOSFET | IPP070N8N3, N-channel | $V_{ds}$ = 80 V, $R_{ds}$ = 7m $\Omega$ |
| Freewheeling diode | Schottky, (UPSC600) | $V_{\text{Breakdown}}$ = 600 V |
| Parallel diode | Schottky, (MBR745) | $V_{\text{Breakdown}}$ = 45 V |
| Load | Resistive | 20 $\Omega$ |

## IV. Simulation Results and Assessment

An electrical circuit with $V_S$ = 311 $V_{peak}$ = 220 $V_{rms}$, L = 20 µH, C = 0.5 mF and MOSFET switch works in $f_{sw}$ = 20 Khz controlled by a control circuit, has been designed and investigated by using Lt-spice simulink program.

1) R-load, inductor (L) and switching frequency of the MOSFET, are three main parameters in this circuit which could be changed in different values in order to find out the optimum design and parameters values in order to get low input $THD_I$ , unity input PF, high efficiency, cheap, not bulky, small size and light converter.
2) Table (I), shows the relationship between different load values comparing it with fundamental input current $P_{in}$, $P_{out}$, $\eta$, $THD_I$ and input PF when L = 20 µH and the switching frequency ($f_{sw}$) is 20 Khz.

*Table II:* Different load values with $THD_I$, PF & $\eta$

| **R**($\Omega$) | $P_{in}$(W) | $P_{out}$ (W) | $\eta$(%) | **THD**(%) | **PF** |
|---|---|---|---|---|---|
| 1 | 46354.5 | 44260 | 95.48 | 5 | 0.999 |
| 10 | 4920.2 | 4851.5 | 98.6 | 11.6 | 0.994 |
| 20 | 2506 | 2473 | 98.68 | 17 | 0.986 |
| 50 | 1038 | 1021 | 98.36 | 28.4 | 0.96 |
| 100 | 543.48 | 525 | 96.6 | 37 | 0.938 |
| 200 | 292.68 | 269.6 | 92.1 | 52.4 | 0.886 |
| 500 | 141 | 110.75 | 78.55 | 83.2 | 0.77 |
| 1000 | 90.2 | 56.1 | 62.2 | 111.7 | 0.667 |

Power factor has been calculated by using equation in [9], P.F = $\frac{1}{\sqrt{1+(THD_I)^2}}$

Global Journal of Researches in Engineering ( F ) Volume XVII Issue V Version I Year 2017

$$I_t = \sqrt{I_1^2 + I_h^2}$$

The total input power, has been calculated via below equation [10]:

$$P_{in} = V_t.I_t.PF$$

The maximum efficiency is 98.68% when input power is 2.5 kw when R-load = 20 Ω and (L) is 20 μH.

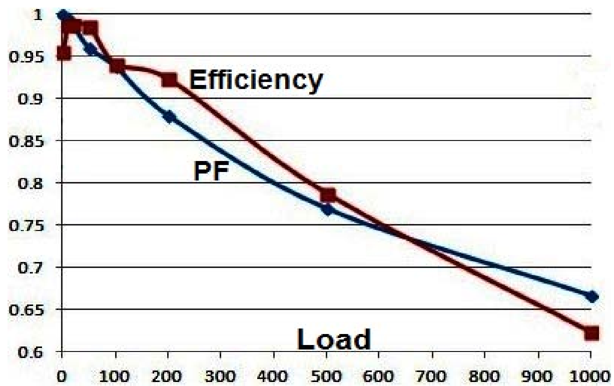


*Fig. 7:* Different load values with PF and $\eta$

It can be concluded, from table (I) and figure (7) that the values of ($\eta$) and input PF, inversely proportion with the increasing of the load value.

3) Table (II) shows the relationship between different inductor values comparing with with $P_{in}$, $P_{out}$, _ and input PF, when R-load = 20 Ω and $f_{sw}$ = 20 Khz.

*Table III:* Different (L) values with $THD_I$, PF & $\eta$

| L(uH) | $P_{in}$(W) | $P_{out}$ (W) | $\eta$(%) | THD(%) | PF |
|---|---|---|---|---|---|
| 1 | 2854.9 | 2679.4 | 93.86 | 55 | 0.876 |
| 10 | 2557.5 | 2510 | 98.1 | 24 | 0.972 |
| 20 | 2506 | 2473 | 98.68 | 17 | 0.986 |
| 50 | 2456 | 2434 | 99.1 | 10.5 | 0.994 |
| 100 | 2434.38 | 2415.5 | 99.2 | 7.2 | 0.997 |
| 200 | 2420.48 | 2403.7 | 99.3 | 4.9 | 0.999 |
| 500 | 2412 | 2395 | 99.3 | 3.5 | 0.999 |
| 1000 | 2407.3 | 2391.8 | 99.36 | 2.5 | 0.999 |

It can be concluded, from table (II) and figure (8) below, that the value of $\eta$ and PF, directly proportion with the increasing of inductor value.

4) Table (III) shows the relationship between different switching frequencies of MOSFET comparing with $P_{in}$, $P_{out}$, $\eta$ and input PF when R-load = 20 Ω and (L) is 20 μH.

It can be concluded from table (III) and figure (9) that, the value of $\eta$ and PF directly proportion with the value of $f_{sw}$.

It can be concluded that, $f_{sw}$ can be kept around (10 - 20) KHz in order to get approximately unity PF (0.98) at the input AC side when (L) is 20 μH for 2.5 kw output power.

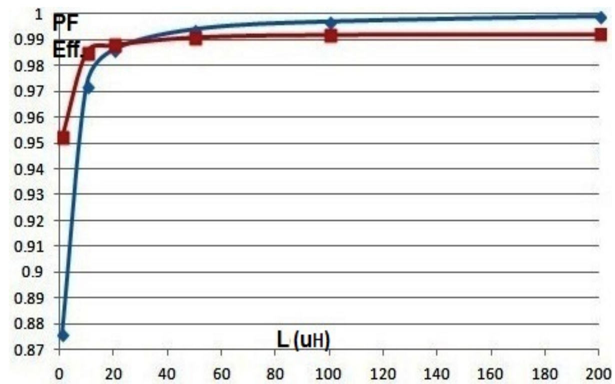


*Fig. 8:* Different (L) values with PF and $\eta$

*Table IV:* Variable (D) for (SW) with $THD_I$, PF & $\eta$

| $f_{sw}$(K) | $P_{in}$(W) | $P_{out}$ (W) | $\eta$(%) | THD(%) | PF |
|---|---|---|---|---|---|
| 5 | 2641 | 2574.8 | 97.5 | 33 | 0.95 |
| 10 | 2561 | 2515 | 98.2 | 23.8 | 0.973 |
| 20 | 2506 | 2473 | 98.68 | 17 | 0.986 |
| 50 | 2456.3 | 2434.2 | 99.1 | 10.6 | 0.994 |
| 100 | 2437.3 | 2415.8 | 99.1 | 7.6 | 0.997 |
| 200 | 2418.9 | 2405 | 99.4 | 5.6 | 0.998 |
| 500 | 2415 | 2397.2 | 99.2 | 3.9 | 0.999 |
| 1000 | 2414.8 | 2396.2 | 99.2 | 3.7 | 0.999 |

5) The figure 10, shows the Fast Fourier Transform (FFT) spectrum of the input source current. The total current harmonic distortion ($THD_I$) is 17%, then the total input power factor is (0.986).
As it is shown in figure (10), the third order harmonic is not exist at the input current waveform, and the only harmonic orders shown are the 5th and 7th order harmonics. This is because (C) was OFF at the middle of the waveform ($t_2 - t_3$) and the load was fed by the source.

6) In the case of the absence of freewheeling diode in the time intervals $t_1 \leq t < t_2$ and $t_3 \leq t < t_4$ (which represent the 2nd and 6th modes), the equation of inductor's voltage is:

$$V_L = L\frac{di_L}{dt} = \frac{L.di_L.f_{sw}}{D}$$

(D) is the duty cycle of (SW) and because of the switching frequency ($f_{sw}$) is (20 KHz), therefore $V_L$ would be a very large value at this moment. Consequently, $V_L$ may be a reason for huge spikes on MOSFET's terminals and may burn the switch.

7) Generally, in this situation a snubber circuit would be proposed as a solution to suppress the high frequency spikes and to protect the MOSFET switch. However in this circuit, the main capacitor (C) would be act as a snubber circuit because of the existence of the freewheeling diode (FWD), which makes $V_C$ charges on the negative value of $V_L$ and prevent high voltage on the terminals of the MOSFET when its in open the status. As shown in figure (11), the inductor voltage does not increases more than 140 $V_{P-P}$ in spite of that the source voltage is 311 $V_{P-P}$, because of the small value of (L).

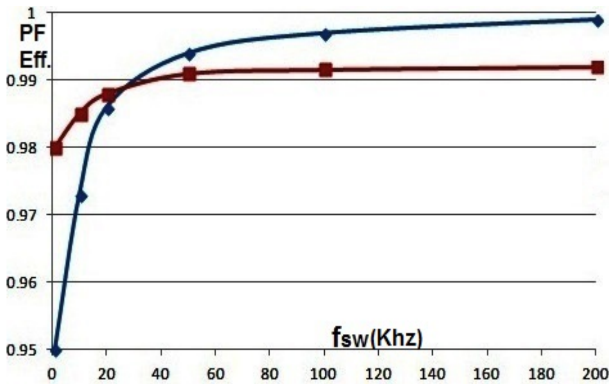


*Fig. 9:* Different $f_{sw}$ values with PF and $\eta$

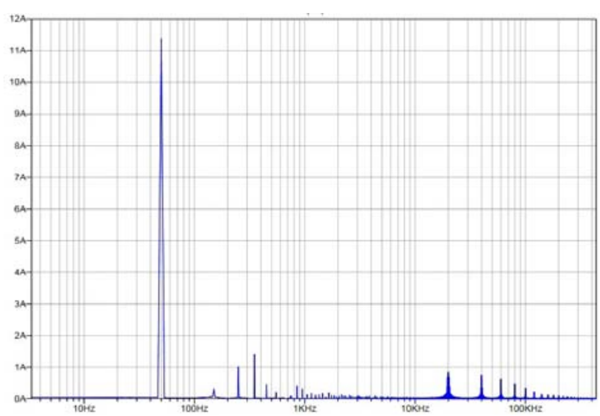

*Fig. 10:* FFT Spectrum of the input current

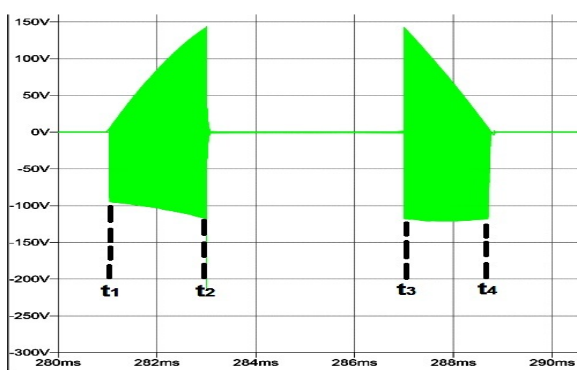


*Fig. 11:* The waveform of $V_L$

8) The required value of the inductance for the same voltage and power ratings in three level boost converter is (L), while the size would be doubled with the using of two inductors (2x2L) for the interleaved boost converter, on the other hand, the inductance would be doubled again (4L) for the conventional boost converter [11].

   The inductor's value used in the literature in [12] for a (3 kw) output power using interleaved boost converter was (270 μH), while the value of inductor (L) in the new proposed circuit is (20 μH) for the same power ratings. This reduction of the inductor's value will effectively contribute in reducing the size, weight and the cost of the converter.

9) One of the significant features of this design, is that the inductor's current is not related to the value of source voltage (except in the 2nd and 6th mode) as usually happens in PFC circuits. This advantage can be utilized in order to reduce the value of (L) into few micro henrys and avoid high $V_L$ values. Consequently, can reduce the size, weight and the cost effectively.

10) Practically, the internal capacitor of the used diodes in the circuit would combine with the stray inductors and compose a parasitic resonant frequency ($f_p$). In order to get rid of the bad effects of ($f_p$), the rising time ($t_r$) or the falling time ($t_f$) can be changed, or alternatively a damper circuit can be added to the circuit or using clamping diodes and that's require additional components and complex design [13].

11) The inductor works like a proper choke or current limiter due to the high negative value of inductor voltage ($V_L$) as its in counter direction of capacitor voltage ($V_C$).

    (L) charges in the time period $t_1 \leq t < t_2$ because $V_S > V_C$. On the other hand, for the time period $t_2 \leq t < t_3$, *IL* is zero because L and C are reverse biased. While, for the time period $t_3 \leq t < t_4$, (L) discharges as a positive current because $V_S > V_C$. However, for time period $t_4 \leq t < t_1$ of the next period, *L* discharges as a negative current because $V_C > V_S$ and the R-load would be fed by $I_L$ which is the same capacitor's current ($I_C = I_L$).

## V. Conclusion

According to the simulation's results, the new proposed PFC circuit was able to reduce the $THD_I$ to 17% with a unity power factor (0.986) at the input side and increases the efficiency to 98.68%.

The topology of reducing the conduction time of the main capacitor via dividing the waveform into three regions ONOFF-ON, can improve the efficiency, the input PF and reduce the $THD_I$ at the input side.

In addition, preventing the capacitor (C) from work in the middle of the time period for about half of the time will eliminate the third order harmonic and shift the harmonics current to the high frequency region and that's will contribute in reducing the size of magnetics due to the small value of the inductor 20 μH which produces a small amount of losses. Accordingly, the small inductor will effectively reduce the size and weight as used just one MOSFET, so the rectifier is not bulky any more, and thats reduces the cost of the converter.

Another advantage of this circuit is that the snubber circuit is not compulsory because of the presence of freewheeling diode. In addition, the design

Global Journal of Researches in Engineering ( F ) Volume XVII Issue V Version I Year 2017

is considered as a high efficient design due to minimum number and small values of components and simple circuit design due to uses single switch.

The performance of this circuit has a wide range of flexibility because, the output ripple voltage, the input PF and $THD_I$ can be improved via controlling the values of duty cycles of (SW), (L) and (C).

From graphical waveforms and tables of results analysis for different values of R-load, inductor (L), and switching frequency, can be concluded that the increasing of inductor value (L) and R-load values is required in order to get a constant unity power factor, small $THD_I$ and high efficiency.

## VI. Acknowledgment

The first author gratefully acknowledge the big support of the Higher Committee for Education Development (HCED) in Iraq.

## References Références Referencias

1. H. Al-bayaty, M. Ambroze, and M. Z. Ahmed, "Utilization of harmonics current in single phase system," in *2016 17th International Conference on Harmonics and Quality of Power (ICHQP),* Oct 2016, pp. 443–447.
2. B. Singh, B. N. Singh, A. Chandra, K. Al-Haddad, A. Pandey, and D. P. Kothari, "A review of single-phase improved power quality ac-dc converters, "*IEEE Transactions on Industrial Electronics*, vol. 50, no. 5, pp. 962–981, 2003.
3. H. Al-bayaty, M. Ambroze, and M. Z. Ahmed, "Taking advantage of the harmonics at the load side using passive filters," in *Systems and Informatics (ICSAI), 2014 2nd International Conference on*, Nov 2014, pp. 169–174.
4. H. Azazi, E. El-Kholy, S. Mahmoud, and S. Shokralla, "Review of passive and active circuits for power factor correction in single phase, low power ac-dc converters," in *Proceedings of the 14th International Middle East Power Systems Conference (MEPCON'10)*, 2010, pp. 217–224.
5. H. Al-bayaty, M. Ambroze, and M. Z. Ahmed, "Feeding loads via harmonics utilization in ac circuit systems," in 2016 *International Conference for Students on Applied Engineering (ICSAE)*, Oct 2016, pp. 224–227.
6. S. Basu, *Single Phase Active Power Factor Correction Converters-Methods for Optimizing EMI, Performance and Costs.* Chalmers University of Technology, 2006.
7. J. P. M. Figueiredo, F. L. Tofoli, and B. L. A. Silva, "A review of singlephase pfc topologies based on the boost converter," in *Industry Applications (INDUSCON), 2010 9th IEEE/IAS International Conference on,* Nov 2010, pp. 1–6.
8. H. al bayaty, A. H. Al-Omari, M. Ambroze, and M. Z. Ahmed, "A novel topology for single phase active pfc circuit," in *2017 IEEE International Conference on Environment and Electrical Engineering and 2017 IEEE Industrial and Commercial Power Systems Europe (EEEIC / I CPS Europe)*, June 2017, pp. 1–6.
9. H. Al-bayaty, M. Ambroze, and M. Z. Ahmed, "New effective power terms and right-angled triangle (rat) power theory*, "International Journal of Electrical Power & Energy Systems,* vol. 88, pp. 133–140, 2017.
10. H. A. bayaty et al., "A new power theory (right-angled triangle theory), "in *2015 IEEE Conference on Energy Conversion (CENCON)*, Oct 2015, pp. 451–456.
11. M. T. Zhang, Y. Jiang, F. C. Lee, and M. M. Jovanovic, "Single-phase three-level boost power factor correction converter," in *Applied Power Electronics Conference and Exposition, 1995. APEC '95. Conference Proceedings 1995., Tenth Annual*, no. 0, Mar 1995, pp. 434–439 vol.1.
12. B. AKIN, "Comparison of conventional and interleaved pfc boost converters for fast and efficient charge of li-ion batteries used in electrical cars," in *International Conference on Power and Energy Systems,* vol. 13, 2012.
13. K. Harada and T. Ninomiya, "Optimum design of rc snubbers for switching regulators, "*IEEE Transactions on Aerospace and Electronic Systems*, no. 2, pp. 209–218, 1979.

Global Journal of Researches in Engineering: F
Electrical and Electronics Engineering
Volume 17 Issue 5 Version 1.0 Year 2017
Type: Double Blind Peer Reviewed International Research Journal
Publisher: Global Journals Inc. (USA)
Online ISSN: 2249-4596 & Print ISSN: 0975-5861

# Optimal Power Flow using a hybrid Particle Swarm Optimizer with Moth Flame Optimizer

By Pradeep Jangir, Siddharth A. Parmar, Indrajit N. Trivedi & Arpita

*Sri Ganganagar College of Ayurvedic Science*

*Abstract-* In this work, the most common problem of the modern power system named optimal power flow (OPF) is optimized using the novel hybrid meta-heuristic optimization algorithm Particle Swarm Optimization-Moth Flame Optimizer (HPSO-MFO) method. Hybrid PSO-MFO is a combination of PSO used for exploitation phase and MFO for exploration phase in an uncertain environment. Position and Speed of particle are reorganized according to Moth and flame location in each iteration. The hybrid PSO-MFO method has a fast convergence rate due to the use of roulette wheel selection method. For the OPF solution, standard IEEE-30 bus test system is used. The hybrid PSO-MFO method is implemented to solve the proposed problem. The problems considered in the OPF are fuel cost reduction, Voltage profile improvement, Voltage stability enhancement, Active power loss minimization and Reactive power loss minimization. The results obtained with hybrid PSO-MFO method is compared with other techniques such as Particle Swarm Optimization (PSO) and Moth Flame Optimizer (MFO).

*Keywords:* *optimal power flow; voltage stability; power system; hybrid PSO-MFO; constraints.*

*GJRE-F Classification:* *FOR Code: 090699*

OPTIMALPOWERFLOWUSINGAHYBRIDPARTICLESWARMOPTIMIZERWITHMOTHFLAMEOPTIMIZER

*Strictly as per the compliance and regulations of:*

# Optimal Power Flow using a hybrid Particle Swarm Optimizer with Moth Flame Optimizer

Pradeep Jangir [α], Siddharth A. Parmar [σ], Indrajit N. Trivedi [ρ] & Arpita [ω]

*Abstract-* In this work, the most common problem of the modern power system named optimal power flow (OPF) is optimized using the novel hybrid meta-heuristic optimization algorithm Particle Swarm Optimization-Moth Flame Optimizer (HPSO-MFO) method. Hybrid PSO-MFO is a combination of PSO used for exploitation phase and MFO for exploration phase in an uncertain environment. Position and Speed of particle are reorganized according to Moth and flame location in each iteration. The hybrid PSO-MFO method has a fast convergence rate due to the use of roulette wheel selection method. For the OPF solution, standard IEEE-30 bus test system is used. The hybrid PSO-MFO method is implemented to solve the proposed problem. The problems considered in the OPF are fuel cost reduction, Voltage profile improvement, Voltage stability enhancement, Active power loss minimization and Reactive power loss minimization. The results obtained with hybrid PSO-MFO method is compared with other techniques such as Particle Swarm Optimization (PSO) and Moth Flame Optimizer (MFO). Results show that hybrid PSO-MFO gives better optimization values as compared with PSO and MFO which verifies the effectiveness of the suggested algorithm.

*Keywords: optimal power flow; voltage stability; power system; hybrid PSO-MFO; constraints.*

## I. Introduction

At the present time, The Optimal power flow (OPF) is a very significant problem and most focused objective for power system planning and operation [1]. The OPF is the elementary tool which permits the utilities to identify the economic operational and secure states in the system [2]. The OPF problem is one of the utmost operating desires of the electrical power system [3]. The prior function of OPF problem is to evaluate the optimum operational state for Bus system by minimizing each objective function within the limits of the operational constraints like equality constraints and inequality constraints [4]. Hence, the optimal power flow problem can be defined as an extremely non-linear and non-convex multimodal optimization problem [5].

From the past few years too many optimization techniques were used for the solution of the Optimal Power Flow (OPF) problem. Some traditional methods used to solve the proposed problem have some limitations like converging at local optima and so they are not suitable for binary or integer problems or to deal with the lack of convexity, differentiability, and continuity [6]. Hence, these techniques are not suitable for the actual OPF situation. All these limitations are overcome by metaheuristic optimization methods. Some of these methods are [7-10]: genetic algorithm (GA) [11], hybrid genetic algorithm (HGA) [12], enhanced genetic algorithm (EGA) [13-14], differential evolution algorithm (DEA) [15-16], artificial neural network (ANN) [17], particle swarm optimization algorithm (PSO) [18], tabu search algorithm (TSA) [19], gravitational search algorithm (GSA) [20], biogeography based optimization (BBO) [21], harmony search algorithm (HSA) [22], krill herd algorithm (KHA) [23], cuckoo search algorithm (CSA) [24], ant colony algorithm (ACO) [25], bat optimization algorithm (BOA) [26], Ant-lion optimizer (ALO) [27-28] and Multi-Verse optimizer (MVO) [29].

In the present work, a newly introduced hybrid meta-heuristic optimization technique named Hybrid Particle Swarm Optimization-Moth Flame Optimizer (HPSO-MFO) is applied to solve the Optimal Power Flow problem. HPSO-MFO comprises of best characteristic of both Particle Swarm Optimization [30] and Moth-Flame Optimizer [31-32] algorithm. The capabilities of HPSO-MFO are finding the global solution, fast convergence rate due to the use of roulette wheel selection, can handle continuous and discrete optimization problems.

According to No Free Lunch Theorem [27,29,30], particular meta-heuristic algorithm is not best for every problem. So, we considered HPSO-MFO for continues optimal power flow problem based on No Free Lunch Theorem. In this work, the HPSO-MFO is presented to standard IEEE-30 bus test system [33] to solve the OPF [34-37] problem. There are five objective cases considered in this paper that have to be optimize using HPSO-MFO technique are Fuel Cost Reduction, Voltage Stability Improvement, Voltage Deviation Minimization, Active Power Loss Minimization and Reactive Power Loss Minimization. The results show the optimal adjustments of control variables in accordance with their limits. The results obtained using HPSO-MFO technique has been compared with Particle Swarm Optimisation (PSO) and Moth Flame Optimizer (MFO) techniques. The results show that HPSO-MFO gives better optimization values as compared to other

*Author α σ: L.E. College, Morbi (Gujarat) India.*
*e-mails: pkjmtech@gmail.com, saparmar92@gmail.com*
*Author ρ: G.E. College, Gandhinagar (Gujarat) India.*
*e-mail: forumtrivedi@gmail.com*
*Author ω: Sri Ganganagar College of Ayurvedic Science & Hospital, Sri Ganganagar (Rajasthan) India. e-mail: apyjangid@gmail.com*

methods which prove the effectiveness of the proposed algorithm.

This paper is summarized as follow: After the first section of the introduction, the second section concentrates on concepts and key steps of standard PSO and MFO techniques and the proposed Hybrid PSO-MFO technique. The third section presents the formulation of Optimal Power Flow problem. Next, we apply HPSO-MFO to solve OPF problem on IEEE-30 bus system in order to optimize the operating conditions of the power system. Finally, the results and conclusion are drawn in the last section.

## II. Standard PSO and Standard MFO

*a) Particle Swarm Optimization*

The particle swarm optimization algorithm (PSO) was discovered by James Kennedy and Russell C. Eberhart in 1995 [30]. This algorithm is inspired by the simulation of social psychological expression of birds and fishes. PSO includes two terms $P_{best}$ and $G_{best}$. Position and velocity are updated over the course of iteration from these mathematical equations:

$$v_{ij}^{t+1} = wv_{ij}^{t} + c_1R_1(Pbest^t - X^t) + c_2R_2(Gbest^t - X^t) \quad (1)$$

$$X^{t+1} = X^t + v^{t+1} \left(\mathrm{i} = 1,\ 2...\mathrm{NP}\right) \text{ And } \left(\mathrm{j} = 1,\ 2...\mathrm{NG}\right) \quad (2)$$

Where

$$w = w^{\max} - \frac{(w^{\max} - w^{\min}) * iteration}{\max iteration}, \quad (3)$$

$w^{max}$=0.4 and $w^{min}$ =0.9.

$v_{ij}^{t}$, $v_{ij}^{t+1}$ is the velocity of a$j^{th}$ member of an$i^{th}$ particle at iteration number ($t$) and ($t+1$). (Usually $C_1$=$C_2$=2), $r_1$ and $r_2$ Random number (0, 1).

*b) Moth-Flame Optimizer*

A novel nature–inspired Moth-Flame optimization algorithm [31] based on the transverse orientation of Moths in space. Transverse orientation for navigation uses a constant angle by Moths with respect to Moon to fly in straight direction in night. In MFO algorithm that Moths fly around flames in a Logarithmic spiral way and finally converges towards the flame. Spiral way expresses the exploration area and it guarantees to exploit the optimum solution [31]:

Moth-Flame optimizer is first introduced by Seyedali Mirjalili in 2015 [31]. MFO is a population - based algorithm; we represent the set of moths in a matrix:

$$M = \begin{bmatrix} m_{1,1}, & m_{1,2} & ,\dots, m_{1,d} \\ m_{2,1,} & m_{2,2} & ,\dots, m_{2,d} \\ \vdots & & \vdots \\ \vdots & & \vdots \\ m_{n,1} & m_{n,2} & ,\dots, m_{n,d} \end{bmatrix} \quad (4)$$

Where $n$ represents a number of moths and d represents a number of variables (dimension).

For all the moths, we also assume that there is an array for storing the corresponding fitness values as follows:

$$OM = \begin{bmatrix} OM_1 \\ OM_2 \\ . \\ . \\ OM_n \end{bmatrix} \quad (5)$$

Where $n$ is the number of moths.

Note that the fitness value is the return value of the fitness (objective) function for each moth. The position vector (first row in the matrix $M$ for instance) of each moth is passed to the fitness function and the output of the fitness function is assigned to the corresponding moth as its fitness function ($OM_1$in the matrix $OM$ for instance).

Other key components in the proposed algorithm are flames. We consider a matrix similar to the moth matrix [31]:

$$F = \begin{bmatrix} FL_{1,1} & FL_{1,2} & . & . & FL_{1,d} \\ FL_{2,1} & FL_{2,2} & . & . & FL_{2,d} \\ . & . & . & . & . \\ . & . & . & . & . \\ FL_{n,1} & FL_{n,2} & . & . & FL_{n,d} \end{bmatrix} \quad (6)$$

Where $n$ shows a number of moths and $d$ represents a number of variables (dimension).

We know that the dimension of M and F arrays are equal. For the flames, we also assume that there is an array for storing the corresponding fitness values [31]:

$$OF = \begin{bmatrix} OFL_1 \\ OFL_2 \\ . \\ . \\ OFL_n \end{bmatrix} \quad (7)$$

Where $n$ is the number of moths.

Here, it must be noted that moths and flames both are solutions. The variance among them is the manner we treat and update them, in the iteration. The moths are genuine search agents that move all over the search space while flames are the finest location of moths that achieves so far. Therefore, every moth searches around a flame and updates it in the case of discovering an enhanced solution. With this mechanism, a moth never loses its best solution.

The MFO algorithm is three rows that approximate the global solution of the problems defined like as follows [31]:

$$\mathrm{MFO} = (\mathrm{I},\ \mathrm{P},\ \mathrm{T}) \quad (8)$$

*I* is the function that yields an uncertain population of moths and corresponding fitness values. The methodical model of this function is as follows:

$$I : \phi \rightarrow \{M, OM\} \quad (9)$$

The *P* function, which is the main function, expresses the moths all over the search space. This function receives the matrix of *M* and takes back its updated one at every time with each iteration.

$$P : M \rightarrow M \quad (10)$$

The *T* returns true and false according to the termination Criterion satisfaction:

$$T : M \rightarrow \{true,\ false\} \quad (11)$$

In order to mathematical model this behavior, we change the location of each Moth regarding a flame with the following equation:

$$M_i = S(M_i, F_j) \quad (12)$$

Where $M_i$ indicate the $i^{th}$ moth, $F_j$ indicates the $j^{th}$ flame and *S* is the spiral function.

In this equation flame $FL_{n,d}$*(search agent * dimension)* of equation (6) modifies the moth matrix of equation (12).

Considering these points, we define a log (logarithmic scale) spiral for the MFO algorithm as follows [31]:

$$S(M_i, F_j) = D_i * e^{bt}\cos(2\pi t) + F_j \quad (13)$$

Where: $D_i$ expresses the distance of the moth for the $j^{th}$ flame, *b* is a constant for expressing the shape of the log (logarithmic) spiral, and *t* is a random value in [-1, 1].

$$D_i = |F_j - M_i| \quad (14)$$

Where: $M_i$ represent the $i^{th}$ moth, $F_j$ represents the $j^{th}$ flame, and where $D_i$ expresses the path length of the $i^{th}$moth for the $j^{th}$ flame.

The no. of flames are adaptively reduced with the iterations. We use the following formulation:

$$flame\,no = round\left(N - l * \frac{N-1}{T}\right) \quad (15)$$

Where *l* is the present number of iteration, *N* is the maximum number of flames, and *T*shows the maximum number of iterations.

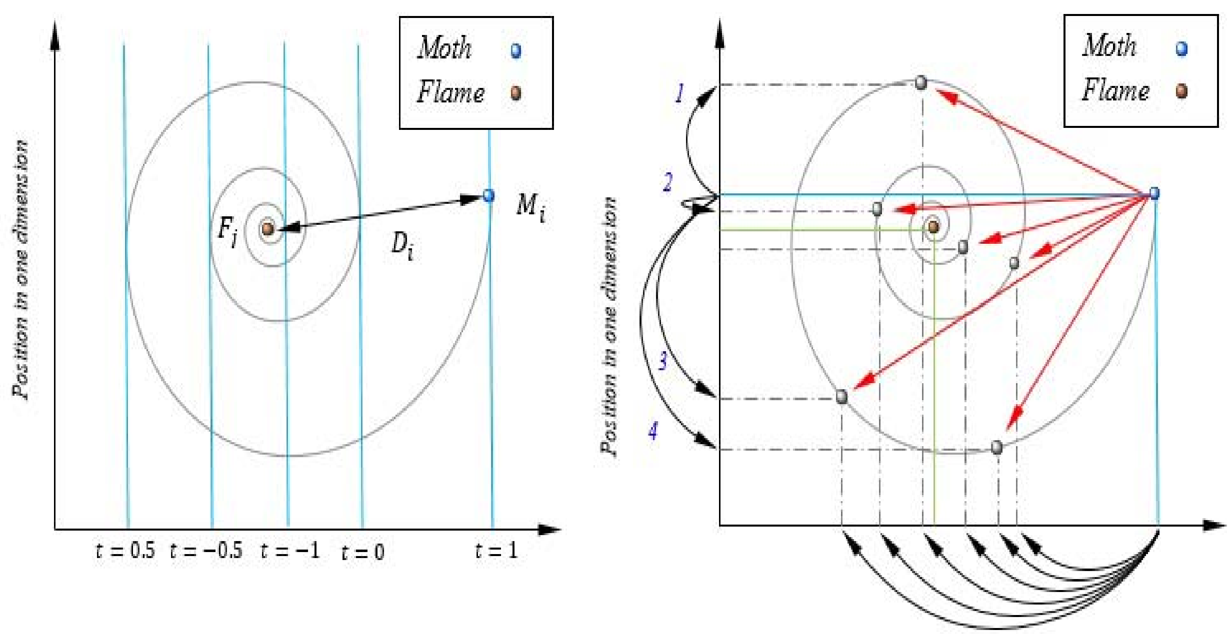


*Fig. 1:* A conceptual model of position updating of a moth around a flame

We utilize Quick sort algorithm, the sorting is in the $o(n\log n)$ best and $o(n^2)$ worst condition, respectively. Considering the *P* function, so, total computational complexity is defined as follows:

$$\mathrm{O}\,(\mathrm{MFO}) = \mathrm{O}\,(\mathrm{t}\,(\mathrm{O}\,(\text{Quick sort}) + \mathrm{O}\,(\text{position update}))) \quad O(MFO) = O(t(n^2 + n*d)) = O(tn^2 + tnd) \tag{16}$$

Where $n$ shows a number of moths, $t$ represents maximum no. of iterations, and $d$ represents no. of variables.

*c) The Hybrid PSO-MFO Algorithm*

The drawback of PSO is the limitation to cover small search space while solving higher order or complex design problem due to constant inertia weight. This problem can be tackled with Hybrid PSO-MFO as it extracts the quality characteristics of both PSO and MFO. Moth-Flame Optimizer is used for exploration phase as it uses logarithmic spiral function so it covers a broader area in uncertain search space. Because both of the algorithms are randomization techniques so we use term uncertain search space during the computation over the course of iteration from starting to maximum iteration limit. Exploration phase means the capability of an algorithm to try out a large number of possible solutions. The position of particle that is responsible for finding the optimum solution to the complex non-linear problem is replaced with the position of Moths that is equivalent to the position of the particle but highly efficient to move solution towards optimal one. MFO directs the particles faster towards optimal value, reduces computational time. As we know that that PSO is a well-known algorithm that exploits the best possible solution for its unknown search space. So the combination of best characteristic (exploration with MFO and exploitation with PSO) guarantees to obtain the best possible optimal solution of the problem that also avoids local stagnation or local optima of the problem.

A set of Hybrid PSO-MFO is the combination of separate PSO and MFO. Hybrid PSO-MFO merges the best strength of both PSO in exploitation and MFO in exploration phase towards the targeted optimum solution.

$$v_{ij}^{t+1} = wv_{ij}^{t} + c_1 R_1 (Moth\_Pos^t - X^t) + c_2 R_2 (Gbest^t - X^t) \tag{17}$$

## III. Optimal Power Flow Problem Formulation

As specified before, OPF is the optimized problem of power flow that provides the optimum values of independent variables by optimizing a predefined objective function with respect to the operating bounds of the system [1]. The OPF problem can be mathematically expressed as a non-linear constrained optimization problem as follows [1]:

$$\text{Minimize} \quad f(a,b) \tag{18}$$

$$\text{Subject to} \quad s(a,b)=0 \tag{19}$$

$$\text{And} \quad h(a,b)\leq 0 \tag{20}$$

Where, $a$=vector of state variables, $b$=vector of control variables, $f(a,b)$=objective function, $s(a,b)$=*different* equality constraints set, $h(a,b)$=different inequality constraints set.
The evaluation function for the OPF problem is given as follows:

Evaluation Function = Search Agents * Maximum Iterations = 40*500= 20000

*a) Variables*

i. *Control variables*

The control variables should be adjusted to fulfill the power flow equations. For the OPF problem, the set for control variables can be formulated as [1], [4]:

$$b^T = [P_{G_2} \ldots P_{G_{NGen}}, V_{G_1} \ldots V_{G_{NGen}}, Q_{C_1} \ldots Q_{C_{NCom}}, T_1 \ldots T_{NTr}] \tag{21}$$

Where,

$P_G$ = Real power output at the *PV(Generator)* buses excluding at the slack (Reference) bus.

$V_G$ = Magnitude of Voltage at *PV* (*Generator*) buses.

$Q_C$ = shunt *VAR* compensation.

$T$ = tap settings of the transformer.

*NGen, NTr, NCom*= No. of generator units, No. of tap changing transformers and No. of shunt *VAR* compensation devices, respectively.

The control variables are the decision variables of the power system which could be adjusted as per the requirement.

ii. *State variables*

There is a need of variables for all OPF formulations for the characterization of the Electrical Power Engineering state of the system. So, the state variables can be formulated as [1], [4]:

$$a^T = [P_{G_1}, V_{L_1} \ldots V_{L_{NLB}}, Q_{G_1} \ldots Q_{G_{NGen}}, S_{l_1} \ldots S_{l_{Nline}}] \tag{22}$$

Where,

$P_{G_1}$ = Real power generation at reference bus.

$V_L$ = Magnitude of Voltage at Loadbuses.

$Q_G$ = Reactive power generation of all generators.

$S_l$ = Transmission line loading.

*NLB*, Nline= No. of *PQ* buses and the No. of transmission lines, respectively.

*b) Constraints*

There are two OPF constraints named inequality and equality constraints. These constraints are explained in the sections given below.

i. *Equality constraints*

The physical condition of the power system is described by the equality constraints of the system. These equality constraints are basically the power flow equations which can be explained as follows [1], [4].

a. *Real power constraints*

The real power constraints can be formulated as follows:

$$P_{Gi} - P_{Di} - V_i \sum_{J=i}^{NB} V_j [G_{ij} Cos(\delta_{ij}) + B_{ij} Sin(\delta_{ij})] = 0 \quad (23)$$

b. *Reactive power constraints*

The reactive power constraints can be formulated as follows:

$$Q_{Gi} - Q_{Di} - V_i \sum_{J=i}^{NB} V_j [G_{ij} Cos(\delta_{ij}) + B_{ij} Sin(\delta_{ij})] = 0 \quad (24)$$

Where, $\delta_{ij} = \delta_i - \delta_j$ is the phase angle of voltage between buses i and j.*NB*= total No. of buses, $P_G$ = real power output, $Q_G$ = reactive power output, $P_D$ = active power load demand, $Q_D$ = reactive power load demand, $B_{ij}$ and $G_{ij}$ = elements of the admittance matrix $Y_{ij} = (G_{ij} + jB_{ij})$ shows the susceptance and conductance between bus i and *j*, respectively, $Y_{ij}$ is the mutual admittance between buses I and j.

ii. *Inequality constraints*

The boundaries of power system devices together with the bounds created to surety system security are given by inequality constraints of the OPF [4], [5].

a. *Generator constraints*

For all generating units including the reference bus: voltage magnitude, real power and reactive power outputs should be constrained within its minimum and maximum bounds as given below [27]:

$$V_{G_i}^{lower} \le V_{G_i} \le V_{G_i}^{upper}, \; i=1,\dots, NGen \quad (25)$$

$$P_{G_i}^{lower} \le P_{G_i} \le P_{G_i}^{upper}, \; i=1,\dots, NGen \quad (26)$$

$$Q_{G_i}^{lower} \le Q_{G_i} \le Q_{G_i}^{upper}, \; i=1,\dots, NGen \quad (27)$$

b. *Transformer constraints*

Tap settings of transformer should be constrained inside their stated minimum and maximum bounds as follows [27]:

$$T_{G_i}^{lower} \le T_{G_i} \le T_{G_i}^{upper}, \; i=1,\dots,NGen \quad (28)$$

c. *Shunt VAR compensator constraints*

Shunt VAR compensation devices need to be constrained within its minimum and maximum bounds as given below [27]:

$$Q_{C_i}^{lower} \le Q_{GC_i} \le Q_{C_i}^{upper}, \; i=1,\dots,NGen \quad (29)$$

d. *Security constraints*

These comprise the limits of a magnitude of the voltage at *PQ* buses and loadings on the transmission line. Voltage for every *PQ* bus should be limited by their minimum and maximum operational bounds. Line flow over each line should not exceed its maximum loading limit. So, these limitations can be mathematically expressed as follows [27]:

$$V_{L_i}^{lower} \le V_{L_i} \le V_{L_i}^{upper}, \; i=1,\dots,NGen \quad (30)$$

$$S_{l_i} \le S_{l_i}^{upper}, \; i=1,\dots,Nline \quad (31)$$

The control variables are self-constraint. The inequality constrained of state variables comprises the magnitude of *PQ* bus voltage, active power production at reference bus, reactive power production and loadings on line may be encompassed into an objective function in terms of quadratic penalty terms. In which, the penalty factor is multiplied by the square of the indifference value of state variables and is included in the objective function and any impractical result achieved is declined [27].

Penalty function may be mathematically formulated as follows:

$$J_{aug} = J + \partial_P \left(P_{G_1} - P_{G_1}^{lim}\right)^2 + \partial_V \sum_{i=1}^{NLB} (V_{L_i} - V_{L_i}^{lim})^2 + \partial_Q \sum_{i=1}^{NGen} + \partial_S \sum_{i=0}^{Nline} (S_{l_i} - S_{l_i}^{max})^2 \quad (32)$$

Where, $\partial_P, \partial_V, \partial_Q, \partial_S$ = penalty factors

$U_{lim}$ = Boundary value of the state variable U.

If U is greater than the maximum limit, $U_{lim}$ takings the value of this one, if *U* is lesser than the minimum limit $U_{lim}$ takings the value of that limit. This can be shown as follows [27]:

$$U^{lim=}\begin{cases} U^{upper} & ;U > U^{upper} \\ U^{lower} & ;U < U^{lower} \end{cases} \qquad (33)$$

## IV. Application and Results

The PSO-MFO technique has been implemented for the OPF solution for standard IEEE 30-bus test system and for a number of cases with dissimilar objective functions. The used software program is written in MATLAB R2014b computing surroundings and used on a 2.60 GHz i5 PC with 4 GB RAM. In this work the HPSO-MFO population size is selected to be 40.

### *a) IEEE 30-bus test system*

With the purpose of elucidating the strength of the suggested HPSO-MFO technique, it has been verified on the standard IEEE 30-bus test system as displays in fig. 2. The standard IEEE 30-bus test system selected in this work has the following features[6], [33]: NGen = No. of generators = 6 at buses *1,2,5,8,11* and *13*, NTr = No. of regulating transformers having off-nominal tap ratio = 4 between buses 4-12, 6-9, 6-10 and 28-27, NCom = No. of shunt VAR Compensators = 9 at buses 10,12,15,17,20,21,23,24 and 29 and NLB = No. of load buses = 24.

In addition, generator cost coefficient data, the line data, bus data, and the upper and lower bounds for the control variables are specified in [33].

In given test system, five diverse cases have been considered for various purposes and all the acquired outcomes are given in Tables 3, 5, 7, 9, 11. The very first column of this tables denotes the optimal values of control variables found where:

- $P_{G1}$ through $P_{G6}$ and $V_{G1}$ through $V_{G6}$ signifies the power and voltages of generator 1 to generator 6.
- $T_{4-12}$, $T_{6-9}$, $T_{6-10}$ and $T_{28-27}$ are the transformer tap settings comprised between buses 4-12, 6-9, 6-10 and 28-27.
- $Q_{C10}$, $Q_{C12}$, $Q_{C15}$, $Q_{C17}$, $Q_{C20}$, $Q_{C21}$, $Q_{C23}$, $Q_{C24}$ and $Q_{C29}$ denote the shunt VAR compensators coupled at buses 10, 12, 15, 17, 20, 21, 23, 24 and 29.

Further, fuel cost *($/hr)*, real power losses *(MW)*, reactive power losses *(MVAR)*, voltage deviation and *Lmax* represent the total generation fuel cost of the system, the total real power losses, the total reactive power losses, the load voltages deviation from 1 and the stability index, respectively. Other particulars for these outcomes will be specified in the next sections.

The control parameters for HPSO-MFO, MFO, PSO used in this problem are given in table 1.

In table 1, no. of variables (dim) shows the six no. of generators used in the 30 bus system. It gives the optimization values for different cases as they depends on the decision variables. In all 5 cases, results are the average value obtained after 10 number of runs.

*Table 1:* Control parameters used in PSO-MFO, MFO and PSO

| Sr. No. | Parameters | Value |
|---|---|---|
| 1 | Population (No. of Search agents) (N) | 40 |
| 2 | Maximum iterations count (t) | 500 |
| 3 | No. of Variables (dim) | 25 |
| 4 | Random Number | [0,1] |
| 5 | source acceleration coefficient ($c\_1$, $c\_2$) | 2 |
| 6 | weighting function (w) | 0.65 |

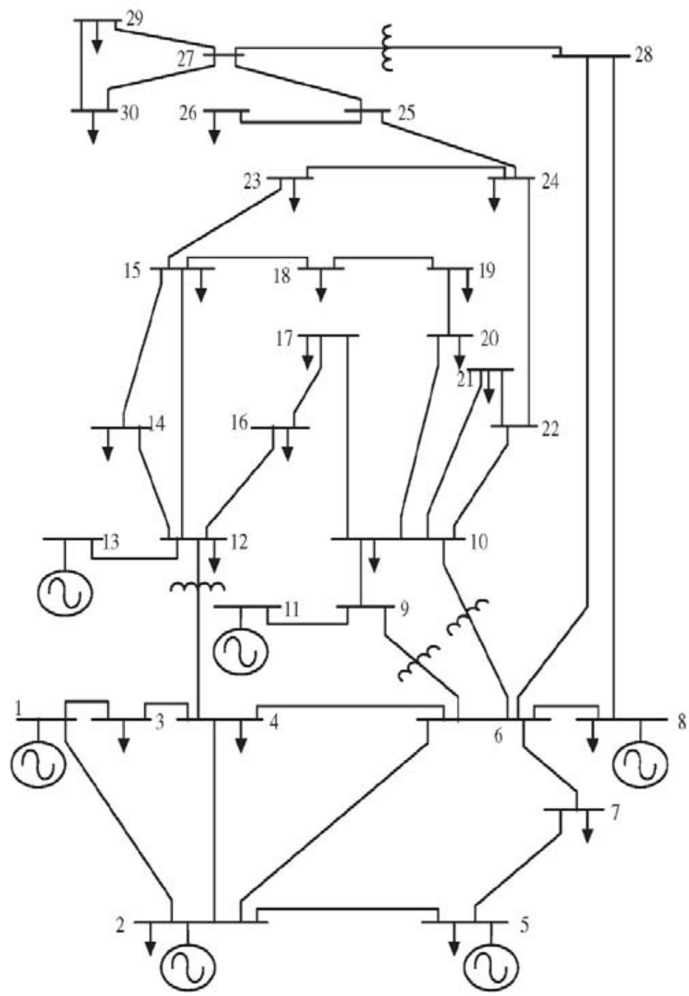


*Fig. 2:* Single line diagram of IEEE 30-bus test system

*Case 1: Minimization of generation fuel cost.*

The very common OPF objective that is generation fuel cost reduction is considered in the case 1. Therefore, the objective function Y indicates the complete fuel cost of total generating units and it is calculated by following equation [1]:

$$Y = \sum_{i=1}^{NGen} f_i(\$/hr) \tag{34}$$

Where, $f_i$ is the total fuel cost of $i^{th}$ generator.

$f_i$, may be formulated as follow:

$$f_i = u_i + v_i P_{Gi} + w_i P_{Gi}^2 (\$/hr) \tag{35}$$

Where, $u_i$, $v_i$ and $w_i$ are the simple, the linear and the quadratic cost coefficients of the $i^{th}$ generator, respectively. The cost coefficients values are specified in [33].

The variation of the total fuel cost with different algorithms over iterations is presented in fig. 2. It demonstrates that the suggested method has outstanding convergence characteristics. The comparison of fuel cost obtained with different methods is shown in table 2 which displays that the results obtained by PSO-MFO are better than the other methods. The optimal values of control variables obtained by different algorithms for case 1 are specified in Table 3. By means of the same settings i.e. control variables boundaries, initial conditions and system data, the results achieved in case 1 with the PSO-MFO technique are compared to some other methods and it display that the total fuel cost is greatly reduced compared to the initial case [6]. Quantitatively, it is reduced from 901.951*$/hr* to 799.056*$/hr*.

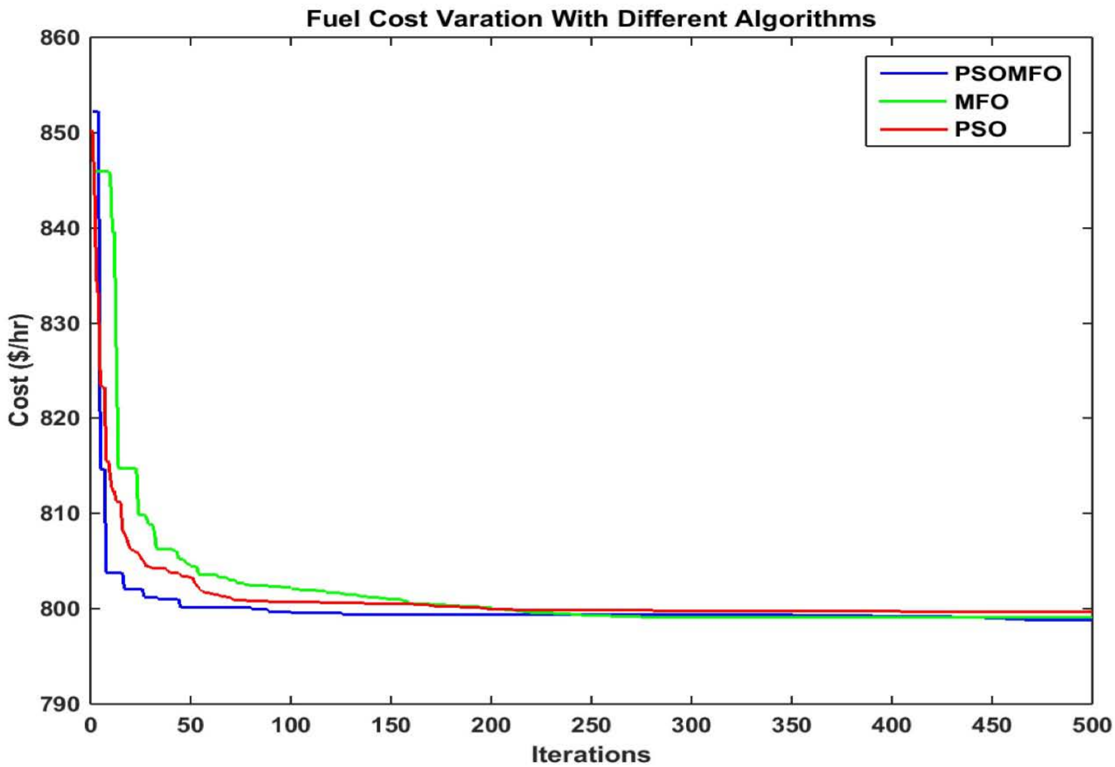


*Fig. 3:* Fuel cost variations with different algorithms

*Table 2:* Comparison of fuel cost obtained with different algorithms

| Method | Fuel Cost ($/hr) | Method Description |
|---|---|---|
| HPSO-MFO | 799.056 | Hybrid Particle Swarm Optimization-Moth Flame Optimizer |
| MFO | 799.072 | Moth Flame Optimizer |
| PSO | 799.704 | Particle Swarm Optimization |
| DE | 799.289 | Differential Evolution [15] |
| BHBO | 799.921 | Black Hole-Based Optimization [6] |

*Table 3:* Optimal values of control variables for case 1 with different algorithms

| Control Variable | Min | Max | Initial | HPSO-MFO | MFO | PSO |
|---|---|---|---|---|---|---|
| $P_{G1}$ | 50 | 200 | 99.2230 | 178.133 | 177.055 | 177.105 |
| $P_{G2}$ | 20 | 80 | 80 | 48.956 | 48.698 | 48.748 |
| $P_{G5}$ | 15 | 50 | 50 | 21.385 | 21.304 | 21.318 |
| $P_{G8}$ | 10 | 35 | 20 | 21.706 | 21.084 | 20.986 |
| $P_{G11}$ | 10 | 30 | 20 | 10.000 | 11.883 | 12.049 |
| $P_{G13}$ | 12 | 40 | 20 | 12.000 | 12.000 | 12.000 |
| $V_{G1}$ | 0.95 | 1.1 | 1.05 | 1.100 | 1.100 | 1.100 |
| $V_{G2}$ | 0.95 | 1.1 | 1.04 | 1.088 | 1.088 | 1.088 |
| $V_{G5}$ | 0.95 | 1.1 | 1.01 | 1.062 | 1.062 | 1.061 |
| $V_{G8}$ | 0.95 | 1.1 | 1.01 | 1.070 | 1.069 | 1.070 |
| $V_{G11}$ | 0.95 | 1.1 | 1.05 | 1.100 | 1.100 | 1.100 |
| $V_{G13}$ | 0.95 | 1.1 | 1.05 | 1.100 | 1.100 | 1.100 |
| $T_{4-12}$ | 0 | 1.1 | 1.078 | 0.939 | 1.044 | 0.976 |
| $T_{6-9}$ | 0 | 1.1 | 1.069 | 1.100 | 0.900 | 0.975 |

| | | | | | | |
|---|---|---|---|---|---|---|
| $T_{6-10}$ | 0 | 1.1 | 1.032 | 1.021 | 0.985 | 1.015 |
| $T_{28-27}$ | 0 | 1.1 | 1.068 | 0.978 | 0.965 | 0.966 |
| $QC_{10}$ | 0 | 5 | 0 | 5.000 | 5.000 | 2.353 |
| $QC_{12}$ | 0 | 5 | 0 | 5.000 | 5.000 | 5.000 |
| $QC_{15}$ | 0 | 5 | 0 | 5.000 | 5.000 | 0.000 |
| $QC_{17}$ | 0 | 5 | 0 | 5.000 | 5.000 | 0.689 |
| $QC_{20}$ | 0 | 5 | 0 | 5.000 | 5.000 | 0.003 |
| $QC_{21}$ | 0 | 5 | 0 | 5.000 | 5.000 | 5.000 |
| $QC_{23}$ | 0 | 5 | 0 | 5.000 | 4.999 | 0.000 |
| $QC_{24}$ | 0 | 5 | 0 | 0.000 | 5.000 | 0.000 |
| $QC_{29}$ | 0 | 5 | 0 | 3.033 | 2.725 | 0.000 |
| Fuel Cost($/hr) | - | - | 901.951 | 799.056 | 799.072 | 799.704 |

*Case 2: Voltage profile improvement*

Bus voltage is considered as most essential and important security and service excellence indices [6]. Here the goal is to reduce the fuel cost and increase voltage profile simultaneously by reducing the voltage deviation of *PQ (load)* buses from the unity 1.0 *p.u*.

Hence, the objective function may be formulated by following equation [4]:

$$Y = Y_{\cos t} + wY_{voltage-deviation} \quad (36)$$

Where, *w* is an appropriate weighting factor, to be chosen by the user to offer a weight or importance to each one of the two terms of the objective function. $Y_{\cos t}$ and $Y_{voltage-deviation}$ are specified as follows [4]:

$$Y_{\cos t} = \sum_{i=1}^{NGen} f_i \quad (37)$$

$$Y_{voltage\_deviation} = \sum_{i=1}^{NGen} |V_i - 1.0| \quad (38)$$

The variation of voltage deviation with different algorithms over iterations is sketched in fig. 3. It demonstrates that the suggested method has good convergence characteristics. The statistical values of voltage deviation obtained with different methods are shown in table 4 which display that the results obtained by PSO-MFO are better than the other methods excluding GSA method. The optimal values of control variables obtained by different algorithms for case 2 are specified in Table 5. By means of the same settings the results achieved in case 2 with the PSO-MFO technique are compared to some other methods and it display that the voltage deviation is greatly reduced compared to the initial case [6]. It has been made known that the voltage deviation is reduced from 1.1496 *p.u*. to 0.1056*p.u*. using PSO-MFO technique.GSA [2] gives better result than the HPSO-MFO method only in case of voltage deviation among five cases. Due to No Free Lunch (NFL) theorem proves that no one can propose an algorithm for solving all optimization problems. This means that the success of an algorithm in solving a specific set of problems does not guarantee solving all optimization problems with different type and nature. NFL makes this field of study highly active which results in enhancing current approaches and proposing new meta-heuristics every year. This also motivates our attempts to develop a new Hybrid meta-heuristic for solving OPF Problem.

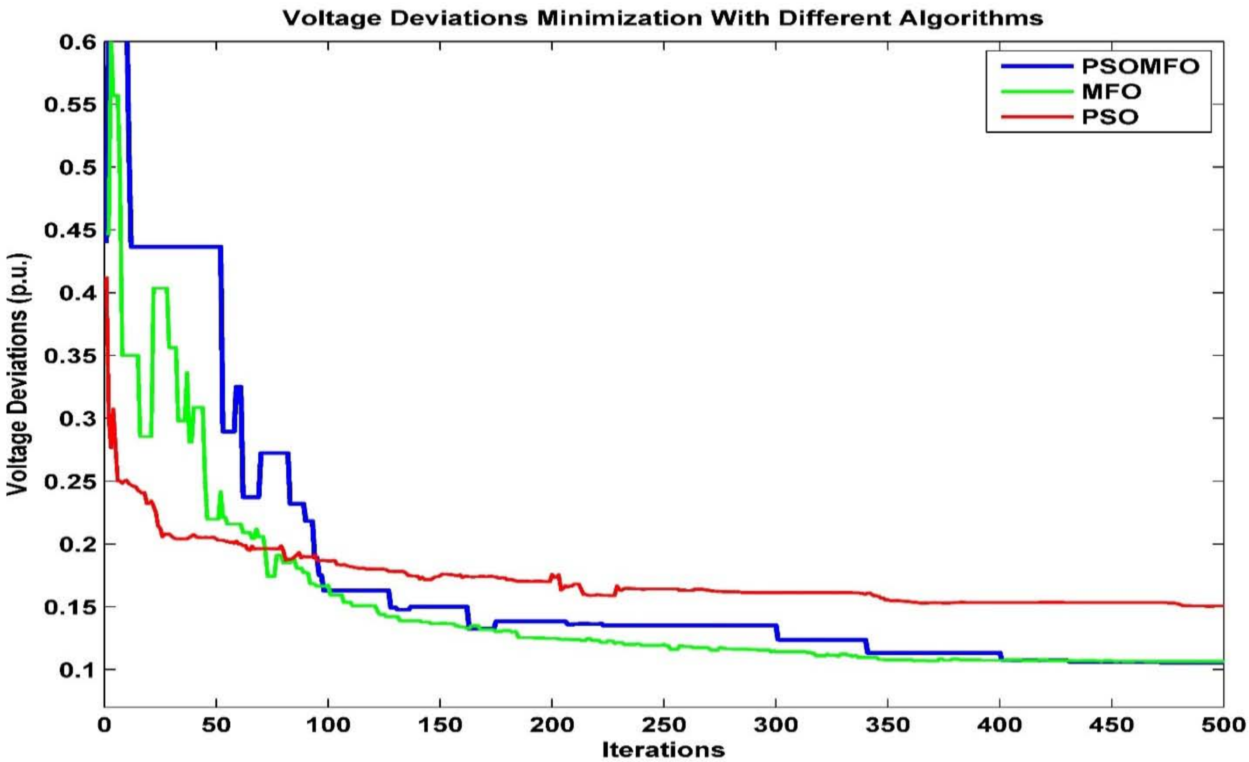


*Fig. 4:* Voltage deviation minimization with different algorithms

*Table 4:* Comparison of voltage deviations obtained with different algorithms

| Method | Voltage Deviation (p.u) | Method Description |
|---|---|---|
| HPSO-MFO | 0.1056 | Hybrid Particle Swarm Optimization-Moth Flame Optimizer |
| MFO | 0.1065 | Moth Flame Optimizer |
| PSO | 0.1506 | Particle Swarm Optimization |
| GSA | 0.0932 | Gravitational Search Algorithm [2] |
| DE | 0.1357 | Differential Evolution [15] |
| BHBO | 0.1262 | Black Hole- Based Optimization [6] |

*Table 5:* Optimal values of control variables for case 2 with different algorithms

| Control Variable | Min | Max | Initial | HPSO-MFO | MFO | PSO |
|---|---|---|---|---|---|---|
| $P_{G1}$ | 50 | 200 | 99.2230 | 177.650 | 180.212 | 175.922 |
| $P_{G2}$ | 20 | 80 | 80 | 49.092 | 49.584 | 46.389 |
| $P_{G5}$ | 15 | 50 | 50 | 15.000 | 15.000 | 21.597 |
| $P_{G8}$ | 10 | 35 | 20 | 10.000 | 24.349 | 19.396 |
| $P_{G11}$ | 10 | 30 | 20 | 30.000 | 12.657 | 17.656 |
| $P_{G13}$ | 12 | 40 | 20 | 12.000 | 12.000 | 12.000 |
| $V_{G1}$ | 0.95 | 1.1 | 1.05 | 1.033 | 1.033 | 1.047 |
| $V_{G2}$ | 0.95 | 1.1 | 1.04 | 1.017 | 1.017 | 1.034 |
| $V_{G5}$ | 0.95 | 1.1 | 1.01 | 1.015 | 1.005 | 0.999 |
| $V_{G8}$ | 0.95 | 1.1 | 1.01 | 0.997 | 0.999 | 1.005 |
| $V_{G11}$ | 0.95 | 1.1 | 1.05 | 1.047 | 1.071 | 0.999 |
| $V_{G13}$ | 0.95 | 1.1 | 1.05 | 1.016 | 1.052 | 1.018 |
| $T_{4\text{-}12}$ | 0 | 1.1 | 1.078 | 1.065 | 1.100 | 0.954 |
| $T_{6\text{-}9}$ | 0 | 1.1 | 1.069 | 0.914 | 0.900 | 0.969 |
| $T_{6\text{-}10}$ | 0 | 1.1 | 1.032 | 0.973 | 1.072 | 0.989 |

| | | | | | | |
|---|---|---|---|---|---|---|
| $T_{28\text{-}27}$ | 0 | 1.1 | 1.068 | 0.960 | 0.960 | 0.960 |
| $QC_{10}$ | 0 | 5 | 0 | 4.080 | 5.000 | 3.948 |
| $QC_{12}$ | 0 | 5 | 0 | 0.165 | 0.000 | 1.765 |
| $QC_{15}$ | 0 | 5 | 0 | 5.000 | 5.000 | 4.844 |
| $QC_{17}$ | 0 | 5 | 0 | 5.000 | 0.000 | 3.075 |
| $QC_{20}$ | 0 | 5 | 0 | 5.000 | 5.000 | 4.687 |
| $QC_{21}$ | 0 | 5 | 0 | 5.000 | 5.000 | 4.948 |
| $QC_{23}$ | 0 | 5 | 0 | 0.000 | 5.000 | 1.623 |
| $QC_{24}$ | 0 | 5 | 0 | 5.000 | 5.000 | 3.559 |
| $QC_{29}$ | 0 | 5 | 0 | 2.248 | 1.315 | 2.034 |
| Vd | - | - | 1.1496 | 0.1056 | 0.1065 | 0.1506 |

*Case 3: Voltage stability enhancement*

Presently, the transmission systems are enforced to work nearby their safety bounds, because of cost-effective and environmental causes. One of the significant characteristics of the system is its capability to retain continuously tolerable bus voltages to each node beneath standard operational environments, next to the rise in load, as soon as the system is being affected by disturbance. The unoptimized control variables may cause increasing and unmanageable voltage drop causing a tremendous voltage collapse [6]. Hence, voltage stability is inviting ever more attention. By using various techniques to evaluate the margin of voltage stability, Glavitch and Kessel have introduced a voltage stability index called L-index depends on the viability of load flow equations for every node [34]. The L-index of a bus shows the probability of voltage collapse circumstance for that particular bus. It differs between 0 and 1 equivalent to zero load and voltage collapse, respectively.

For the given system with *NB, N Gen* and *NLB* buses signifying the total no. of buses, the total no. of generator buses and the total no. of load buses, respectively. The buses can be distinct as *PV (generator)* buses at the head and *PQ (load)* buses at the tail as follows [4]:

$$\begin{bmatrix} I_L \\ I_G \end{bmatrix} = [Y_{bus}] \begin{bmatrix} V_L \\ V_G \end{bmatrix} = \begin{bmatrix} Y_{LL} & Y_{LG} \\ Y_{GL} & Y_{GG} \end{bmatrix} \begin{bmatrix} V_L \\ V_G \end{bmatrix} \tag{39}$$

Where, $Y_{LL}$, $Y_{LG}$, $Y_{GL}$ and $Y_{GG}$ are co-matrix of $Y_{bus}$. The subsequent hybrid system of equations can be expressed as:

$$\begin{bmatrix} V_L \\ I_G \end{bmatrix} = [H] \begin{bmatrix} I_L \\ V_G \end{bmatrix} = \begin{bmatrix} H_{LL} & H_{LG} \\ H_{GL} & H_{GG} \end{bmatrix} \begin{bmatrix} I_L \\ V_G \end{bmatrix} \tag{40}$$

Where matrix *H* is produced by the partially inverting of $Y_{bus}$, $H_{LL}$, $H_{LG}$, $H_{GL}$ and $H_{GG}$ are the co-matrix of *H*, $V_G$, $I_G$, $V_L$ and $I_L$ are voltage and current vector of Generator buses and load buses, respectively.

The matrix *H* is given by:

$$[H] = \begin{bmatrix} Z_{LL} & -Z_{LL}Y_{LG} \\ Y_{GL}Z_{LL} & Y_{GG} - Y_{GL}Z_{LL}Y_{LG} \end{bmatrix} Z_{LL} = Y_{LL}^{-1} \tag{41}$$

Hence, the L-index denoted by $L_j$ of bus j is represented as follows:

$$L_j = \left| 1 - \sum_{i=1}^{NGen} H_{LG_{ji}} \frac{v_i}{v_j} \right| \quad j=1,2\ldots,NL \tag{42}$$

Hence, the stability of the whole system is described by a global indicator $L_{\max}$ which is given by [6],

$$L_{\max} = \max(L_j) \qquad j=1,2\ldots,NL \tag{43}$$

The system is more stable as the value of $L_{\max}$ is lower.

The voltage stability can be enhanced by reducing the value of voltage stability indicator *L-index* at every bus of the system. [6].

Thus, the objective function may be given as follows:

$$Y = Y_{\text{cost}} + wY_{voltage\_Stability\_Enhancement} \tag{44}$$

Where, $$Y_{\text{cost}} = \sum_{i=1}^{NGen} f_i \tag{45}$$

$$Y_{voltage\_stability\_enhancement} = L_{\max} \tag{46}$$

The variation of the *Lmax* index with different algorithms over iterations is presented in fig. 4. The statistical results obtained with different methods are shown in table 6 which display that PSO-MFO method gives better results than the other methods. The optimal values of control variables obtained by different algorithms for case 3 are given in Table 7. After applying the PSO-MFO technique, it appears from Table 7 that the value of *Lmax* is considerably decreased in this case compared to initial [6] from *0.1723* to *0.1126*. Thus, the distance from breakdown point is improved.

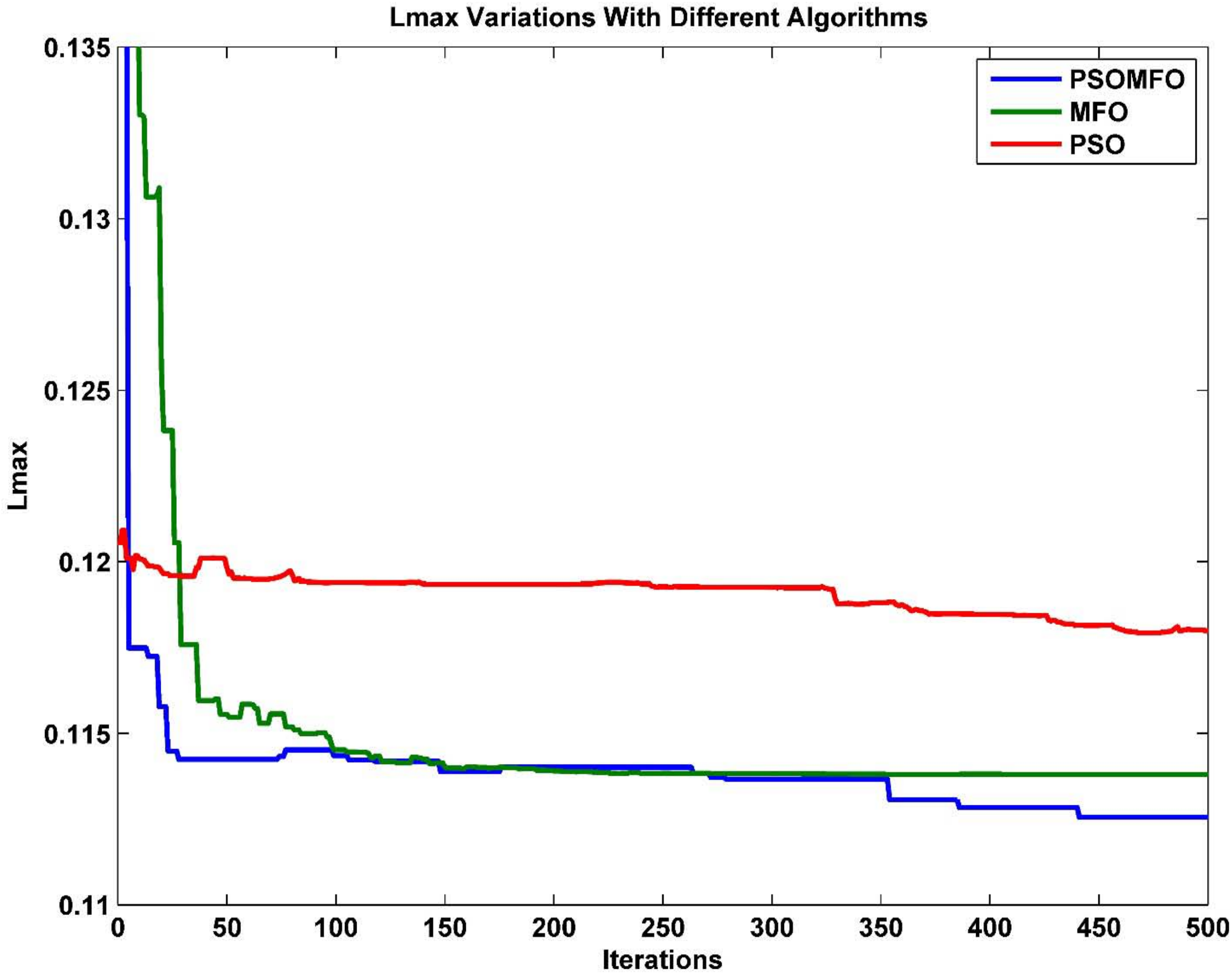


*Fig. 5:* *Lmax* variations with different algorithms

*Table 6:* Comparison of *Lmax* index obtained with different algorithms

| Method | $L_{max}$ | Method Description |
|---|---|---|
| HPSO-MFO | 0.1126 | Hybrid Particle Swarm Optimization-Moth Flame Optimizer |
| MFO | 0.1138 | Moth Flame Optimizer |
| PSO | 0.1180 | Particle Swarm Optimization |
| GSA | 0.1162 | Gravitational Search Algorithm [2] |
| DE | 0.1219 | Differential Evolution [15] |
| BHBO | 0.1167 | Black Hole- Based Optimization [6] |

*Table 7:* Optimal values of control variables for case 3 with different algorithms

| Control Variable | Min | Max | Initial | HPSO-MFO | MFO | PSO |
|---|---|---|---|---|---|---|
| $P_{G1}$ | 50 | 200 | 99.2230 | 182.308 | 177.299 | 158.331 |
| $P_{G2}$ | 20 | 80 | 80 | 45.360 | 48.792 | 49.050 |
| $P_{G5}$ | 15 | 50 | 50 | 21.109 | 21.316 | 18.956 |
| $P_{G8}$ | 10 | 35 | 20 | 21.557 | 20.351 | 31.224 |
| $P_{G11}$ | 10 | 30 | 20 | 10.000 | 12.370 | 15.906 |
| $P_{G13}$ | 12 | 40 | 20 | 12.000 | 12.012 | 17.801 |
| $V_{G1}$ | 0.95 | 1.1 | 1.05 | 1.100 | 1.100 | 1.098 |

| | | | | | | |
|---|---|---|---|---|---|---|
| $V_{G2}$ | 0.95 | 1.1 | 1.04 | 1.086 | 1.089 | 1.090 |
| $V_{G5}$ | 0.95 | 1.1 | 1.01 | 1.063 | 1.063 | 1.043 |
| $V_{G8}$ | 0.95 | 1.1 | 1.01 | 1.077 | 1.055 | 1.058 |
| $V_{G11}$ | 0.95 | 1.1 | 1.05 | 1.100 | 1.100 | 1.081 |
| $V_{G13}$ | 0.95 | 1.1 | 1.05 | 1.098 | 1.100 | 1.100 |
| $T_{4-12}$ | 0 | 1.1 | 1.078 | 1.034 | 0.996 | 0.900 |
| $T_{6-9}$ | 0 | 1.1 | 1.069 | 0.900 | 0.900 | 1.007 |
| $T_{6-10}$ | 0 | 1.1 | 1.032 | 0.973 | 0.964 | 1.071 |
| $T_{28-27}$ | 0 | 1.1 | 1.068 | 0.968 | 0.955 | 0.933 |
| $QC_{10}$ | 0 | 5 | 0 | 5.000 | 5.000 | 3.286 |
| $QC_{12}$ | 0 | 5 | 0 | 5.000 | 5.000 | 1.221 |
| $QC_{15}$ | 0 | 5 | 0 | 5.000 | 5.000 | 4.601 |
| $QC_{17}$ | 0 | 5 | 0 | 5.000 | 5.000 | 1.082 |
| $QC_{20}$ | 0 | 5 | 0 | 5.000 | 5.000 | 0.444 |
| $QC_{21}$ | 0 | 5 | 0 | 5.000 | 5.000 | 0.399 |
| $QC_{23}$ | 0 | 5 | 0 | 5.000 | 5.000 | 2.446 |
| $QC_{24}$ | 0 | 5 | 0 | 5.000 | 5.000 | 4.753 |
| $QC_{29}$ | 0 | 5 | 0 | 5.000 | 4.984 | 3.887 |
| $L_{max}$ | - | - | 0.1723 | **0.1126** | 0.1138 | 0.1180 |

*Case 4: Minimization of active power transmission losses*

In the case 4 the Optimal Power Flow objective is to reduce the active power transmission losses, which can be represented by power balance equation as follows [6]:

$$J = \sum_{i=1}^{NGen} P_i = \sum_{i=1}^{NGen} P_{Gi} - \sum_{i=1}^{NGen} P_{Di} \qquad (47)$$

Fig. 5 show the tendency for reducing the total real power losses objective function using the different techniques. The active power losses obtained with different techniques are shown in table 8 which made sense that the results obtained by PSO-MFO give better values than the other methods. The optimal values of control variables obtained by different algorithms for case 4 are displayed in Table 9. By means of the same settings the results achieved in case 4 with the PSO-MFO technique are compared to some other methods and it display that the real power transmission losses are greatly reduced compared to the initial case [6] from 5.821 MW to 2.831 MW.

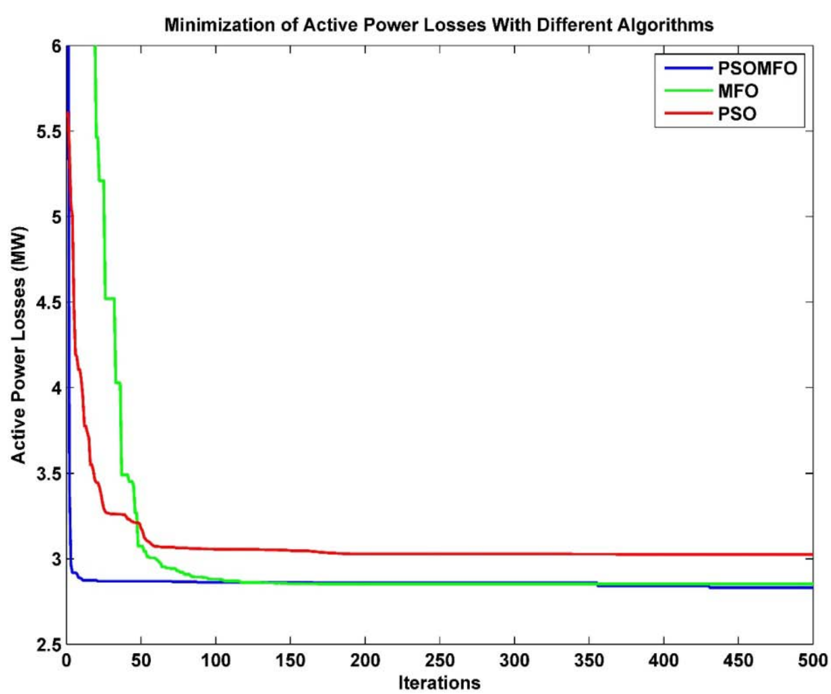


*Fig. 6:* Minimization of active power losses with different algorithms

Global Journal of Researches in Engineering ( F ) Volume XVII Issue V Version I Year 2017

*Table 8:* Comparison of active power transmission losses obtained with different algorithms

| Method | Active Power Loss (MW) | Method Description |
|---|---|---|
| HPSO-MFO | 2.831 | Hybrid Particle Swarm Optimization-Moth Flame Optimizer |
| MFO | 2.853 | Moth Flame Optimizer |
| PSO | 3.026 | Particle Swarm Optimization |
| BHBO | 3.503 | Black Hole- Based Optimization [6] |

*Table 9:* Optimal values of control variables for case 4 with different algorithms

| Control Variable | Min | Max | Initial | HPSO-MFO | MFO | PSO |
|---|---|---|---|---|---|---|
| $P_{G1}$ | 50 | 200 | 99.2230 | 51.269 | 51.253 | 51.427 |
| $P_{G2}$ | 20 | 80 | 80 | 80.000 | 80.000 | 80.000 |
| $P_{G5}$ | 15 | 50 | 50 | 50.000 | 50.000 | 50.000 |
| $P_{G8}$ | 10 | 35 | 20 | 35.000 | 35.000 | 35.000 |
| $P_{G11}$ | 10 | 30 | 20 | 30.000 | 30.000 | 30.000 |
| $P_{G13}$ | 12 | 40 | 20 | 40.000 | 40.000 | 40.000 |
| $V_{G1}$ | 0.95 | 1.1 | 1.05 | 1.100 | 1.100 | 1.100 |
| $V_{G2}$ | 0.95 | 1.1 | 1.04 | 1.100 | 1.098 | 1.100 |
| $V_{G5}$ | 0.95 | 1.1 | 1.01 | 1.082 | 1.080 | 1.083 |
| $V_{G8}$ | 0.95 | 1.1 | 1.01 | 1.086 | 1.087 | 1.090 |
| $V_{G11}$ | 0.95 | 1.1 | 1.05 | 1.100 | 1.100 | 1.100 |
| $V_{G13}$ | 0.95 | 1.1 | 1.05 | 1.100 | 1.100 | 1.100 |
| $T_{4\text{-}12}$ | 0 | 1.1 | 1.078 | 1.044 | 1.056 | 0.977 |
| $T_{6\text{-}9}$ | 0 | 1.1 | 1.069 | 0.901 | 0.900 | 1.100 |
| $T_{6\text{-}10}$ | 0 | 1.1 | 1.032 | 0.993 | 0.982 | 1.100 |
| $T_{28\text{-}27}$ | 0 | 1.1 | 1.068 | 0.987 | 0.973 | 0.998 |
| $QC_{10}$ | 0 | 5 | 0 | 5.000 | 5.000 | 4.065 |
| $QC_{12}$ | 0 | 5 | 0 | 4.570 | 5.000 | 0.000 |
| $QC_{15}$ | 0 | 5 | 0 | 4.969 | 3.070 | 5.000 |
| $QC_{17}$ | 0 | 5 | 0 | 4.942 | 5.000 | 5.000 |
| $QC_{20}$ | 0 | 5 | 0 | 4.337 | 5.000 | 0.000 |
| $QC_{21}$ | 0 | 5 | 0 | 5.000 | 5.000 | 5.000 |
| $QC_{23}$ | 0 | 5 | 0 | 5.000 | 5.000 | 5.000 |
| $QC_{24}$ | 0 | 5 | 0 | 5.000 | 5.000 | 0.000 |
| $QC_{29}$ | 0 | 5 | 0 | 2.412 | 2.508 | 0.000 |
| PLoss (MW) | - | - | 5.8219 | 2.831 | 2.853 | 3.026 |

*Case 5: Minimization of reactive power transmission losses*

The accessibility of reactive power is the main point for static system voltage stability margin to support the transmission of active power from the source to sinks [6].

Thus, the minimization of *VAR* losses are given by the following expression:

$$J = \sum_{i=1}^{NGen} Q_i = \sum_{i=1}^{NGen} Q_{Gi} - \sum_{i=1}^{NGen} Q_{Di} \tag{48}$$

It is notable that the reactive power losses are not essentially positive. The variation of reactive power losses with different methods shown in fig. 6. It demonstrates that the suggested method has good convergence characteristics. The statistical values of reactive power losses obtained with different methods are shown in table 10 which display that the results obtained by hybrid PSO-MFO method are better than the other methods. The optimal values of control variables obtained by different algorithms for case 5 are given in Table 11. It is shown that the reactive power losses are greatly reduced compared to the initial case [6] from -4.6066 MVAR to -25.335MVAR using hybrid PSO-MFO method.

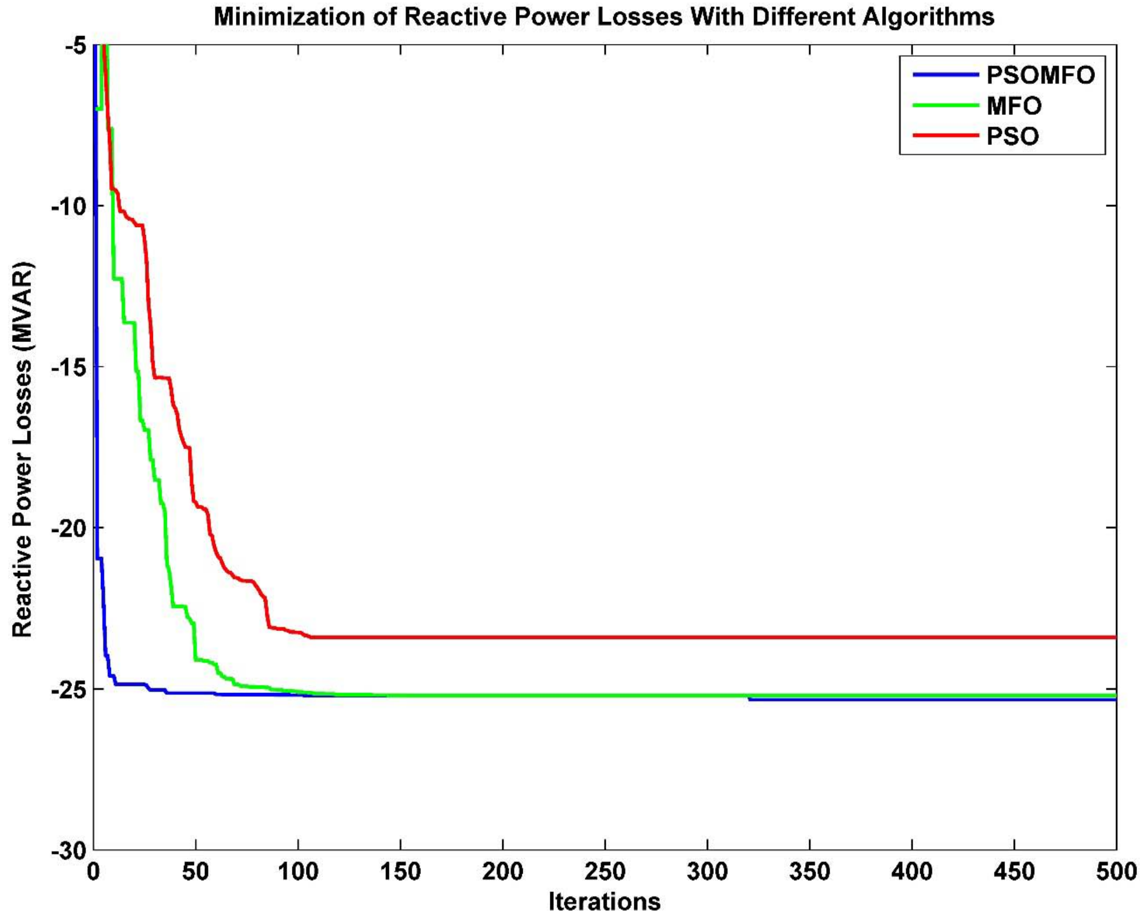


*Fig. 7:* Minimization of reactive power transmission losses with different algorithms

*Table 10:* Comparison of reactive power losses obtained with different algorithms

| Method | Reactive Power Loss (MVAR) | Method Description |
|---|---|---|
| HPSO-MFO | -25.335 | Hybrid Particle Swarm Optimization-Moth Flame Optimizer |
| MFO | -25.204 | Moth Flame Optimizer |
| PSO | -23.407 | Particle Swarm Optimization |
| BHBO | -20.152 | Black Hole- Based Optimization [6] |

*Table 11:* Optimal values of control variables for case 5 with different algorithms

| Control Variable | Min | Max | Initial | HPSO-MFO | MFO | PSO |
|---|---|---|---|---|---|---|
| $P_{G1}$ | 50 | 200 | 99.2230 | 51.318 | 51.356 | 51.644 |
| $P_{G2}$ | 20 | 80 | 80 | 80.000 | 80.000 | 80.000 |
| $P_{G5}$ | 15 | 50 | 50 | 50.000 | 50.000 | 50.000 |
| $P_{G8}$ | 10 | 35 | 20 | 35.000 | 35.000 | 35.000 |
| $P_{G11}$ | 10 | 30 | 20 | 30.000 | 30.000 | 30.000 |
| $P_{G13}$ | 12 | 40 | 20 | 40.000 | 40.000 | 40.000 |
| $V_{G1}$ | 0.95 | 1.1 | 1.05 | 1.100 | 1.100 | 1.100 |
| $V_{G2}$ | 0.95 | 1.1 | 1.04 | 1.100 | 1.100 | 1.100 |
| $V_{G5}$ | 0.95 | 1.1 | 1.01 | 1.092 | 1.092 | 1.100 |
| $V_{G8}$ | 0.95 | 1.1 | 1.01 | 1.100 | 1.100 | 1.100 |
| $V_{G11}$ | 0.95 | 1.1 | 1.05 | 1.100 | 1.100 | 1.100 |
| $V_{G13}$ | 0.95 | 1.1 | 1.05 | 1.100 | 1.100 | 1.100 |
| $T_{4\text{-}12}$ | 0 | 1.1 | 1.078 | 1.002 | 0.974 | 0.962 |
| $T_{6\text{-}9}$ | 0 | 1.1 | 1.069 | 0.965 | 1.100 | 1.100 |
| $T_{6\text{-}10}$ | 0 | 1.1 | 1.032 | 0.987 | 0.984 | 0.961 |

| | | | | | | |
|---|---|---|---|---|---|---|
| $T_{28\text{-}27}$ | 0 | 1.1 | 1.068 | 0.986 | 0.981 | 0.964 |
| $QC_{10}$ | 0 | 5 | 0 | 5.000 | 5.000 | 5.000 |
| $QC_{12}$ | 0 | 5 | 0 | 0.000 | 5.000 | 0.000 |
| $QC_{15}$ | 0 | 5 | 0 | 5.000 | 5.000 | 0.000 |
| $QC_{17}$ | 0 | 5 | 0 | 5.000 | 5.000 | 0.000 |
| $QC_{20}$ | 0 | 5 | 0 | 5.000 | 5.000 | 0.000 |
| $QC_{21}$ | 0 | 5 | 0 | 5.000 | 5.000 | 0.000 |
| $QC_{23}$ | 0 | 5 | 0 | 5.000 | 5.000 | 0.000 |
| $QC_{24}$ | 0 | 5 | 0 | 5.000 | 5.000 | 5.000 |
| $QC_{29}$ | 0 | 5 | 0 | 3.393 | 3.407 | 0.000 |
| QLoss (MVAR) | - | - | -4.6066 | **-25.335** | -25.204 | -23.407 |

Table 12 show the comparison of elapsed time taken by the different methods to optimize the different objective cases. The comparison shows that the time taken by all three algorithms is not same which indicates the different evaluation strategy of different methods.

*Table 12:* Comparison of Elapsed time in seconds for MFO, PSO and HPSO-MFO for all cases

| Case No. | Elapsed Time (Seconds) | | |
|---|---|---|---|
| | MFO | PSO | HPSO-MFO |
| 1 | 166.2097 | 250.2674 | 211.7915 |
| 2 | 191.8238 | 266.5375 | 229.6873 |
| 3 | 196.6275 | 270.3358 | 243.2919 |
| 4 | 161.6395 | 248.8739 | 259.9731 |
| 5 | 173.5987 | 253.3971 | 209.4387 |

## V. Robustness Test

In order to check the robustness of the HPSO-MFO for solving continues Optimal Power Flow problems, 10 times trials with various search agents for cases Case 1, Case 2, Case 3, Case 4 and Case 5. Table 2, Table 3, Table 4, Table 5, Table 6, Table 7, Table 8, Table 9, Table 10 and Table 11 presents the statistical results achieved by the HPSO-MFO, MFO and PSO algorithms for OPF problems for various cases. From these tables, it is clear that the optimum objective function values obtained by HPSO-MFO are near to every trial and minimum compare to MFO and PSO algorithms. It proves the robustness of hybrid PSO-MFO algorithm (HPSO-MFO) to solve OPF problem.

## VI. Conclusion

Particle Swarm Optimization-Moth Flame Optimizer (PSO-MFO), Moth Flame Optimizer and Particle Swarm Optimization Algorithm are successfully applied to standard IEEE 30-bus test systems to solve the optimal power flow problem for the various types of cases. The results give the optimal settings of control variables with different methods which demonstrate the effectiveness of the different techniques. The solutions obtained from the hybrid PSO-MFO method approach has good convergence characteristics and gives the better results compared to MFO and PSO methods which confirm the effectiveness of proposed algorithm.

## VII. Acknowledgment

The authors would like to thank Professor Seyedali Mirjalili for his valuable comments and support. http://www.alimirjalili.com/MFO.html.

## References Références Referencias

1. H.R.E.H. Bouchekara, M.A. Abido, A.E. Chaib, R. Mehasni, Optimal power flow using the league championship algorithm: a case study of the Algerian power system, Energy Convers. Manag. 87 (2014) 58–70.
2. Duman S, Güvenç U, Sönmez Y, Yörükeren N. Optimal power flow using gravitational search algorithm. Energy Convers Manag2012; 59:86–95.
3. Niknam T, R Narimani M, Jabbari M, Malekpour AR. A modified shuffle frogleaping algorithm for multi-objective optimal power flow. Energy 2011; 36(11): 6420–32.
4. J. Carpentier, Contribution à l'étude du Dispatching Economique, Bull. Soc. Fran-caise Electriciens (1962) 431–447.
5. H.R.E.H. Bouchekara, M.A. Abido, M. Boucherma, Optimal power flow using Teaching-Learning-Based Optimization technique, Electr. Power Syst. Res. 114(2014) 49–59.
6. H.R.E.H. Bouchekara, Optimal power flow using black-hole-based optimization approach, Appl. Soft Comput. (2013) (under review).
7. S. Frank, I. Steponavice, S. Rebennack, Optimal power flow: a bibliographicsurvey I, formulations

and deterministic methods, Energy Syst. 3 (3) (2012)221–258.
8. M.R. AlRashidi, M.E. El-Hawary, Applications of computational intelligence techniques for solving the revived optimal power flow problem, Electr. Power Syst. Res. 79 (4) (2009) 694–702.
9. S. Frank, I. Steponavice, S. Rebennack, Optimal power flow: a bibliographic survey II, non-deterministic and hybrid methods, Energy Syst. 3 (3) (2012)259–289.
10. A.R. Yildiz, A comparative study of population-based optimization algorithms for turning operations, Inf. Sci. (Ny) 210 (2012) 81–88.
11. LJ Cai, I Erlich and G Stamtsis. Optimal choice and allocation of FACTS devices in deregulated electricity market using genetic algorithms. *IEEE*. 2004.
12. TS Chung and YZ Li. A hybrid GA approach for OPF with consideration of FACTS devices. *IEEE Power Engineering Review*. 2001; 47-50.
13. K Kalaiselvi, V Kumar, and K Chandrasekar. Enhanced Genetic Algorithm for Optimal Electric Power Flow using TCSC and TCPS. Proc. World. 2010; (II).
14. AG Bakirtzis. P Biskas, CE Zoumas, and V Petridis. Optimal power flow by enhanced genetic algorithm. *Power Syst, IEEE Trans*. 2002; 17(2): 229–236.
15. A.A. Abou El Ela, M.A. Abido, Optimal power flow using differential evolution algorithm, Electr. Power Syst. Res. 80 (7) (2010) 878–885.
16. Slimani L, Bouktir T. Optimal Power Flow Solution of the Algerian Electrical Network using Differential Evolution Algorithm. *TELKOMNIKA Indonesian Journal of Electrical Engineering*. 2012; 10(2): 199–210.
17. Badrul H Chowdhury. Towards the concept of integrated security: optimal dispatch under static and dynamic security constraints. *Electric Power Syst, Research*.1992; 25: 213-225.
18. M Saravanan, SM Slochanal, P Venkatesh, J Abraham. Application of particle swarm optimization technique for optimal location of FACTS devices considering cost of installation and system loadability. *Electric Power Syst, Research*. 2007; 77: 276-283.
19. Abido MA. Optimal power flow using tabu search algorithm. *Electric Power Compon Syst*. 2002; 30: 469–83.
20. S Duman U Güvenç, Y Sönmez and N Yörükeren. Optimal power flow using gravitational search algorithm. *Energy Convers, Manag*. 2012; 59: 86–95.
21. A Bhattacharya and PChattopadhyay. Application of biogeography-based optimisation to solve different optimal power flow problems. *IET Gener, Transm. Distrib*. 2011; 5(1): 70.
22. N Sinsupan, U Leeton and T Kulworawanichpong. *Application of Harmony Search to Optimal Power Flow Problems*. 2010:219–222.
23. A Mukherjee and V Mukherjee. *Solution of optimal power flow using chaotic krill herd algorithm*. Chaos, Solitons & Fractals. 2015; 78: 10–21.
24. M Rama, Mohana Rao and AV NareshBabu. Optimal Power Flow Using Cuckoo Optimization Algorithm. *IJAREEIE*. 2013: 4213–4218.
25. J Soares. T Sousa. ZA Vale. H Morais. and P Faria. Ant colony search algorithm for the optimal power flow problem. *IEEE Power Energy Soc, Gen, Meet*. 2011; 1–8.
26. Indrajit N. Trivedi, Motilal Bhoye, Pradeep Jangir, Siddharth A. Parmar, Narottam Jangir and Arvind Kumar, "Voltage stability enhancement and voltage deviation minimization using BAT optimization algorithm," *2016 3rd International Conference on Electrical Energy Systems (ICEES)*, Chennai, India, 2016, pp. 112-116. doi: 10.1109/ICEES.2016.7510626.
27. Optimal power flow with enhancement of voltage stability and reduction of power loss using ant-lion optimizer, Indrajit N. Trivedi, Pradeep Jangir & Siddharth A. Parmar, Cogent Engineering (2016), 3: 1208942.
28. Indrajit N. Trivedi, Siddharth A. Parmar, R.H. Bhesdadiya, Pradeep Jangir, "Voltage stability enhancement and voltage deviation minimization using Ant-Lion optimizer algorithm", *2016 2nd International Conference on Advances in Electrical, Electronics, Information, Communication and Bio-Informatics (AEEICB)*, Chennai, India, 2016, pp. 263-267. doi: 10.1109/AEEICB.2016.7538286.
29. Indrajit N. Trivedi, Pradeep Jangir, Narottam Jangir, Siddharth A. Parmar, Motilal Bhoye and Arvind Kumar, "Voltage stability enhancement and voltage deviation minimization using Multi-Verse optimizer algorithm," *2016 International Conference on Circuit, Power and Computing Technologies (ICCPCT)*, Nagercoil, India, 2016, pp. 1-5. doi: 10.1109/ICCPCT.2016.7530136.
30. J. Kennedy, R. Eberhart, Particle swarm optimization, in: Proceedings of the IEEE International Conference on Neural Networks, Perth, Australia, 1995, pp. 1942–1948.
31. Seyedali Mirjalili, "Moth-flame optimization algorithm: A novel nature-inspired heuristic paradigm," Knowledge-Based System, vol. 89, pages 228-249, 2015.
32. Narottam Jangir, Mahesh H. Pandya, Indrajit N. Trivedi, R. H. Bhesdadiya, Pradeep Jangir and Arvind Kumar, "Moth-Flame optimization Algorithm for solving real challenging constrained engineering optimization problems," *2016 IEEE Students' Conference on Electrical, Electronics and Computer*

*Science (SCEECS)*, Bhopal, India, 2016, pp. 1-5. doi: 10.1109/SCEECS.2016.7509293.
33. K. Lee, Y. Park, J. Ortiz, A united approach to optimal real and reactive power dispatch, IEEE Trans. Power App. Syst. 104 (5) (1985) 1147–1153.
34. P. Kessel, H. Glavitsch, Estimating the voltage stability of a power system, IEEETrans. Power Deliv. 1 (3) (1986) 346–354.
35. W. Ongsakul, T. Tantimaporn, Optimal power flow by improved evolutionary programming, Electr. Power Compon. Syst. 34 (1) (2006) 79–95.
36. C.A. Belhadj, M.A. Abido, An optimized fast voltage stability indicator, in: Electric Power International Conference on Engineering, Power Tech Budapest, 1999, pp. 79–83.
37. S.A.H. Soliman, A.H. Mantawy, Modern Optimization Techniques with Applications in Electric Power Systems, Energy Systems, Springer, New York/Heidelberg/Dordrecht/London, 2012.

Global Journal of Researches in Engineering: F
Electrical and Electronics Engineering
Volume 17 Issue 5 Version 1.0 Year 2017
Type: Double Blind Peer Reviewed International Research Journal
Publisher: Global Journals Inc. (USA)
Online ISSN: 2249-4596 & Print ISSN: 0975-5861

# Detecting Defective Bypass Diodes in Photovoltaic Modules using Mamdani Fuzzy Logic System

By Mahmoud Dhimish, Violeta Holmes, Bruce Mehrdadi, Mark Dales & Peter Mather

*University of Huddersfield, United Kingdom*

*Abstract- In* this paper, the development of fault detection method for PV modules defective bypass diodes is presented. Bypass diodes are nowadays used in PV modules in order to enhance the output power production during partial shading conditions. However, there is lack of scientific research which demonstrates the detection of defective bypass diodes in PV systems. Thus, this paper propose a PV bypass diode fault detection classification based on Mamdani fuzzy logic system, which depends on the analysis of Vdrop, Voc , and Isc obtained from the I-V curve of the examined PV module.

The fuzzy logic system depends on three inputs, namely percentage of voltage drop (PVD), percentage of open circuit voltage (POCV), and the percentage of short circuit current (PSCC). The proposed fuzzy system can detect up to 13 different faults associated with defective and non-defective bypass diodes. In addition, the proposed system was evaluated using two different PV modules under various defective bypass conditions. Finally, in order to investigate the variations of the PV module temperature during defective bypass diodes and partial shading conditions, i5 FLIR thermal camera was used.

*Keywords: photovoltaic module, fault detection, fuzzy logic, thermal detection, bypass diodes.*

*GJRE-F Classification: FOR Code: 290901*

DETECTINGDEFECTIVEBYPASSDIODESINPHOTOVOLTAICMODULESUSING MAMDANIFUZZYLOGICSYSTEM

*Strictly as per the compliance and regulations of:*

# Detecting Defective Bypass Diodes in Photovoltaic Modules using Mamdani Fuzzy Logic System

Mahmoud Dhimish [α], Violeta Holmes [σ], Bruce Mehrdadi [ρ], Mark Dales [Ѡ] & Peter Mather [¥]

*Abstract- In* this paper, the development of fault detection method for PV modules defective bypass diodes is presented. Bypass diodes are nowadays used in PV modules in order to enhance the output power production during partial shading conditions. However, there is lack of scientific research which demonstrates the detection of defective bypass diodes in PV systems. Thus, this paper propose a PV bypass diode fault detection classification based on Mamdani fuzzy logic system, which depends on the analysis of Vdrop, Voc , and Isc obtained from the I-V curve of the examined PV module.

The fuzzy logic system depends on three inputs, namely percentage of voltage drop (PVD), percentage of open circuit voltage (POCV), and the percentage of short circuit current (PSCC). The proposed fuzzy system can detect up to 13 different faults associated with defective and non-defective bypass diodes. In addition, the proposed system was evaluated using two different PV modules under various defective bypass conditions. Finally, in order to investigate the variations of the PV module temperature during defective bypass diodes and partial shading conditions, i5 FLIR thermal camera was used.

*Keywords: photovoltaic module, fault detection, fuzzy logic, thermal detection, bypass diodes.*

## I. Introduction

As prices in the photovoltaic (PV) industry have decreased considerably in the last few years, reliability questions have been proportional increased interest. The performance and efficiency of PV modules are affected by several factor such as solar irradiance, ambient temperature, humidity, and wind [1-3]. In addition, several work have studied and evaluated the performance of PV modules under different climate conditions, in particular the effect of sand dust accumulation and partial shading on the output power of PV modules and PV arrays [4 & 5].

In addition, PV modules output power performance could be decreased due to the PV cracks [6 & 7]. As reported in [8], PV cracks occur in PV solar cells due to partial shading conditions affecting some solar cells while the rest are under normal operation mode, also it might occur due to the dust and hot spots in PV modules. To solve this problem in PV modules, a bypass diodes connection to the PV strings is recommended.

As a result of these factors impacting the PV performance, a fault detection methods is indeed important to be employed and further investigate in PV systems. In general, fault detection method in PV systems can be grouped as visual (discoloration, surface soiling, and delamination), thermal (hot spots and PV micro cracks), and electrical (I-V, and P-V curve analysis, and transmittance line diagnosis) [9 & 10]. In this paper, we focus on an electrical method. Multiple PV fault detection based electrical methods for PV system are based on:

1. Methods do not require climate data (such as solar irradiance and PV module temperature). In [11] the authors developed a method based on the Earth Capacitance Measurements (ECM) to detect the disconnection of a PV module. The first Time-Domain Reflectometry (TDR) technique was proposed by [12]. This technique is used to detect the disconnection of PV strings as well as the impedance change due to PV degradation. Finally, [13-15] proposed a statistical analysis PV fault detection method based on t-test and standard deviation, which can be used to detect PV failure, and faults associated with maximum power point tracking (MPPT) units.
2. Methods based on the analysis of the current-voltage I-V characteristics. In [16], the analysis of the I-V and P-V curve was used to investigate the performance of the PV module, thus, detecting possible faults such as partial shading and faulty PV strings. In [17 & 18], the authors calculate the fill factor (FF), series resistance (Rs), and the shunt resistance (Rsh) from the I-V curve to investigate the performance of multiple PV configuration systems.

Methods based on artificial intelligence (AI) techniques. In [19 & 20] the authors proposed a PV fault detection algorithm which can identify the partial shading conditions in PV modules based on a fuzzy logic system. However, the proposed technique cannot identify the impact of bypass diodes in PV modules, which has been investigated by [21 & 22]. In addition, a learning method based on Expert Systems is developed by [23-25] to identify faults in PV modules due to partial

About α σ ρ Ѡ ¥: School of Computing and Engineering, University of Huddersfield, United Kingdom, HD1 3DH.
e-mails: mahmoud.dhimish2@hud.ac.uk, v.holmes@hud.ac.uk, b.mehrdadi@hud.ac.uk, m.r.dales@hud.ac.uk & p.j.mather@hud.ac.uk

shading and inverter's failure. Furthermore, in [26], an artificial neural network (ANN) is used in order to classify different types of faults occurring in a PV array. In this case, the ANN takes as inputs the current and the voltage at maximum power point, and the temperature of the PV module. Different methods based on the Takagie Sugeno Kahn Fuzzy Rule (TSKFRBS) have been described in [27 & 28].

The main contribution of this work is to present a new PV fault detection method based on Mamdani fuzzy logic system, which can detects the defective bypass diodes and partial shading conditions. The fuzzy logic system depends on three inputs:

1. Percentage of voltage drop (PVD)
2. Percentage of open circuit voltage (POCV)
3. Percentage of short circuit current (PSCC)

Finally, in order to investigate the variations of the PV module temperature during defective bypass diodes and partial shading conditions, i5 FLIR thermal camera was used. Several test have been carried out using two diffident PV modules with nominal peak power 220 Wp and 130 Wp.

## II. Examined PV Module Characteristics

The PV system used in this work comprises a PV plant containing 9 polycrystalline silicon PV modules each with a nominal power of 220 Wp. The photovoltaic modules are organized in 3 strings and each string is made up of 3 series-connected PV modules. Using a photovoltaic connection unit which is used to enable or disable the connected of any PV modules from the entire GCPV plant, each photovoltaic string is connected to a Maximum Power Point Tracker (MPPT) which has an output efficiency not less than 98.5% [29]. The existing PV system is shown in Figure 1a.

The SMT6 (60) P solar module manufactured by Romag has been used in this work. The tilt angle of the PV installation is 42°. The electrical characteristics of the solar module are shown in Table 1. Additionally, the standard test condition (STC) for these solar panels are: solar irradiance (G): 1000 W/m$^2$ and PV module temperature (T): 25 °C.

Each examined PV module comprises three bypass diodes which are connected in parallel to each PV string. Figure 1b shows the connection of the bypass diodes, where Figure 1c shows the junction box placed at the back of the PV modules.

*Table 1:* Examined PV electrical characteristics

| PV module electrical characteristics | Value |
|---|---|
| Power at maximum power point ($P_{mpp}$) | 220 W |
| Voltage at maximum power point ($V_{mpp}$) | 28.7 V |
| Current at maximum power point ($I_{mpp}$) | 7.67 A |
| Open Circuit Voltage ($V_{oc}$) | 36.74 V |
| Short Circuit Current ($I_{sc}$) | 8.24 A |
| Number of cells connected in series | 60 |
| Number of cells connected in parallel | 1 |

## III. Inspection and Validation Method

In this work, the MPPT units were used to measure the voltage, and current using the internal sensors embedded with this device. Subsequently, the MPPT units are connected to a Virtual instrumentation (VI) LabVIEW software in order to simulate the current-voltage (I-V) curve of the examined PV modules.

Furthermore, the investigation of the temperature variations during partial shading and faulty bypass diodes (bypass diode disconnected from the PV modules) have been captured using i5 FLIR thermal camera. This camera has the following specification:

- Thermal image quality: 100x100 pixels
- Field of view: 21° (H) x 21° (V)
- Thermal sensitivity: 32.18 F

## IV. Experimental Results

*a) I-V curve characteristics under partial shading conditions*

The first test will demonstrate the impact of partial shading conditions on the I-V curve for a standalone PV module. The first PV module in the PV system will be coved by an opaque object to examine the PV module under various partial shading conditions as shown in Figure 3a.

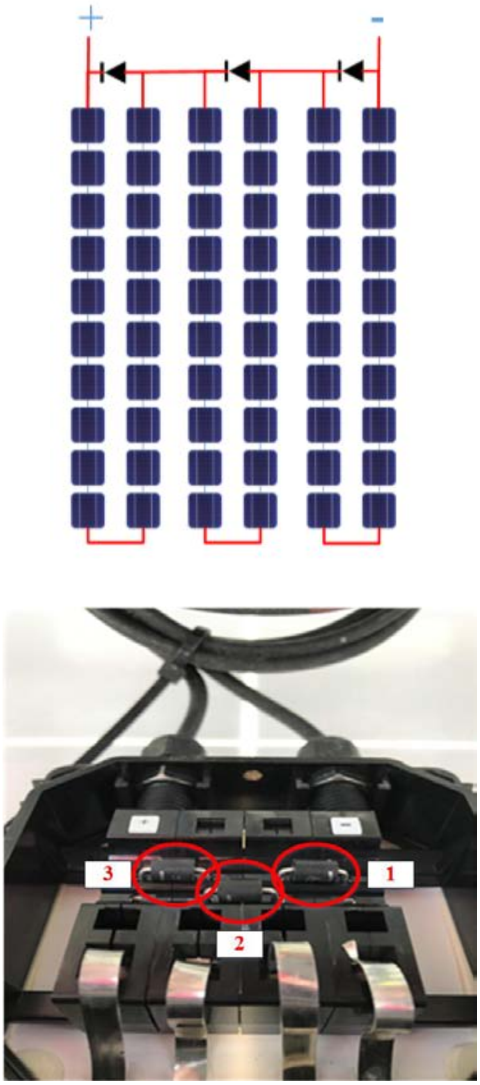


*Fig. 1:* (a) Examined PV system installed at the University of Huddersfield, United Kingdom, (b) Internal bypass connection for each PV module, (c) Junction box placed at the back of the PV modules

Multiple experiments have been conducted under various partial shading conditions, starting from 10% and ending up with 90%. Three thermal images of the examined PV module under partial shading conditions (10%, 30%, and 60%) are shown in Figure 3. In addition, all experiments were performed while there is no defective bypass diodes connected in the tested PV module.

Figure 2a and Figure 2b show the experiment output for the I-V and P-V curves for all tested shading conditions. As can be noticed, while increasing the percentage of shading the Voc of the PV module decrease. However, the I sc remains the same at 8.18 A.

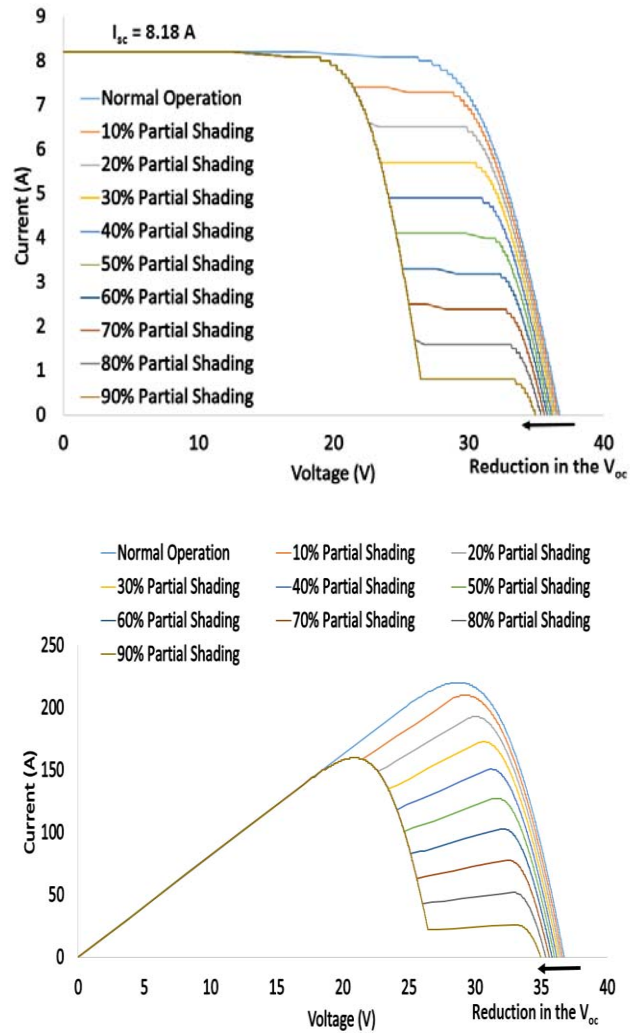


*Fig. 2:* (a) I-V curve characteristics under various partial shading conditions affecting the PV module, (b) P-V curve characteristics under various partial shading conditions affecting the PV module

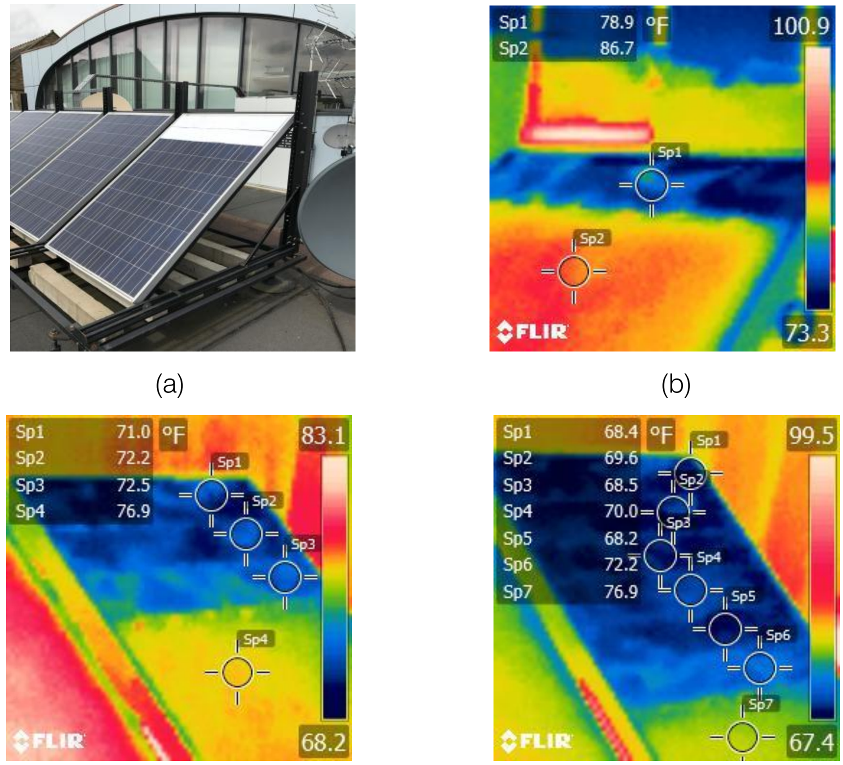


(a) (b)

(c) (d)

*Fig. 3:* (a) Real image of the examined PV module coved by opaque object, (b) 10% partial shading, (c) 30% partial shading, (d) 60% partial shading

*b) I-V curve characteristics under 90% partial shading condition and faulty bypass diodes*

This test was experimentally evaluated while disconnecting one, two, and three bypass diodes in the PV module under 90% partial shading condition (worst case scenario).

As shown in Figure 4a, during 90% partial shading and no disconnection of PV module bypass diodes, PV module I-V curve started to drop its $I_{sc}$ at 18 V, we called this drop as $V_{drop}$ in the I-V curve. However, the first drop in the I-V curve while disconnecting one bypass diode is equal to 16 V. Faster drop is associated with 90% partial shading and 2 faulty bypass diodes in the PV module.

The last case, when all PV module bypass diodes completely removed during 90% partial shading condition. In this case, the drop in the $I_{sc}$ is obtained at the start of the I-V curve (at 0~2.87 V). This loss in the current will affect the output power of the PV module significantly. The output power obtained in each case scenario is presented as follows:

- No fault in the bypass diodes:
    - Pmpp = 159.8 W
- Disconnecting 1 bypass diode:
    - Pmpp = 141.5 W
- Disconnecting 2 bypass didoes:
    - $P_{mpp}$ = 104.8 W
- Disconnecting all bypass didoes:
    - $P_{mpp}$ = 18.84 W

While disconnecting the bypass diodes from the PV module during partial shading conditions, the PV module output power will decrease. This phenomenon occur due to the impact of the reverse-bias feature of the bypass diodes.

Furthermore, Figure 4b shows that while disconnecting one bypass diode from the examined PV module, the temperature raises in the PV string associated with the faulty bypass diode location. The increase of the PV sting temperature will decrease the PV output power. According to Figure 4b, the increase of the PV string temperature is equal to:

Increase in the PV string temperature =

66.2 F (PV string without bypass diode) - 62.9 F (adjacent PV strings with bypass diodes)

= 3.3 F

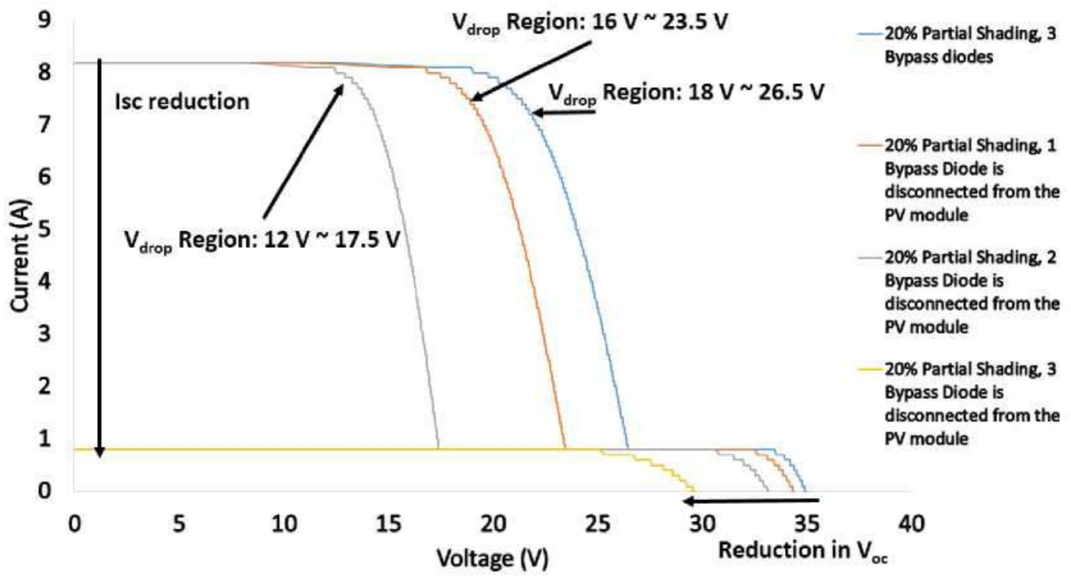


(a)

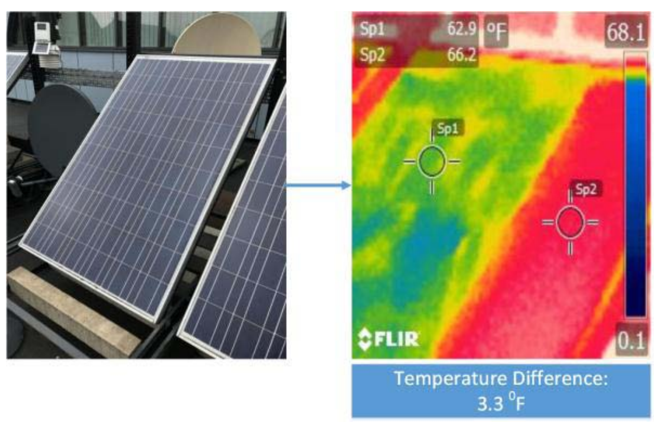


(b)

*Fig. 4:* (a) I-V curves under various conditions affecting the examined PV module, (b) Real image and thermography image of the examined PV module while disconnecting one bypass diode from the first PV string

Since the voltage drop ($V_{drop}$) has been measured during worst case scenario at each $I_{sc}$ level of the examined I-V curves, it has been found that the $V_{drop}$ in each examined case can be classified as the following:

- No fault in the bypass diodes:
  - o $V_{drop}$ Region: 18 ~ 26.5 V
- Disconnecting 1 bypass diode:
  - o $V_{drop}$ Region: 16 ~ 23.5 V
- Disconnecting 2 bypass didoes:
  - o $V_{drop}$ Region: 12 ~ 17.5 V
- Disconnecting all bypass didoes:
  - o $V_{drop}$ Region: 0 ~ 2.87 V

In order to generalize the findings of the $V_{drop}$, the percentage of $V_{mpp}$ has been compared with the $V_{drop}$ values, which can be formalized as stated in (1) by the voltage drop percentage (PVD).

$$\text{Percentage of Voltage Drop (PVD)} = \frac{V_{drop}}{V_{mpp}} \times 100 \quad (1)$$

The following calculations show the percentage of voltage drop based on (1) which is validated using the examined I-V curve shown in Figure 4a.

No fault in the bypass diodes:

$$PVD = \frac{17.5 \sim 26.5}{28.7} \times 100 = 61.0\% \sim 92.3\%$$

Disconnecting 1 bypass diode:

$$PVD = \frac{15 \sim 23.5}{28.7} \times 100 = 52.2\% \sim 81.9\%$$

Disconnecting 2 bypass didoes:

$$PVD = \frac{10.5 \sim 17.5}{28.7} \times 100 = 36.5\% \sim 61\%$$

Disconnecting all bypass didoes:

$$PVD = \frac{0 \sim 2.87}{28.7} \times 100 = 0\% \sim 10\%$$

As can be noticed, the regions of the PVD are overlapping, and in order to increase the detection accuracy of the bypass diodes regions, the percentage of open circuit voltage (POCV) is used. The POCV is calculated using (2).

$$\text{Percentage of open circuit voltage} = \frac{\text{Measured Voc}}{\text{Theoretical Voc}} \times 100 \quad (2)$$

From the results obtained previously in Figure 4a, the POVC for each tested case scenario has been calculated as the following:

No fault in the bypass diodes:

$$POVC = \frac{36.74 \sim 35}{36.74} \times 100 = 100\% \sim 95.3\%$$

Disconnecting 1 bypass diode:

$$POVC = \frac{36.74 \sim 33.5}{36.74} \times 100 = 100\% \sim 91.2\%$$

Disconnecting 2 bypass didoes:

$$POVC = \frac{36.74 \sim 32.1}{36.74} \times 100 = 100\% \sim 87.3\%$$

It is also worthy to mention the behavior of the I-V curves based on the measured $I_{sc}$ for each examined case. Since $I_{sc}$ is another variable which could be used to examine the faulty bypass diodes in PV modules. For that reason, percentage of short circuit current drop (PSCC) has been used and presented by (3).

$$\text{Percentage of Short Circuit Current} = \frac{\text{Measured Isc}}{\text{Theoretical Isc}} \times 100 \quad (3)$$

The PSCC is equal to 1 in the first 3 cases (no fault in the bypass diodes, disconnecting 1 bypass diode, and disconnecting 2 bypass diodes). However, the PSCC was evaluated using partial shading conditions between 0% up to 90% while disconnecting all bypass diodes in the examined PV module. The PSCC results are shown in Table 2, where I-V curves are presented in Figure 5.

The result shows that the percentage of PSCC depends on the percentage of shading affecting the PV module. An increase in the partial shading results a decrease in the PSCC percentage.

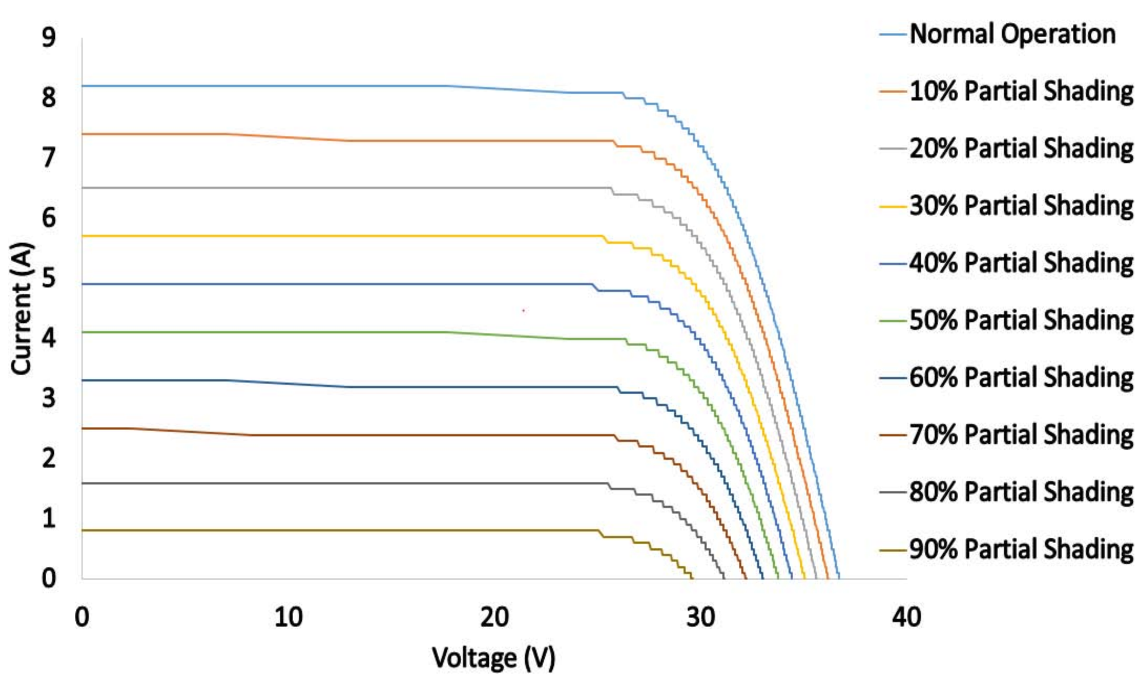


*Fig. 5:* I-V curve simulation under various partial shading conditions while disconnecting all bypass diodes from the examined PV module.

*Table 2:* PSCC Results for an Examined PV module while disconnecting all bypass diodes

| Shading Percentage % | Measured $I_{sc}$ (A) | PSCC % |
|---|---|---|
| Normal Operation | 8.18 | 100 |
| 10% | 7.37 | 90 |
| 20% | 6.55 | 80 |
| 30% | 5.73 | 70 |
| 40% | 4.91 | 60 |
| 50% | 4.09 | 50 |
| 60% | 3.28 | 40 |
| 70% | 2.46 | 30 |
| 80% | 1.64 | 20 |
| 90% | 820 mA | 10 |

## V. Proposed Fault Detection System

In this section, the proposed PV bypass diode fault detection system will be presented. Firstly, the fault detection system proposed in this paper is capable of detecting faults associated with bypass diodes and partial shading conditions affecting the PV modules.

The detection system is based on the variations of the IV curve $V_{drop}$, I-V curve $V_{oc}$, and I-V curve $I_{sc}$. Next, Mamdani fuzzy logic system is used to detect the faults in the examined PV module. The general fuzzy system architecture is illustrated in Figure 6.

Subsequently, the fuzzy system is based on three inputs:

1. PVD
2. POVC
3. PSCC

All inputs are processed by the fuzzy logic system based on the membership functions shown in Figure 7a, where all the percentages are discussed previously in section IV.

The output of the fuzzy logic system can classify 13 different type of fault associated with PV bypass diodes and partial shading conditions. Furthermore, Figure 7b illustrates the output membership function used in the fuzzy system. In addition, the list of the faults are shown in Figure 7c.

The fuzzy logic system rule are based on: if, and statement. All selected rules in the fuzzy logic is presented in Appendix A.

The main question related to the structure of the fuzzy logic system, that if the rules and classification could be used in other PV modules? - The answer will be briefly answered next section, however, as can be seen in Figure 6, the PVD, POCV and PSCC depends on the ratio of the measured and theoretical PV parameters, thus, these ratios are fixed through any tested PV module. As a result of that, the fuzzy logic could be used to classify the faulty bypass diodes in other PV modules as appropriate.

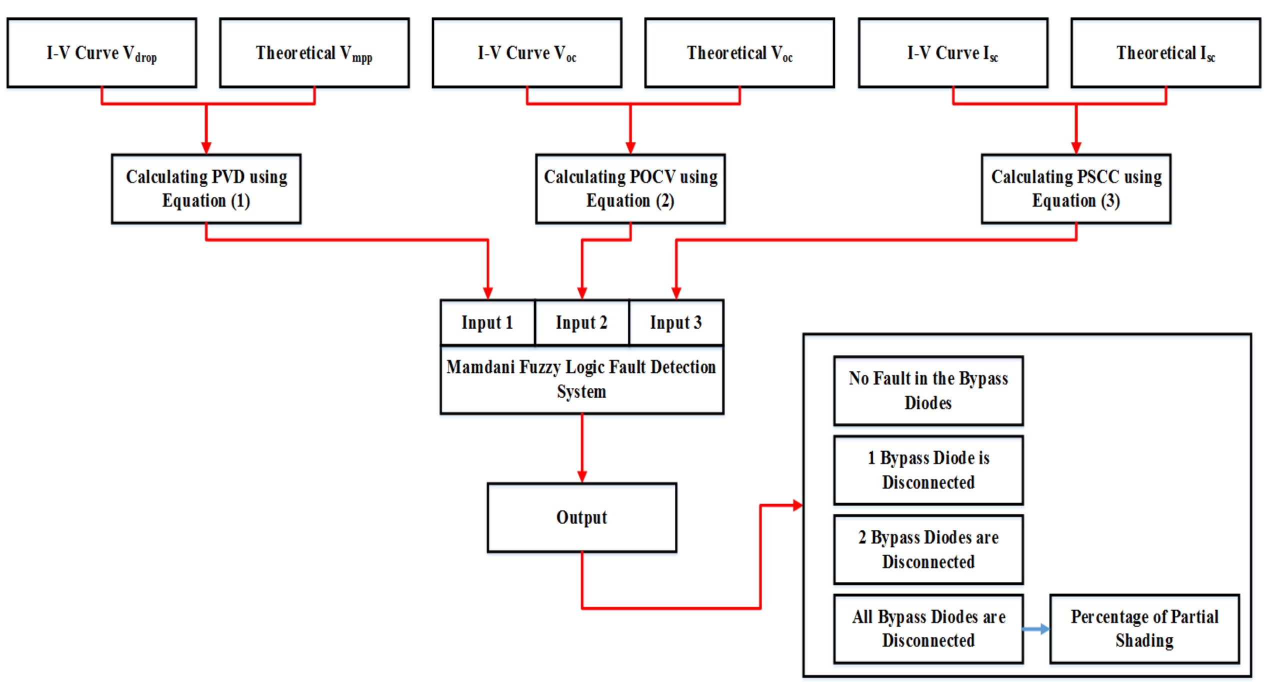


*Fig. 6:* Proposed fault detection system using Mamdani fuzzy logic system

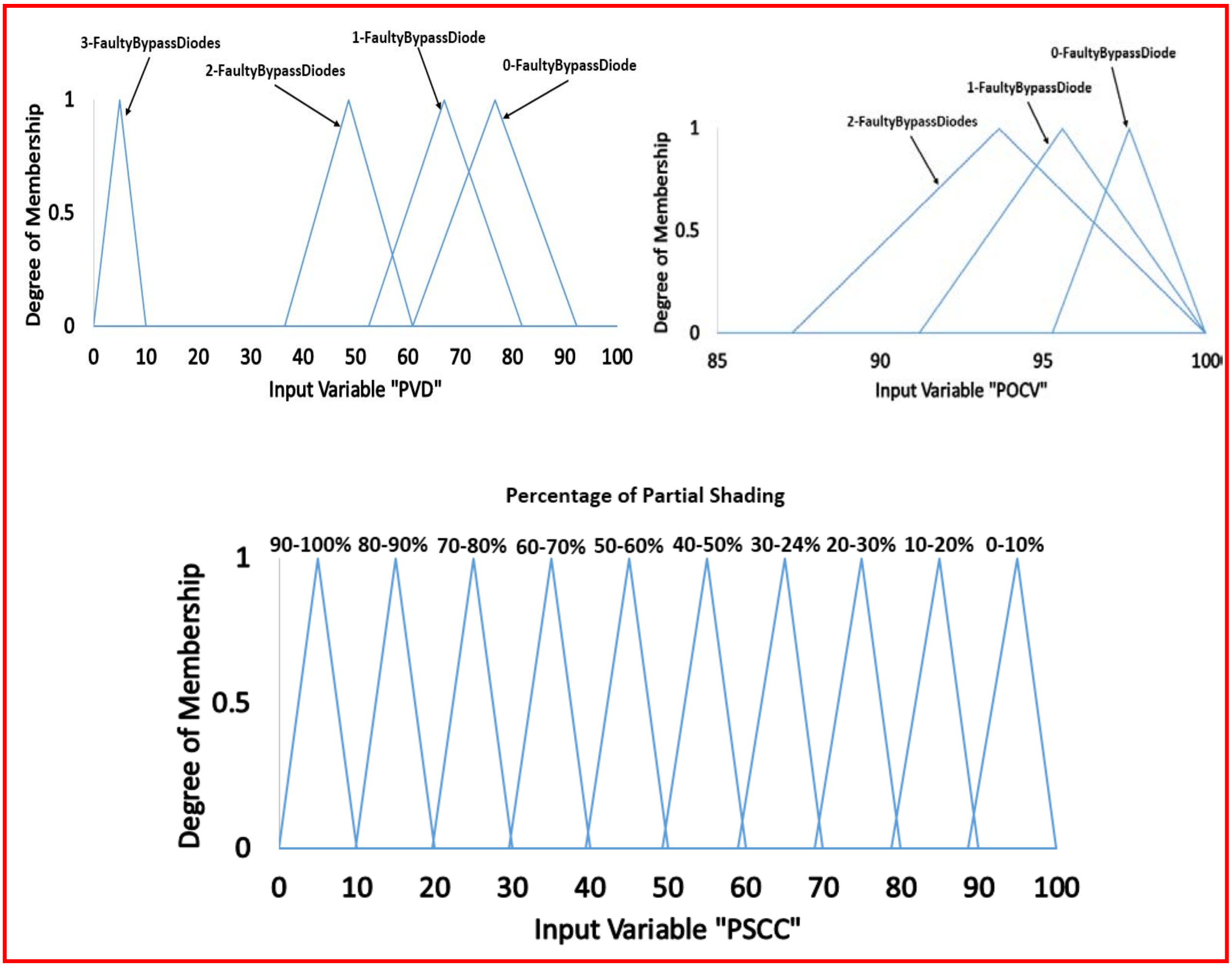


(a)

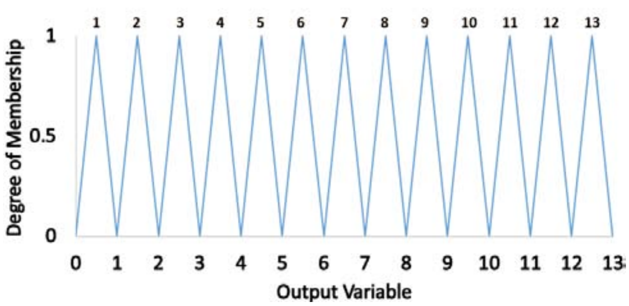


(b)

1 >> No Faults in the Bypass Diodes
2 >> 1 Fualty Bypass Diode
3 >> 2 Faulty Bypass Diodes
4 >> 3 Faulty Bypass Diodes & 0-10% Partial Shading
5 >> 3 Faulty Bypass Diodes & 10-20% Partial Shading
6 >> 3 Faulty Bypass Diodes & 20-30% Partial Shading
7 >> 3 Faulty Bypass Diodes & 30-40% Partial Shading
8 >> 3 Faulty Bypass Diodes & 40-50% Partial Shading
9 >> 3 Faulty Bypass Diodes & 50-60% Partial Shading
10 >> 3 Faulty Bypass Diodes & 60-70% Partial Shading
11 >> 3 Faulty Bypass Diodes & 70-80% Partial Shading
12 >> 3 Faulty Bypass Diodes & 80-90% Partial Shading
13 >> 3 Faulty Bypass Diodes & 90-100% Partial Shading

(c)

*Fig. 7:* (a) Input variables for the proposed fuzzy logic fault detection system, (b) output variable for the fuzzy logic fault detection systems, (c) List of faults which can be detected using the fuzzy logic system

## VI. Validate the Proposed Fault Detection System using KC130GHT PV Module

In this section, the proposed fault detection system will be evaluated using a different PV module installed at the University of Huddersfield, where the electrical characteristics of the PV module is shown in Table 3. Real image of the PV module is shown in Figure 7. Additionally, the PV strings are connected to three bypass diodes.

In this section, two case scenarios will be evaluated, the first case is when the PV module under one defective bypass diode, where the second case where the PV module under three defective bypass diodes.

*a) PV module under one defective bypass diode and 35% partial shading*

This test was evaluated when the PV module has one defective bypass diode. The PV module output parameters: $V_{drop}$, $V_{oc}$, and $I_{sc}$ are shown in Figure 9a.

The percentages PVD, POVC, PSCC are equal to 58.52%, 99.08% and 100%. Next, these percentages are processed by the fuzzy logic system.

*Table 3:* KC130GHT PV module electrical characteristics

| PV module electrical characteristics | Value |
|---|---|
| Power at maximum power point (Pmpp) | 130 W |
| Voltage at maximum power point (Vmpp) | 17.6 V |
| Current at maximum power point (Impp) | 7.39 A |
| Open Circuit Voltage (Voc) | 21.9 V |
| Short Circuit Current (Isc) | 8.02 A |
| Number of cells connected in series | 36 |
| Number of cells connected in parallel | 1 |

*Fig. 8:* Real image of KC130GHT PV module

As shown in Figure 9a, the output of the fuzzy system is equal to 1.91, which is between the region "1-2". This region indicates that there is one defective bypass diode in the PV module. In addition, the classifications of all regions are previously described in Figure 7c.

In conclusion, this test was performed by the fuzzy logic, and it has successfully detected the defective bypass diode in the PV module.

*b) PV module under three defective bypass diodes and 65% partial shading*

The second test, was performed when the PV module has three defective bypass diodes (all bypass diodes has been removed) and this test was evaluated while covering 65% of the PV module using an opaque paper. The output performance of the PV module parameters is shown in Figure 9b. The theoretical Isc dropped down to 2.81A after 0.3V. The percentage as PVD, POVC and PSCC are equal to 1.70%, 91.32%, and 35.04%.

The output of the fuzzy system is equal to 9.5, which is between the regions "9-10". This region indicates that there is 3 faulty bypass diodes and 60-70% partial shading affects the PV module.

Both tests indicate that the proposed detection system is capable of detecting the defective bypass diodes in the PV module. Subsequently, there is a high accuracy in the fuzzy logic system output results comparing to the faulty conditions affecting the examined PV module.

## VII. Conclusion

This paper proposed a fault detection method for PV module defective bypass diodes. The detection method is based on Mamdani fuzzy logic system, which depends on the analysis of $V_{drop}$, $V_{oc}$, and $I_{sc}$ obtained from the I-V curve of the examined PV module.

The fuzzy logic system depends on three inputs, namely percentage of voltage drop (PVD), Percentage of open circuit voltage (POCV), and the percentage of short circuit current (PSCC). The proposed fuzzy system can detect up to 13 different faults associated with defective and non-defective bypass diodes.

The detection system achieved high detection accuracy during the validation process. In addition, the fuzzy system was evaluated using two different PV modules installed at the University of Huddersfield. Finally, in order to investigate the variations of the PV module temperature during defective bypass diodes and partial shading conditions, i5 FLIR thermal camera was used.

In future, it is intended to extend the present work to detect the faults in PV bypass diodes using the analysis of the series resistance ($R_s$) and shunt resistance ($R_{sh}$) of the PV module. In addition, the fuzzy system could be replaced with artificial neural network (ANN).

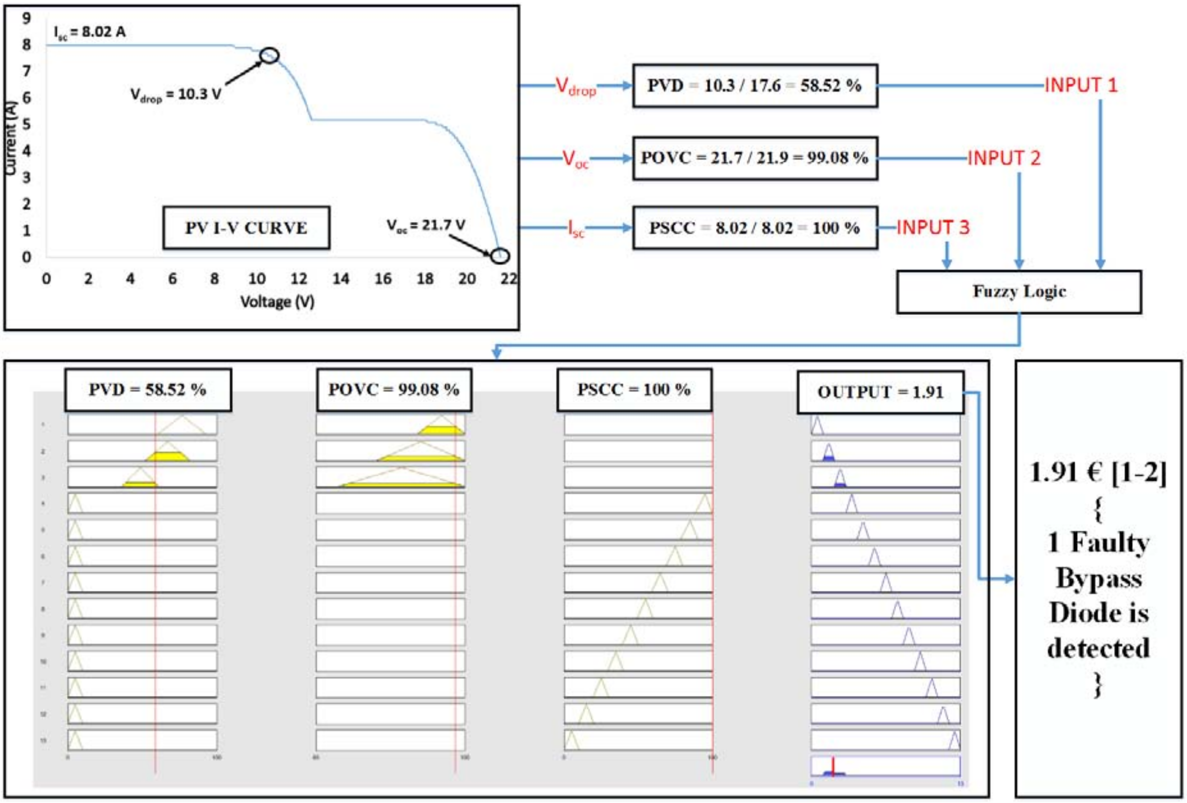


(a)

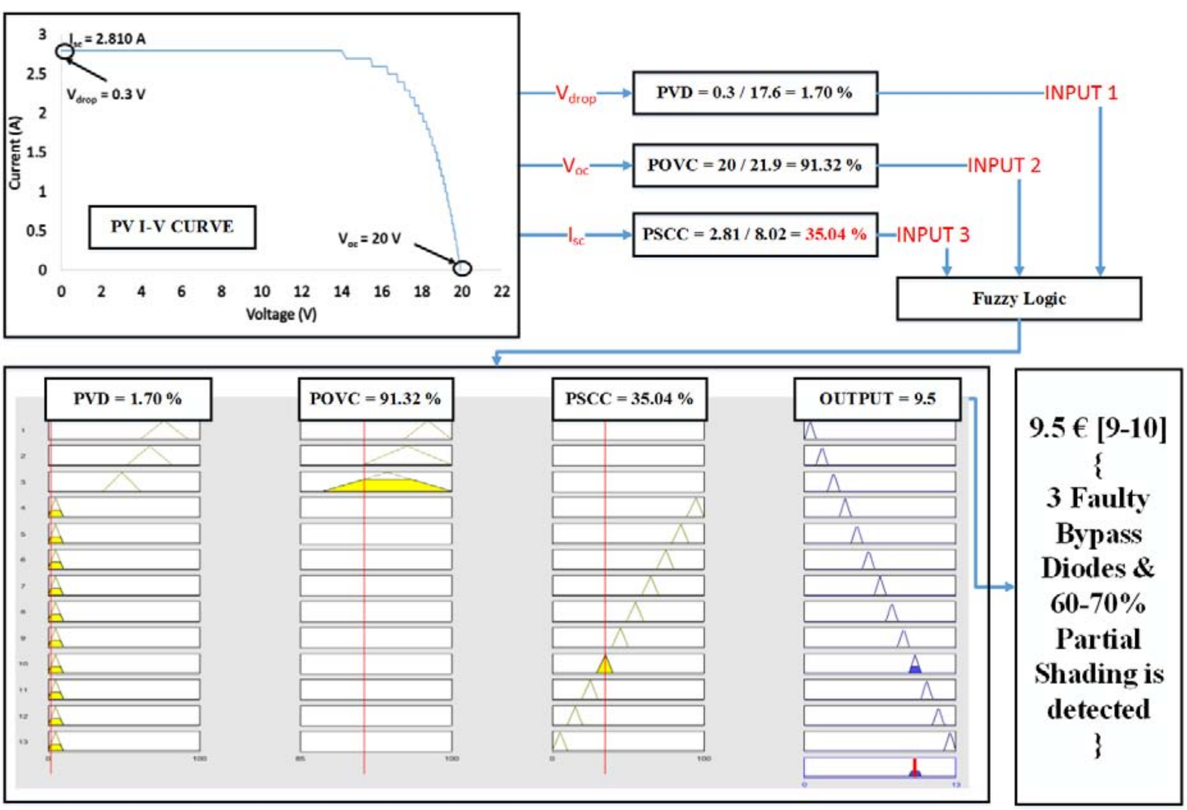


(b)

*Fig. 9:* (a) Output results for 1 faulty bypass diode "case senario1", (b) Output results for 3 faulty bypass diodes & 60-70% partial shading "case scenario 2"

## References Références Referencias


1. Kaldellis, J. K., Kapsali, M., & Kavadias, K. A. (2014). Temperature and wind speed impact on the efficiency of PV installations. Experience obtained from outdoor measurements in Greece. Renewable Energy, 66, 612-624.
2. Eke, R., & Betts, T. R. (2017). Spectral irradiance effects on the outdoor performance of photovoltaic modules. *Renewable and Sustainable Energy Reviews,* 69, 429-434.
3. Dhimish, M., & Holmes, V. (2016). Fault detection algorithm for grid-connected photovoltaic plants. *Solar Energy*, 137, 236-245.
4. Saidan, M., Albaali, A. G., Alasis, E., & Kaldellis, J. K. (2016). Experimental study on the effect of dust deposition on solar photovoltaic panels in desert environment. *Renewable Energy,* 92, 499-505.
5. Ramli, M. A., Prasetyono, E., Wicaksana, R. W., Windarko, N. A., Sedraoui, K., & Al-Turki, Y. A. (2016). On the investigation of photovoltaic output power reduction due to dust accumulation and weather conditions. *Renewable Energy,* 99, 836-844.
6. Dhimish, M., Holmes, V., Mehrdadi, B., & Dales, M. (2017). The Impact of Cracks on Photovoltaic Power Performance. *Journal of Science: Advanced Materials and Devices.*
7. Dolara, A., Lazaroiu, G. C., Leva, S., Manzolini, G., & Votta, L. (2016). Snail trails and cell microcrack impact on PV module maximum power and energy production. *IEEE Journal of Photovoltaics, 6(5),* 1269-1277.
8. Dhimish, M., Holmes, V., Dales, M., & Mehrdadi, B. (2017). The effect of micro cracks on photovoltaic output power: case study based on real time long term data measurements. *Micro & Nano Letters*.
9. Alam, M. K., Khan, F., Johnson, J., & Flicker, J. (2015). A comprehensive review of catastrophic faults in PV arrays: types, detection, and mitigation techniques. *IEEE Journal of Photovoltaics, 5(3),* 982-997.
10. Tsanakas, J. A., Ha, L., & Buerhop, C. (2016). Faults and infrared thermographic diagnosis in operating c-Si photovoltaic modules: A review of research and future challenges. *Renewable and Sustainable Energy Reviews, 62,* 695-709.
11. Takashima, T., Yamaguchi, J., Otani, K., Oozeki, T., Kato, K., & Ishida, M. (2009). Experimental studies of fault location in PV module strings. *Solar Energy Materials and Solar Cells, 93(6),* 1079-1082.
12. Schirone, L., Califano, F. P., & Pastena, M. (1994). Fault detection in a photovoltaic plant by time domain reflectometry. *Progress in Photovoltaics: Research and Applications, 2(1),* 35-44.
13. Dhimish, M., Holmes, V., & Dales, M. (2017). Parallel fault detection algorithm for grid-connected photovoltaic plants. *Renewable Energy,* 113, 94-111.
14. Silvestre, S., da Silva, M. A., Chouder, A., Guasch, D., & Karatepe, E. (2014). New procedure for fault detection in grid connected PV systems based on the evaluation of current and voltage indicators. *Energy Conversion and Management, 86,* 241-249.
15. Vergura, S., Acciani, G., Amoruso, V., Patrono, G. E., & Vacca, F. (2009). Descriptive and inferential statistics for supervising and monitoring the operation of PV plants. *IEEE Transactions on Industrial Electronics, 56(11),* 4456-4464.
16. Miwa, M., Yamanaka, S., Kawamura, H., & Ohno, H. (2006, May). Diagnosis of a power output lowering of PV array with a (-dI/dV)-V characteristic. In *Photovoltaic Energy Conversion, Conference Record of the 2006 IEEE 4th World Conference on* (Vol. 2, pp. 2442-2445). IEEE.
17. Dhimish, M., Holmes, V., Mehrdadi, B., Dales, M., Chong, B., & Zhang, L. (2017). Seven indicators variations for multiple PV array configurations under partial shading and faulty PV conditions. *Renewable Energy*.
18. Lappalainen, K., & Valkealahti, S. (2017). Output power variation of different PV array configurations during irradiance transitions caused by moving clouds. *Applied Energy, 190*, 902-910.
19. Saidan, M., Albaali, A. G., Alasis, E., & Kaldellis, J. K. (2016). Experimental study on the effect of dust deposition on solar photovoltaic panels in desert environment. *Renewable Energy, 92,* 499-505.
20. Ramli, M. A., Prasetyono, E., Wicaksana, R. W., Windarko, N. A., Sedraoui, K., & Al-Turki, Y. A. (2016). On the investigation of photovoltaic output power reduction due to dust accumulation and weather conditions. *Renewable Energy, 99,* 836-844.
21. Dhimish, M., Holmes, V., Mehrdadi, B., & Dales, M. (2017). Diagnostic method for photovoltaic systems based on six layer detection algorithm. *Electric Power Systems Research, 151*, 26-39.
22. Dhimish, M., Holmes, V., Mehrdadi, B., & Dales, M. (2017). Multi-Layer Photovoltaic Fault Detection Algorithm. *High Voltage*.
23. Roy, S. S., Mallik, A., Gulati, R., Obaidat, M. S., & Krishna, P. V. (2017, January). A Deep Learning Based Artificial Neural Network Approach for Intrusion Detection. In *International Conference on Mathematics and Computing* (pp. 44-53). Springer, Singapore.
24. Kow, K. W., Wong, Y. W., Rajkumar, R. K., Rajkumar, R. K., & Isa, D. (2017). Incremental Unsupervised Learning Algorithm for Power Fluctuation Event Detection in PV Grid-Tied Systems. In *9th International Conference on Robotic, Vision, Signal Processing and Power Applications* (pp. 673-679). Springer Singapore.
25. Mallor, F., León, T., De Boeck, L., Van Gulck, S., Meulders, M., & Van der Meerssche, B. (2017). A method for detecting malfunctions in PV solar

panels based on electricity production monitoring. *Solar Energy, 153*, 51-63.
26. Li, Z., Wang, Y., Zhou, D., & Wu, C. (2012). An intelligent method for fault diagnosis in photovoltaic array. *System Simulation and Scientific Computing*, 10-16.
27. Ducange, P., Fazzolari, M., Lazzerini, B., & Marcelloni, F. (2011, November). An intelligent system for detecting faults in photovoltaic fields. In *Intelligent systems design and applications (ISDA), 2011 11th international conference on* (pp. 1341-1346). IEEE.
28. Bonsignore, L., Davarifar, M., Rabhi, A., Tina, G. M., & Elhajjaji, A. (2014). Neuro-fuzzy fault detection method for photovoltaic systems. *Energy Procedia*, 62, 431-441.
29. Dhimish, M., Holmes, V., Dales, M., Mather, P., Sibley, M., Chong, B., & Zhang, L. (2017, June). Fault detection algorithm for multiple GCPV array configurations. In *Power Tech, 2017 IEEE Manchester* (pp. 1-6). IEEE.

## Appendix A

Fuzzy logic system rules:

1. If (PVD is 0-FaultyBypassDiode) and (POCV is 0-FaultyBypassDiode) then (Output is 1) (1)
2. If (PVD is 1-FaultyBypassDiode) and (POCV is 1-FaultyBypassDiode) then (Output is 2) (1)
3. If (PVD is 2-FaultyBypassDiodes) and (POCV is 2-FaultyBypassDiodes) then (Output is 3) (1)
4. If (PVD is 3-FaultyBypassDiodes) and (PSCC is 0-10%PartialShading) then (Output is 4) (1)
5. If (PVD is 3-FaultyBypassDiodes) and (PSCC is 10-20%PartialShading) then (Output is 5) (1)
6. If (PVD is 3-FaultyBypassDiodes) and (PSCC is 20-30%PartialShading) then (Output is 6) (1)
7. If (PVD is 3-FaultyBypassDiodes) and (PSCC is 30-40%PartialShading) then (Output is 7) (1)
8. If (PVD is 3-FaultyBypassDiodes) and (PSCC is 40-50%PartialShading) then (Output is 8) (1)
9. If (PVD is 3-FaultyBypassDiodes) and (PSCC is 50-60%PartialShading) then (Output is 9) (1)
10. If (PVD is 3-FaultyBypassDiodes) and (PSCC is 60-70%PartialShading) then (Output is 10) (1)
11. If (PVD is 3-FaultyBypassDiodes) and (PSCC is 70-80%PartialShading) then (Output is 11) (1)
12. If (PVD is 3-FaultyBypassDiodes) and (PSCC is 80-90%PartialShading) then (Output is 12) (1)
13. If (PVD is 3-FaultyBypassDiodes) and (PSCC is 90-100%PartialShading) then (Output is 13) (1)

Global Journal of Researches in Engineering: F
Electrical and Electronics Engineering
Volume 17 Issue 5 Version 1.0 Year 2017
Type: Double Blind Peer Reviewed International Research Journal
Publisher: Global Journals Inc. (USA)
Online ISSN: 2249-4596 & Print ISSN: 0975-5861

# Review-Reservoir Computing Trend on Software and Hardware Implementation

By Yongbo Liao & Hongmei Li
*University of Electronic Science and Technology of China*

*Abstract-* Since Reservoir Computing proposed, it has progressed in two directions, software and hardware implementation, both sharing the same goal of better performance. While applying on the former, the chosen task is increasingly complex and practical, even blending noise to close to physical situation. Meanwhile, the latter, evaluated by benchmark tasks, is proposed as a compensation of software implementation, which will be utilized for complex and practical tasks in the future when it matures. Here will give a brief introduction of conception, methodology, benchmark tasks, developments and some applications of RC.

*Keywords: reservoir computing, software implementation, hardware implementation.*

*GJRE-F Classification: FOR Code: 290903*

# Review-Reservoir Computing Trend on Software and Hardware Implementation

Yongbo Liao [α] & Hongmei Li [σ]

*Abstract-* Since Reservoir Computing proposed, it has progressed in two directions, software and hardware implementation, both sharing the same goal of better performance. While applying on the former, the chosen task is increasingly complex and practical, even blending noise to close to physical situation. Meanwhile, the latter, evaluated by benchmark tasks, is proposed as a compensation of software implementation, which will be utilized for complex and practical tasks in the future when it matures. Here will give a brief introduction of conception, methodology, benchmark tasks, developments and some applications of RC.

*Keywords: reservoir computing, software implementation, hardware implementation.*

## I. Introduction

Reservoir Computing(RC) has been a preferred research topic when the conception raised for training Recurrent Neural Network (RNN)in the first time. The approach that reinvigorates RNN is a collection of Echo State Network (ESN) [1] and Liquid State Machine (LSM) [2], the former tending to engineering applications while the latter to neurophysiology. RC retains input weights and reservoir weights initialized and only supervised readout weights are trained to obtain excellent performance in many tasks, provided RC possesses certain generic properties. Notably, tasks based on RC model should be time-dependent.

RC is renowned for less time consumption and resource occupancy. Therefore, many researchers attempt to improve existing research results in their arena by applying RC. After survey comprehensively, the research of RC falls into two general categories: software and hardware implementation. In software implementation, the mainstream is exploring a practicability of applying RC in a new arena or an improvement of existing results by RC, while in hardware implementation, the research is more challenge, and so far the aim is building a RC structure on hardware platform and performing simply tasks successfully. With the dedication of researchers, delay-based RC [4] and mask conception [5] emerged and improved hardware implementation.

The emphasis of RC research switches from software to hardware implementation, therefore, this paper will focus on hardware implementation, and will also introduce emerging works based on software implementation as well as some classical benchmark tasks.

## II. RC Methodology

Before introduce implementation, the basic knowledge of RC should be mentioned. In consideration of that every works related to RC involving basic RC idea, here will briefly and concisely introduce basic knowledge of RC and list out key equations.

The first key equation is reservoir state update equation, which is slightly alterable due to researcher's thoughts and the actual task. The classic reservoir state update equation [1] is as simply as:

$$\mathbf{x}(n+1) = f(\mathbf{W}^{in}\mathbf{u}(n+1) + \mathbf{W}\mathbf{x}(n) + \mathbf{W}^{back}\mathbf{y}_{target}(n)) \quad (1)$$

For the sake of a better dynamic behavior, a complex reservoir state update equation with a leaky integration [1, 6] is proposed as:

$$\mathbf{x}(n+1) = (1-a)\mathbf{x}(n) + f(\mathbf{W}^{in}\mathbf{u}(n+1) + \mathbf{W}\mathbf{x}(n) + \mathbf{W}^{back}\mathbf{y}_{target}(n)) \quad (2)$$

where n is discrete time, $\mathbf{u}(n+1) \in \mathbf{R}^{N_u}$ is the input signals, $\mathbf{x}(n) \in \mathbf{R}^{N_x}$ is the reservoir states, $\mathbf{y}_{target}(n) \in \mathbf{R}^{N_y}$ is the target output signals applied for producing error feedback by comparing with signals calculated by readout output equation, f(· )is a nonlinear continuous function, typically sigmoid or hyperbolic tangent function, $\mathbf{W}^{in} \in \mathbf{R}^{N_x \times N_u}$, $\mathbf{W} \in \mathbf{R}^{N_x \times N_x}$ and $\mathbf{W}^{back} \in \mathbf{R}^{N_x \times N_y}$ are the input weight matrix, reservoir weight matrix and the output feedback weight matrix respectively, indicating the connections among nodes. And parameter a in equation (2) is a leaky integration constant confined in the range of 0 to 1.

The second key equation is readout output equation [1]:

$$\mathbf{y}(n+1) = f_{out}(\mathbf{W}^{out}(\mathbf{u}(n+1), \mathbf{x}(n+1), \mathbf{y}(n))) \quad (3)$$

where $\mathbf{y}(n) \in \mathbf{R}^{N_y}$ is the readout output signals, $f_{out}$(· )is a linear continuous function, typically identity function, $\mathbf{W}^{out} \in \mathbf{R}^{N_y \times (N_u + N_x)}$ is output weight matrix, $(\mathbf{u}(n+1), \mathbf{x}(n+1), \mathbf{y}(n))$ is the concatenation of the input signals, reservoir state and previous readout output vectors.

*Author α: University of Electronic Science and Technology of China, School of Energy Science and Engineering, State key Laboratory of Electronic Thin Films and Integrated Devices, Chengdu 611731, People's Republic of China. e-mail: lyb@uestc.edu.cn*
*Author σ: University of Electronic Science and Technology of China, School of Energy Science and Engineering*
*e-mail: lhm3551@qq.com*

The third key equation is training output weight matrix [1], which calculated by equation (1) via ridge regression as (there assumes **y** equals to $\mathbf{y}_{target}$, i.e. error is zero) [1]:

$$\mathbf{W}^{out} = \mathbf{Y}_{target}\mathbf{X}^{T}(\mathbf{X}\mathbf{X}^{T}+\alpha^{2}\mathbf{I})^{-1} \qquad (4)$$

where Y target is the collection of y target(n+1), X is the collection of (u(n+1),x(n+1)), I is identity matrix and **α** is regularization parameter which is applied for the optimization of RC structure. $(\bullet)^{-1}$ is matrix inversion.

The final equation is a normalized root-mean-square error (NRMSE)[7], which should be minimized during the training, also as a typical standard measures results:

$$E(\mathbf{y},\mathbf{y}_{target}) = \sqrt{\frac{<\|\mathbf{y}(n)-\mathbf{y}_{target}(n)\|^{2}>}{<\|\mathbf{y}_{target}(n)-<\mathbf{y}_{target}(n)>\|^{2}>}} \qquad (5)$$

where ||· || stands for the Euclidean distance, and <· > for mean function.

## III. Preprocessing

Before feeding data into RC system, raw data should be preprocessed to meet some index for a higher performance expectation. To our knowledge, the present existing preprocessing approaches are normalization, masking and Fourier transformation of images.

Normalization preprocessing. Normalization is an approach preferred in preprocessing, benefitted from its simplicity. There are several advantages in adopting normalization preprocessing, which can be exemplified by conveniently processing data, accelerating network training, improving network stability and making the average of input data close to zero or possessing a smaller mean square error. The basic concept of this approach is limiting the amplitude of the input data to the range of 0 to 1 or -1 to 1. After training and obtaining the normalization output data, anti-normalization should be applied on them to obtain genuine output data.

Masking preprocessing. There are two masking approaches including digital binary mask [5, 8] and analog chaos mask [5], both are periodic mask and emerge for delay-based RC based on semiconductor laser subjected to optical feedback and injection. Masking preprocessing can be expressed as [5]:

$$M(\mathrm{t}) = \mathrm{mask}(\mathrm{t})\times \mathrm{u}(n)\times\gamma \qquad (7)$$

where M(t) stands for masked signal, mask(t) for mask signal with a periodicity T, and $\gamma$ for scaling factor.

In [8], Schneider explained how to conduct the preprocessing of digital binary mask in detail, holding input signal a sample time by a zero-order holder which produces a piecewise-constant signal, subsequently doing periodic amplitude modulation on piecewise-constant signal by a mask signal whose periodicity equals to sample time. In [9], Tezuka simplified the digital binary mask by utilizing a step waveform as a mask signal at the cost of losing variability. In [5], Nakayama introduced analog chaos mask which differs to digital binary mask approach in mask signal. Indeed, he compared this two mask approaches in prediction task and the results are similar to original signals in both cases but response in analog case is more complex and error is smaller.

## IV. Training

The essence of the training is computing the weight matrix $W^{out}$ by given input driven signals and target readout output signals while other weight matrixes $W^{in}$, W, $W^{back}$ keep fixed. Note that, regularization parameter **α** is also fixed after it is determined by optimal strategy. After $W^{out}$ is determined, feeding the input signals, harvesting the corresponding output readout signals, and calculating the NRMSE.

The values of fixed weight matrix $W^{in}$, W and $W^{back}$ are arbitrarily initialized by random number generator or Gaussian probability distribution [10] depending on specific circumstances. Once determined, they keep unchanged in the whole training and testing duration.

While the number of the reservoir internal nodes is arbitrarily determined, it should satisfy two constraints, i.e. the structure should be as simple as possible which means the number of reservoir nodes should be small, the another is the NRMSE should be sufficiently small which needs reservoir to be complex and large contrary to the aforementioned constraint [11]. Therefore, a compromise scheme indicating the optimal number of reservoir nodes is considered in experiment.

Training algorithm varies with different applications, but the variation merely is function selection, staying the basic concept unchanged. In electrocardiogram classification application [11], logistic regression algorithm was applied to cope readout process. In multiclass prediction[10], support vector machine was utilized to replace the traditional linear readout layer. In visual contents detection [12], traditional algorithm hyperbolic tangent function was applied. There is another typical function frequently used, namely sigmoid function also called S function.

## V. Benchmark Tasks

Benchmark tasks are frequently harnessed to evaluate upgraded reservoir computing structure in many masterpiece works, indicating benchmark tasks possess a vital place in RC research. Therefore, subsequent contents within this section are center on benchmark tasks.

The extremely popular benchmark task is time series prediction due to the time-dependent property, including Mackey Glass chaotic time series prediction [13] and Santa-Fe time series prediction [14, 9]. The other long-standing benchmark task is classification covering simple signal classification. Recognition benchmark task is also noticeable, such as isolated spoken digit recognition and digital handwriting recognition[8]. Meanwhile, there are other frequently harnessed benchmark tasks such as the 10th order nonlinear auto regressive moving average (NARMA) system [13, 15, 4], 5-Bit Parity [4] and nonlinear channel equalization [14, 15, 16].

## VI. Application

RC approaches has been widely applied in academic arena. These application spans from bioscience field (in this field RC named LSM) to engineering domain (in this field RC named ESN) that are amenable to supervised model. Meanwhile, the platform constructing the neural network model has transited from software to hardware.

What follows is the application of RC in the last three years.

Classification. Since the classification application will not confine to simple task, the development direction is achieving complex real-time task. One of the examples is electrocardiogram classification [11], where the novel reservoir computing with logistic regression was applied, instead of standard reservoir computing with linear regression. The methodology requires a computationally inexpensive preprocessing of the electrocardiographic signals, which leads to a fast algorithm, approaching a real-time classification solution. Another is classifying three types of wind power ramp events (WPRE)[17] by ESN with support vector machine (SVM), to be specific, ESN for WPRE recognition and SVM for WPRE classification and training this novel model for multiple WPRE prediction.

Recognition. With the passage of time, the recognition contents are increasingly widespread. In [18], a visual contents obtained by a surveillance camera was for detecting the status of a door by a leaky integration RC. In [19], High speed recognition of dispersive Fourier images was achieved by a photonic RC system. In [20], activity recognition, which is vital in activity assistance and smart homes, was achieved by appropriate configuration of RC with low cost and good accuracy.

Prediction. The most research about prediction is temporal task. As the RC technology matures, forecasting short-term stream flow [21], wind power ramp events [17] and BBS score via balance assessment [22] become increasingly accurate. In line with minimizing downstream flood damage and maximizing the generated power with low costs, Bezerra[21] devoted to water source study and attempt to short-term stream flow forecasting with the aid of RC model, which do achieve better performance than traditional approaches. In [17], Manuel investigated alleviating the impact of wind power ramp events by forecasting it via RC model that was modified slightly for better performance. Reference [22] devoted to improving health monitoring in the elderly, Gallicchio conducted measurement campaign on elderly volunteers and obtained Balance dataset including weight value recorded by Wii Balance Board and target BBS score. The whole experiment was conducted on a variant of RC model, a leaky integration Echo State Network model suitable for dealing with the characteristics of the temporal data generated from sensors.

Optical implementation. Semiconductor laser based on optical feedback and injection due to its potential high speed processing capacity repeatedly serves for perfecting RC model. Respecting to how to apply laser, idea differs to everyone. Harnessing only one drive laser converting input signals into optical signals [23, 24, 25], or two lasers including a drive laser and a response laser [5], or nanophotonic crystal cavities [26] diminishing model size, or a ring laser simultaneously computing two unrelated input signals [27], or a mutually coupled optoelectronic system compensating slowly masking preprocess [9], is the response of aforementioned different applying ideas, which will increase with researchers' unremitting efforts. While adding optical implementation in RC model reaps great performance, classic readout layer may need necessary alters for specific optical methods. Coupling to an analogelectronic readout eliminates offline post-processing [23].In [26], the approach about design full optical readout layer is a problem urgently solved.

## References Références Referencias


1. Jaeger, H. (2010). The " echo state " approach to analysing and training recurrent neural networks – with an Erratum note 1. GMD Report, (148), 1–47. https://doi.org/citeulike-article-id:9635932.
2. Maass, W., Natschl, Ger, T., & Markram, H. (2002). Real-time computing without stable states: a new framework for neural computation based on perturbations. Neural Computation, 14(11), 2531-2560.
3. Yi, Y., Liao, Y., Wang, B., Fu, X., Shen, F., Hou, H., & Liu, L. (2015). FPGA based spike-time dependent encoder and reservoir design in neuromorphic computing processors. Microprocessors and Microsystems, 46, 175–183. https://doi.org/10.1016/j.micpro.2016.03.009.
4. Schumacher, J., Toutounji, H., & Pipa, G. (2015). An Introduction to Delay-Coupled Reservoir

Computing. Artificial Neural Networks. Springer International Publishing.

5. Nakayama, J., Kanno, K., & Uchida, A. (2016). Laser dynamical reservoir computing with consistency: an approach of a chaos mask signal. Optics Express, 24(8), 8679. https://doi.org/10.1364/OE.24.008679.
6. Lun, S. X., Yao, X. S., Qi, H. Y., & Hu, H. F. (2015). A novel model of leaky integrator echo state network for time-series prediction. Neurocomputing, 159(1), 58-66.
7. Lukoševičius, Mantas, & Jaeger, H. (2009). Survey: reservoir computing approaches to recurrent neural network training. Computer Science Review, 3(3), 127-149.
8. Schneider, B., Dambre, J., & Bienstman, P. (2016). Using digital masks to enhance the bandwidth tolerance and improve the performance of on-chip reservoir computing systems. IEEE Transactions on Neural Networks & Learning Systems, 27(12), 1-6.
9. Tezuka, M., Kanno, K., & Bunsen, M. (2016). Reservoir computing with a slowly modulated mask signal for preprocessing using a mutually coupled optoelectronic system. , 55(8S3), 08RE06.
10. Manuel Dorado-Moreno, Antonio Manuel Dur´an-Rosal, David Guijo-Rubio, Pedro Antonio Guti´Errez1, L. P., Sancho Salcedo-Sanz, and C., & As-Mart´, esar H. (2016). Multiclass Prediction of Wind Power Ramp Events Combining Reservoir Computing and Support Vector Machines. Canadian Conference on AI, 9868, 300–309. https://doi.org/10.1007/978-3-319-44636-3_28
11. Escalona-Morán, M. A., Soriano, M. C., Fischer, I., & Mirasso, C. R. (2015). Electrocardiogram classification using reservoir computing with logistic regression. IEEE Journal of Biomedical and Health Informatics, 19(3), 892–898. https://doi.org/10.1109/JBHI.2014.2332001
12. Jalalvand, A., Wallendael, G. Van, & Walle, R. Van De. (2015). Real-Time Reservoir Computing Network-Based Systems for Detection Tasks on Visual Contents. Proceedings - 7th International Conference on Computational Intelligence, Communication Systems and Networks, CICSyN 2015, 146–151. https://doi.org/10.1109/CICSyN.2015.35
13. Scardapane, S., Panella, M., Comminiello, D., Hussain, A., & Uncini, A. (2016). Distributed reservoir computing with sparse readouts [research frontier]. IEEE Computational Intelligence Magazine, 11(4), 59-70.
14. Modeste Nguimdo, R., Verschaffelt, G., Danckaert, J., & Van Der Sande, G. (2015). Simultaneous computation of two independent tasks using reservoir computing based on a single photonic nonlinear node with optical feedback. IEEE Transactions on Neural Networks and Learning Systems, 26(12), 3301–3307. https://doi.org/10.1109/TNNLS.2015.2404346
15. Vinckier, Q., Duport, F., Smerieri, A., Massar, S., & Haelterman, M. (2016). Autonomous bio-inspired photonic processor based on reservoir computing paradigm. IEEE 2016 Summer Topicals Meeting Series. IEEE.
16. Appeltant, L., Soriano, M. C., Sande, G. V. D., Danckaert, J., Massar, S., & Dambre, J., et al. (2011). Information processing using a single dynamical node as complex system. Nature Communications, 2(9), 468.
17. Manuel Dorado-Moreno, Antonio Manuel Dur´an-Rosal, David Guijo-Rubio, Pedro Antonio Guti´Errez1, L. P., Sancho Salcedo-Sanz, and C., & As-Mart´, esar H. (2016). Multiclass Prediction of Wind Power Ramp Events Combining Reservoir Computing and Support Vector Machines. Canadian Conference on AI, 9868, 300–309. https://doi.org/10.1007/978-3-319-44636-3_28
18. Jalalvand, A., Wallendael, G. Van, & Walle, R. Van De. (2015). Real-Time Reservoir Computing Network-Based Systems for Detection Tasks on Visual Contents. Proceedings - 7th International Conference on Computational Intelligence, Communication Systems and Networks, CICSyN 2015, 146–151. https://doi.org/10.1109/CICSyN.2015.35
19. Mesaritakis, C., Bogris, A., Kapsalis, A., & Syvridis, D. (2015). High-speed all-optical pattern recognition of dispersive fourier images through a photonic reservoir computing subsystem. Optics Letters, 40(14), 3416-3419.
20. Palumbo, F., Gallicchio, C., Pucci, R., & Micheli, A. (2015). Human activity recognition using multisensor data fusion based on reservoir computing. Journal of Ambient Intelligence & Smart Environments, 8(2), 87--107.
21. Bezerra, S. G. T. A., Andrade, C. B. D., & Valença, M. J. S. (2016).Using Reservoir Computing and Trend Information for Short-Term Stream flow Forecasting. Artificial Neural Networks and Machine Learning – ICANN 2016.
22. Gallicchio, C., Micheli, A., Pedrelli, L., Fortunati, L., Vozzi, F., & Parodi, O. (2016). A Reservoir Computing Approach for Balance Assessment. Advanced Analysis and Learning on Temporal Data. Springer International Publishing.
23. Vinckier, Q., Duport, F., Smerieri, A., Massar, S., & Haelterman, M. (2016). Autonomous bio-inspired photonic processor based on reservoir computing paradigm. IEEE 2016 Summer Topicals Meeting Series. IEEE.
24. Takeda, S., Nakano, D., Yamane, T., Tanaka, G., Nakane, R., & Hirose, A., et al. (2016). Photonic Reservoir Computing Based on Laser Dynamics

with External Feedback. Neural Information Processing. Springer International Publishing.

25. Nguimdo, R. M., Lacot, E., Jacquin, O., Hugon, O., Van, d. S. G., & Guillet, d. C. H. (2017). Prediction performance of reservoir computing systems based on a diode-pumped erbium-doped microchip laser subject to optical feedback. Optics Letters, 375-378.
26. Salehi, M. R., & Dehyadegari, L. (2016). Nanophotonic reservoir computing for noisy speech recognition. Optical and Quantum Electronics, 48(5), 1-18.
27. Nguimdo, R. M., Verschaffelt, G., Danckaert, J., & Van, d. S. G. (2015). Simultaneous computation of two independent tasks using reservoir computing based on a single photonic nonlinear node with optical feedback. IEEE Trans Neural Netw Learn Syst, 26(12), 3301.

This page is intentionally left blank

Global Journal of Researches in Engineering: F
Electrical and Electronics Engineering
Volume 17 Issue 5 Version 1.0 Year 2017
Type: Double Blind Peer Reviewed International Research Journal
Publisher: Global Journals Inc. (USA)
Online ISSN: 2249-4596 & Print ISSN: 0975-5861

# Numerical Analysis of Electrical Characteristics in a Squared Channel EHD Gas Pump

By Rezaur Rahman & Dr. A. K. M Monayem Hossain Mazumder
*Lamar Univeristy, United States*

*Abstract-* Corona discharge characteristic is highly dependable on working medium, the system setup, and the ambient condition. With a numerical analysis, the impact of high voltages on the electrical characteristics during EHD (electro hydrodynamic) pumping in a square channel is investigated with a wide range of high applied voltages. The conductor setup is settled with three types of pin configuration. Also, each conductor is tested for three different width ground plates. Simulation model consists of a conductor, ground plate, and square flow channel (6.0-inch). The material for the square channel is glass; copper is selected for both conductor and ground plate. The results of the numerical study showed that the use of different numbers of conductor pin and change in ground plate width have a great impact on the EHD electrical characteristics with a significant deviation of forces on ground plate, conductor, test region and square channel are found.

*Keywords: corona wind, electrohydrodynamic, ionic flow, ansoff maxwell, numerical analysis, FEM, force flow.*

*GJRE-F Classification: FOR Code: 090699*

NUMERICALANALYSISOFELECTRICALCHARACTERISTICSINASQUAREDCHANNELEHDGASPUMP

*Strictly as per the compliance and regulations of:*

# Numerical Analysis of Electrical Characteristics in a Squared Channel EHD Gas Pump

Rezaur Rahman α & Dr. A.K.M Monayem Hossain Mazumder σ

*Abstract-* Corona discharge characteristic is highly dependable on working medium, the system setup, and the ambient condition. With a numerical analysis, the impact of high voltages on the electrical characteristics during EHD (electro hydrodynamic) pumping in a square channel is investigated with a wide range of high applied voltages. The conductor setup is settled with three types of pin configuration. Also, each conductor is tested for three different width ground plates. Simulation model consists of a conductor, ground plate, and square flow channel (6.0-inch). The material for the square channel is glass; copper is selected for both conductor and ground plate. The results of the numerical study showed that the use of different numbers of conductor pin and change in ground plate width have a great impact on the EHD electrical characteristics with a significant deviation of forces on ground plate, conductor, test region and square channel are found.

*Keywords: corona wind, electrohydrodynamic, ionic flow, ansoff maxwell, numerical analysis, FEM, force flow.*

## I. Introduction

When a gas discharged from the place where geometry confines the gas ionizing processes to high-field ionization regions around an active electrode [1](Goldman, A. Goldman, and Sigmond, 1985). The American Standards Association defines "Corona is a luminous discharge due to ionization of the air surrounding a conductor around which, exists a voltage gradient exceeding a certain critical value" [2](What is Corona? Hubbell Power System, 2004).

So far two types of flow generated per the working principle. One is displacement type and another one is a dynamic type[3] (Laser and Santiago, 2004) which distinguishes between the reciprocating and continuous flow [4](Chen, 2005).

Corona discharge mainly occurred with two asymmetric electrodes, one of its very sharp on curvature shape (needle, pin or wire) and another one has a very curvy geometry (rod or plate). The curved electrode contains a very high charge potential which is created by supplying a very high voltage from an outer source. By creating a plasma state, the electrode with high curvature ionized the nearest gas molecules which tend to migrate to the ground low curved electrode and this procedure is fully controlled by Coulomb force. Coronas can be either positive or negative. The voltage supplied to the curved electrode determines whether it is positive or negative. If the voltage supplied to the electrode is positive the corona discharge is positive otherwise it is negative if the supplied voltage is negative.

The ionized ions generate thrust on the other molecules near them by creating a collision while they try to move to the ground plate (low curved electrode). This continuous migration process creates a bulk flow, which is called ionic wind or corona wind (Fig 1).

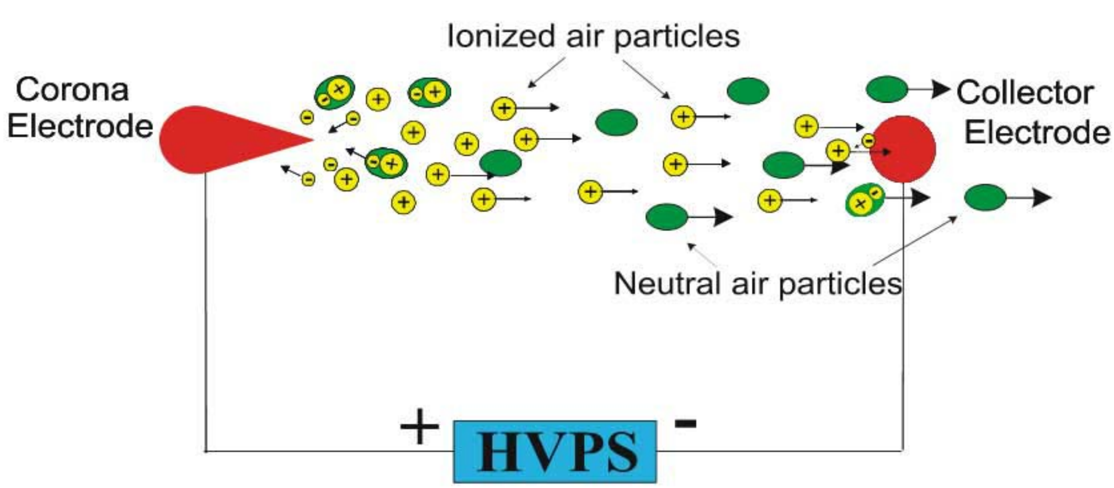


*Figure 1:* A basic schematic diagram for Corona wind generation with corona discharge[5](Genuth, 2013).

*Author α σ: Lamar University, USA. e-mail: rezas.arena@gmail.com*

## II. Experimental Setup

The main design parameters followed here is the same as[6] (Mazumder and Lai, 2014), two stage EHD pumping procedure, but for this type of study, we only consider a single stage model. A glass box is the main structure where the other apparatuses are mounted. This box also works as a passage to the EHD flow which is induced after providing very high voltage and reaches the initial limit. Other main two parts of this setup are a conductor (emitter pin) and ground plate.

In this study, the whole design procedure is done using PTC Creo Parametric 3.0 m010. The main glass box is taken with an inner dimension of 4 in by 4 in by 12 in. The thickness of the glass is 0.25 inches. The conductor is made with copper material of 20 GA which gives this wire a diameter of .032 inches. The Ground plate thickness is 0.025 inches. The emitter pin is also made with the same copper wire and their length is 1.0 inches from the top to the ground plate. Whole conductor setup is attached to the glass box just 1.0 inches below the top of the box see fig 2.6. The gap between the conductor and ground plate is 2.5 inches that also concludes that the pin end point to the ground plate beginning is 1.5 inches (Fig 2.6), this gap is necessary to achieve the successful EHD pumping. Three types of the ground plate, as well as three types of conductor setup, are used in this study. The ground plate with a height of 0.5 inch, 1.0 inch and 2.0 inch and conductor with 4 pins, 12 pins, and 28 pin emitters are considered and designed for this numerical analysis process.

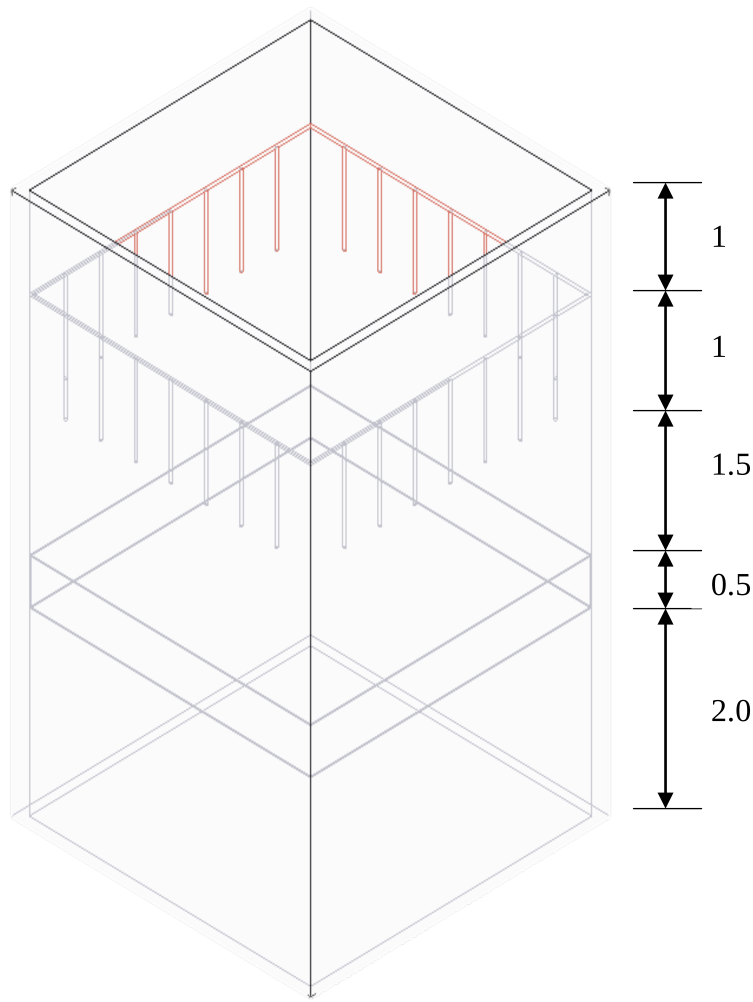


*Figure 2:* Schematic figure of 28 pin conductor setup with a 0.5-inchgroundplate.

Cases of study

4 pin conductor with 0.5 inch of groundplate.
4 pin conductor with 1.0 inch of groundplate.
4 pin conductor with 2.0 inch of groundplate.
12 pin conductor with 0.5 inch of groundplate.
12 pin conductor with 1.0 inch of groundplate.
12 pin conductor with 2.0 inch of groundplate.
28 pin conductor with 0.5 inch of groundplate.
28 pin conductor with 1.0 inch of groundplate.
28 pin conductor with 2.0 inch of groundplate.

## III. Theory and Simulation Set Up

The electrostatic theory is derived from Gauss's Law and from Faraday's law of induction. Gauss's Law shows that the net electric flux passing through any closed surface is equal to the net positive charge enclosed by that surface. This derives that in differential format

$$\nabla \cdot D = \rho \tag{1}$$

Here $D$ (x, y) is the charge density. We also know that the charge density can be pulled out by multiplying the relative permittivity $\varepsilon_r$, $\varepsilon_o$ is the permittivity of free space, $8.854 \times 10^{-12}$ F/m and Field Intensity $E$. So, we can conclude with another equation:

$$D = \varepsilon_r \cdot \varepsilon_o \cdot E \tag{2}$$

With the help of Faraday's law of induction, it is known that

$$E = -\nabla \cdot \phi \tag{3}$$

Where $\phi$ (x,y) is the electric potential.
So, the final field equation is

$$\nabla \cdot (\varepsilon_r \cdot \varepsilon_o - \nabla \cdot \phi(x,y)) = -\rho \tag{4}$$

This is the equation that the electrostatic field simulator solves using the finite element method.

To analyze the results a datum line is created by Maxwell just in the middle of the model with a total height of 6-inch top to bottom. This datum line is used to create the data plots after finishing the simulation process. Also, parameters like force, torque, and matrix distribution are set up on each part of the model to get the final output after final pass in the simulation process. An empty box is created just in the middle of the main canal to cover the highest maximum volume to get a visual of voltage, charge, electric field distribution after completing the simulation work.

Solution setup is the main part before starting the solution, where we can put the percentage of error, we will allow in this particular study with the number of passes allowed. Here we put the percentage of error allowed is 0.5 % with a number of passes 10 for all cases. So, the Maxwell software will perform the passes till it reaches the error percentage allowed. If we put the whole procedure in a flow chart we can conclude with the below flow chart.

## IV. Results and Discussion

Electric Field Intensity

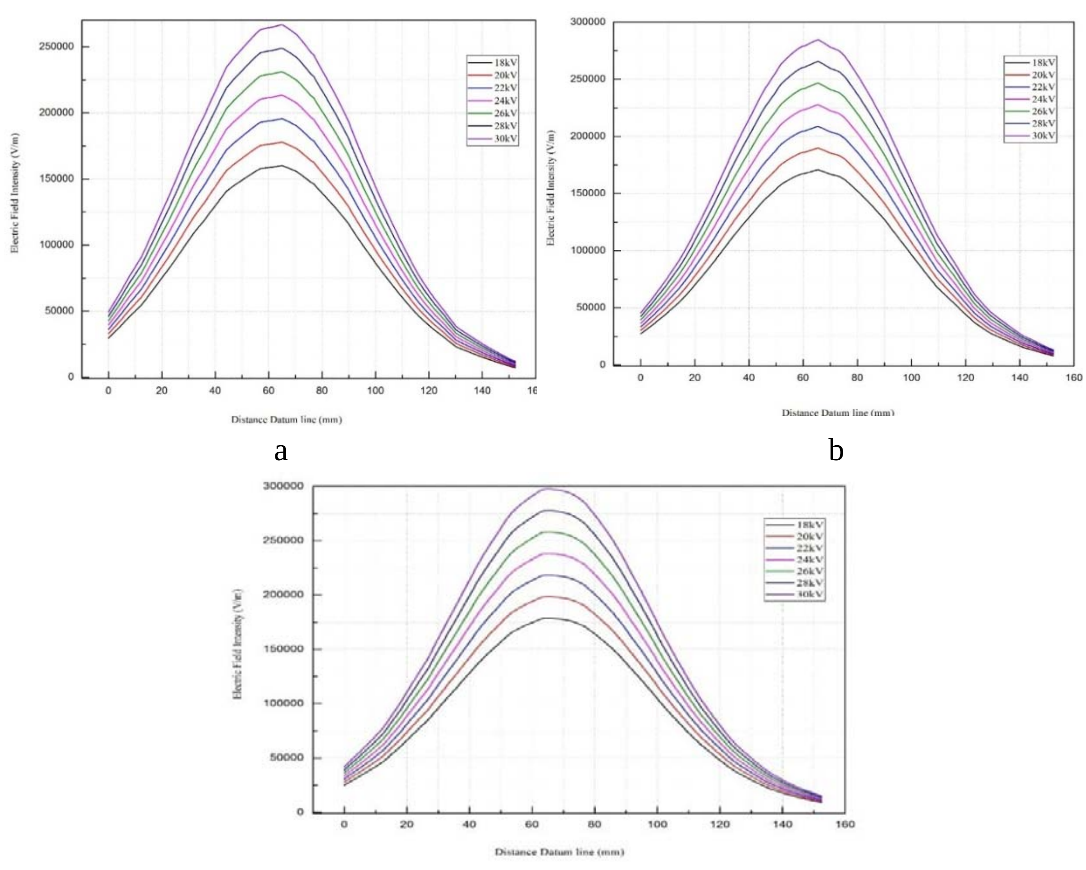


*Figure 3:* Electric field intensity (v/m) distribution with 0.5-inch ground plate along the datum line (a) for 4 pin emitter (b) for 12 pin emitter (c) for 28 pin emitter

The use of the different height of ground plate poses different lines in the graph which also represents the change of electric field intensity. The replacement of ground plate with larger width shows a greater range of field intensity with the same amount of voltage input.

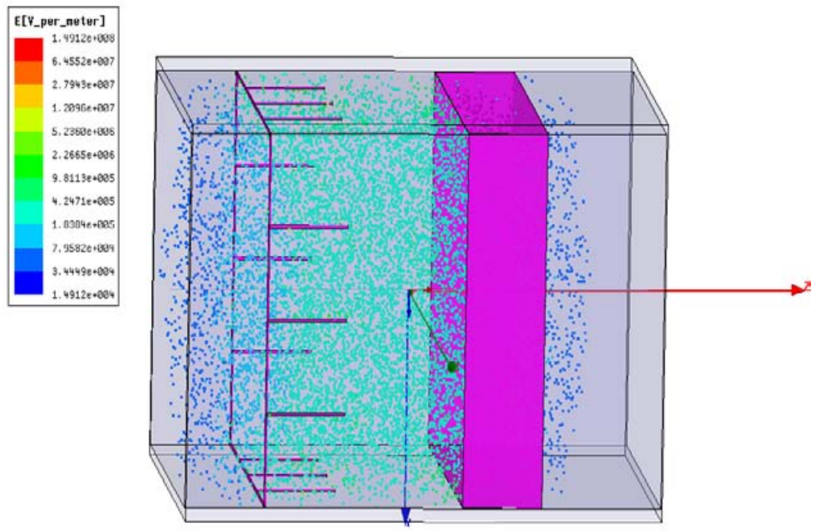


a

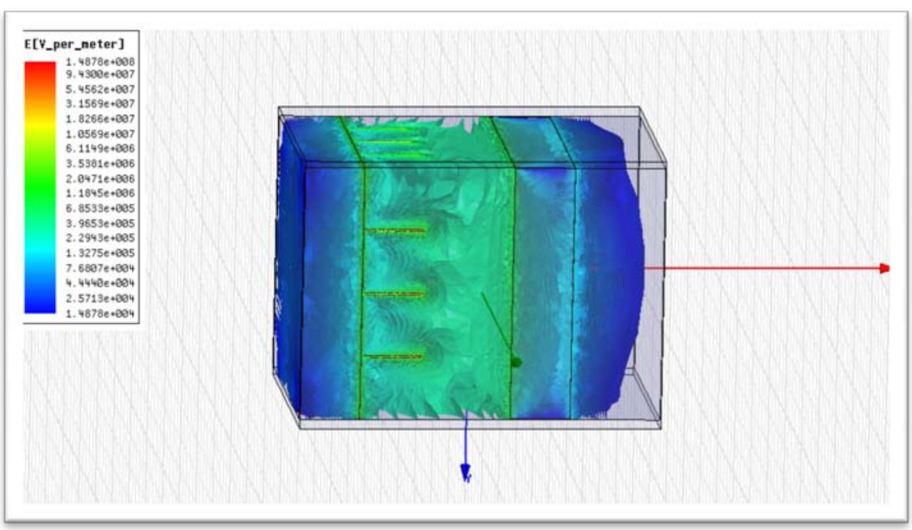


b

*Figure 4:* Electric field intensity distribution in for 12 pin, 1.0-inch ground plate 24 kV applied voltage (a) Cloud view (b) Isovalsurface view

From figure 4 observation, which the same setup in field overlay with a much detail view, it is found the air near the conductor pin have greater field intensity than the air on the top and bottom of the passage. Also, the highly intense field layer is also found on the top on the ground plate. The top part of the ground plate portion remarkably carries high electrical field intensity though the input voltage in this portion is 0 kV. It indicates that the charged ionic air near the conductor jumps to the ground plate. The migrated air particles are causing the ionic wind and the flow of fluid medium in the canal.

## V. Highest Field Intense Position

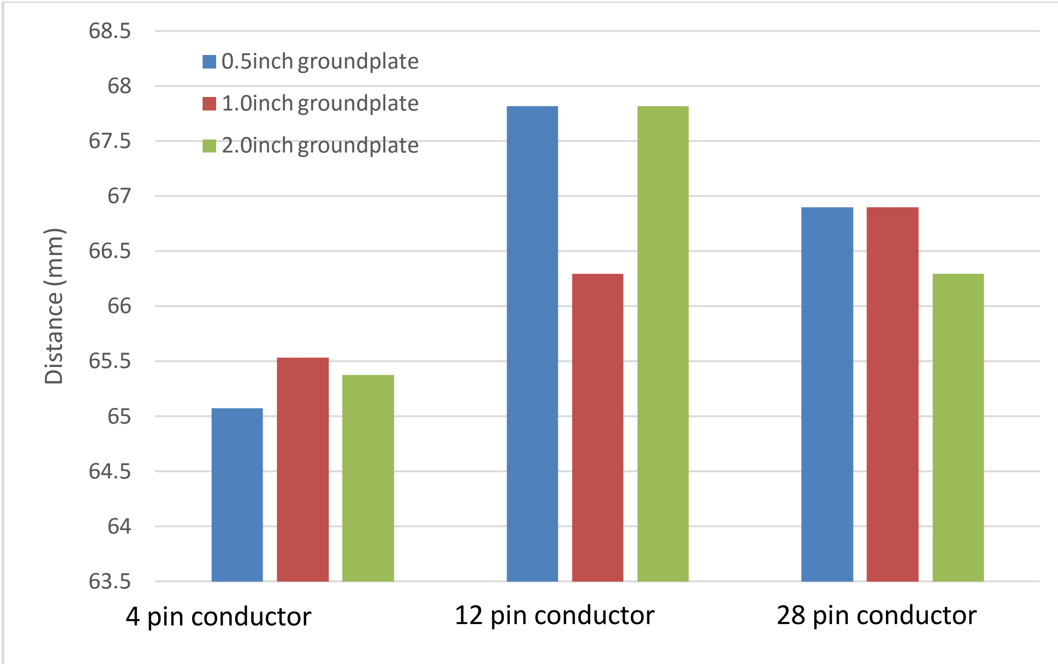


*Figure 5:* Highest field intensity points from the top of the channel

For each type of Ground plate setup, it is created single case, so for 0.5-inch, 1.0-inch and 2.0-inch ground plate 3 types of pin combination taken each time to build 3 fields of study. For 0.5-inch ground plate the far most position found for 12 pin conductor set up and closest found for 4 pin conductor. 1.0-inch ground plate setup showed interesting data that both 4 and 28 pin setup have the same point of highest intensity, but both of them went far from the point they have for 4 pin setup, 12 pin setup in this case lacked behind from both of them and created the point nearest to the top with an increase from 0.5-inch ground plate setup. 2.0-inch ground plate with 4 pin conductor has far most and 28 pin conductor closest points of electric field. So, it can be concluded from table 4.1 that the far most point found for the 1.0-inch ground plate with 4 and 28 pin conductor setup.

## VI. Forces on Test Region

It is already discussed that the test region is created inside the channel and the material is assigned as Air to see the impact inside the channel which also worked as a working fluid domain. The table 4.2 indicates that the forces in X-axis for 4 pins are always negative and comparatively larger than 12 pin and 28 pin conductor. As the concern is the forces acting in the positive Z-axis direction as it has the potential to create the force which can drive the fluid from top to bottom of the channel. For 4 and 12 pin the Z direction force is larger, but it is negative, which means a very poor or negative potential to create the flow in the Z direction. Found forces here are very low compared to the forces created in other parts of the experimental domain. For each pin set up for every direction despite their positivity forces increase with the increase of voltage applied. The maximum total force found in the 12 pin conductor setup which is 230 $\mu$N. As the forces in X or Y or Z axis found negative in different cases which mean the force is not exerting on the outside of the channel it basically creating a collision within the region. For 4 and 12 pin the X and Z axis force pushing inwards whereas the Y axis forces are exerting on the region wall.

*Table 1:* Force distribution for 0.5-inch ground plate in test region

| Voltage | $F_{XY}$ Force ($\mu$N) | $F_Y$ Force ($\mu$N) | $F_Z$ Force ($\mu$N) | Total Force ($\mu$N) | Conductor Typed |
|---|---|---|---|---|---|
| 18 | -59.437 | 26.893 | -12.602 | 66.444 | |
| 20 | -73.379 | 33.201 | -15.558 | 82.029 | |
| 22 | -88.788 | 40.174 | -18.825 | 99.255 | |
| 24 | -105.67 | 47.81 | -22.404 | 118.12 | |
| 26 | -124.01 | 56.11 | -26.293 | 138.63 | 4 Pin Conductor |
| 28 | -143.82 | 65.075 | -30.494 | 160.78 | |
| 30 | -165.1 | 74.703 | -35.006 | 184.57 | |

| | | | | | |
|---|---|---|---|---|---|
| 18 | -6.3726 | 81.071 | -16.404 | 82.959 | 12 Pin Conductor |
| 20 | -7.8674 | 100.09 | -20.252 | 102.42 | |
| 22 | -9.5195 | 121.11 | -24.505 | 123.93 | |
| 24 | -11.329 | 144.13 | -29.163 | 147.48 | |
| 26 | -13.296 | 169.15 | -34.226 | 173.09 | |
| 28 | -15.42 | 196.17 | -39.695 | 200.74 | |
| 30 | -17.702 | 225.2 | -45.568 | 230.44 | |
| 18 | -49.719 | -19.857 | 1.1611 | 53.55 | 28 Pin Conductor |
| 20 | -61.381 | -24.515 | 1.4335 | 66.111 | |
| 22 | -74.271 | -29.663 | 1.7345 | 79.994 | |
| 24 | -88.389 | -35.301 | 2.0642 | 95.2 | |
| 26 | -103.73 | -41.43 | 2.4226 | 111.73 | |
| 28 | -120.31 | -48.049 | 2.8096 | 129.58 | |
| 30 | -138.11 | -55.158 | 3.2253 | 148.75 | |

## VII. Conclusion

The present study has investigated the electrical characteristics of a square channel single stage EHD pump. Three types of conductor (4, 12, 28 pin) are created and each conductor have three (0.5-inch, 1.0-inch and 2.0-inch) ground plate set up with the glass channel. A lost voltage always found for every applied voltage in a conductor. The pattern of the charge distribution, electric field distribution and energy distribution are same along the datum line. All the simulations are converged within the selected maximum number of pass and energy error percentage (0.5 %). Tetrahedral meshes are created by the adaptive meshing system in each validation pass. For the same number of pins if the width of ground plate is increased the percentage of ionized air is increased. For the same ground plate width, it is found that the ionized air is increased if the pin number in conductor increased. The electric field intensity is increased by the increment of the conductor pin number and width of ground plate.

The far most point of highest electrical field intensity is the 1.0-inch ground plate with 4 and 28 pin conductor setup. The position of the highest value of electric field gradually decreases from the top the channel if the pin number is increased for 0.5-inch ground plate setup. Highest field intensity is found nearest for 12 pin conductor with a 1.0-inch ground plate and for 2.0-inch ground plate nearest field intensity created for 28 pin conductor.

Forces acting on Ground Plate, Conductor and Channel are increased with if the applied voltage is increased, which are independent of the width of ground plate, but also larger range of forces are found with the increase of pin number. The experimental domain forces are very low compared to the forces. Forces are increased when applied voltage increased despite their direction.

This study has opened a lot of opportunities to work on different shapes of sizes of EHD pump as the electric field potential and forces are measured successfully. This same simulation can be tied up with ansys fluent. This can be effective to find the flow pattern and flow velocity directly from the ionized air. Any kind of dielectric fluid can be analyzed in micro scale.

## References Références Referencias


1. Goldman, M., A. Goldman, and R. S. Sigmond. "The Corona Discharge, Its Properties and Specific Uses." Pure and Applied Chemistry 57, no. 9 (1985). doi:10.1351/pac198557091353.
2. "What Is Corona?" Hubbell Power Systems (2004). Accessed October 25, 2016. http://www.hubbell powersystems.com/literature/insulators/EU1234-H.pdf.
3. Laser, D. J., and J. G. Santiago. "A Review of Micropumps." Journal of Micromechanics and Microengineering 14, no. 6 (2004). doi:10.1088 /0960-1317/14/6/r01.
4. Chen, L. "Fabrication and Characterization of a Multi-stage Electroosmotic Pump for Liquid Delivery." Sensors and Actuators B: Chemical 104, no. 1 (2005): 117-23. doi:10.1016/j.snb.2004. 05.013.
5. Genuth, I. "Ionic Wind – Chillin' the PC." TFOT. 2013. Accessed September 02, 2016. http://thefutureof things.com/3057-ionic-wind-chillin-the-pc/.
6. Mazumder, A. K. M. Monayem Hossain, and F. C. Lai. "Enhancement in Gas Pumping in a Square Channel With Two-Stage Corona Wind Generator." IEEE Transactions on Industry Applications 50, no. 4 (2014): 2296-305. doi:10.1109/tia.2013.2290864.

Global Journal of Researches in Engineering: F
Electrical and Electronics Engineering
Volume 17 Issue 5 Version 1.0 Year 2017
Type: Double Blind Peer Reviewed International Research Journal
Publisher: Global Journals Inc. (USA)
Online ISSN: 2249-4596 & Print ISSN: 0975-5861

# Real Power Loss Reduction by Revolutionary Algorithm

By Dr. K. Lenin

*Prasad V. Potluri Siddhartha Institute of Technology*

*Abstract-* In this paper, Kidney Search (KS) algorithm is proposed for solving reactive power problem. When using KS algorithm, solutions are rated based on the average value of the objective function in a particular population of particular round. Optimal solutions are identified in the filtered blood and the rest are considered as inferior solutions. As the algorithm proposed by the name of kidney, it reproduces various processes from the system of a biological kidney. Proposed Kidney search (KS) algorithm has been tested on standard IEEE 30 bus test system and simulation results show clearly about the better performance of the proposed KS algorithm in reducing the real power loss.

*Keywords: optimal reactive power, transmission loss, kidney search algorithm.*

GJRE-F Classification: *FOR Code: 090607*

# Real Power Loss Reduction by Revolutionary Algorithm

Dr. K. Lenin

*Abstract-* In this paper, Kidney Search (KS) algorithm is proposed for solving reactive power problem. When using KS algorithm, solutions are rated based on the average value of the objective function in a particular population of particular round. Optimal solutions are identified in the filtered blood and the rest are considered as inferior solutions. As the algorithm proposed by the name of kidney, it reproduces various processes from the system of a biological kidney. Proposed Kidney search (KS) algorithm has been tested on standard IEEE 30 bus test system and simulation results show clearly about the better performance of the proposed KS algorithm in reducing the real power loss.

*Keywords: optimal reactive power, transmission loss, kidney search algorithm.*

## I. Introduction

Optimal reactive power problem is a multi-objective optimization problem that minimizes the real power loss and bus voltage deviation. Various mathematical techniques like the gradient method [1-2], Newton method [3] and linear programming [4-7] have been adopted to solve the optimal reactive power dispatch problem. Both the gradient and Newton methods have the complexity in managing inequality constraints. If linear programming is applied then the input- output function has to be uttered as a set of linear functions which mostly lead to loss of accuracy. The problem of voltage stability and collapse play a major role in power system planning and operation [8]. Global optimization has received extensive research awareness, and a great number of methods have been applied to solve this problem. Evolutionary algorithms such as genetic algorithm have been already proposed to solve the reactive power flow problem [9, 10]. Evolutionary algorithm is a heuristic approach used for minimization problems by utilizing nonlinear and non-differentiable continuous space functions. In [11], Genetic algorithm has been used to solve optimal reactive power flow problem. In [12], Hybrid differential evolution algorithm is proposed to improve the voltage stability index. In [13] Biogeography Based algorithm is projected to solve the reactive power dispatch problem. In [14], a fuzzy based method is used to solve the optimal reactive power scheduling method. In [15], an improved evolutionary programming is used to solve the optimal reactive power dispatch problem. In [16], the optimal reactive power flow problem is solved by integrating a genetic algorithm with a nonlinear interior point method. In [17], a pattern algorithm is used to solve ac-dc optimal reactive power flow model with the generator capability limits. In [18], F. Capitanescu proposes a two-step approach to evaluate Reactive power reserves with respect to operating constraints and voltage stability. In [19], a programming based approach is used to solve the optimal reactive power dispatch problem. In [20], A. Kargarian et al present a probabilistic algorithm for optimal reactive power provision in hybrid electricity markets with uncertain loads. Kidney search algorithm (KS) is a new evolutionary optimization algorithm that derives its functionality from the kidney process in the body of a human being, and was initially introduced by [21]. When using the KS algorithm, the solutions are rated based on the average value of the objective functions of the solutions in a particular populace in a particular round. Optimal solutions are identified in the filtered blood and the rest are considered as inferior solutions. This process simulates the process of filtration known as glomerular in the human kidney. The inferior solutions once again are considered during other reiterations, and if they don't satisfy the filtration rate after the application of a set of movement operators, they are ejected from the set of solutions. This also stimulates the reabsorption and secretion features of a kidney. Additionally, a solution termed as the optimal solution is expelled if it does not prove to be better than the solutions classified in the worst sets; this simulates the blood secretion process by the kidney. After placing each of the solutions in a set, the optimal solutions are ranked, and the filtered and waste blood is combined to form another population that is subjected to an updated filtration rate. Filtration offers the needed manipulation to generate a new solution and reabsorption provides further examination. This paper proposes Kidney Search (KS) algorithm to solve the optimal reactive power problem. Proposed KS algorithm has been evaluated in standard IEEE 30 bus test system and the simulation results show that the proposed approach outperforms all the entitled reported algorithms in minimization of real power loss.

## II. Problem Formulation

The optimal power flow problem is treated as a general minimization problem with constraints, and can be mathematically written in the following form:

*Author: Professor, Department of EEE, Prasad V. Potluri Siddhartha Institute of Technology, Kanuru, Vijayawada, Andhra Pradesh -520007. e-mail: gklenin@gmail.com*

$$\text{Minimize } f(x, u) \tag{1}$$

subject to

$$g(x,u)=0 \tag{2}$$

and

$$h(x, u) \leq 0 \tag{3}$$

where f(x,u) is the objective function. g(x.u) and h(x,u) are respectively the set of equality and inequality constraints. x is the vector of state variables, and u is the vector of control variables.

The state variables are the load buses (PQ buses) voltages, angles, the generator reactive powers and the slack active generator power:

$$x = \left(P_{g1}, \theta_2, .., \theta_N, V_{L1}, ., V_{LNL}, Q_{g1}, .., Q_{gng}\right)^T \tag{4}$$

The control variables are the generator bus voltages, the shunt capacitors/reactors and the transformers tap-settings:

$$u = \left(V_g, T, Q_c\right)^T \tag{5}$$

or

$$u = \left(V_{g1}, \dots, V_{gng}, T_1, .., T_{Nt}, Q_{c1}, .., Q_{cNc}\right)^T \tag{6}$$

Where ng, nt and nc are the number of generators, number of tap transformers and the number of shunt compensators respectively.

## III. Objective Function

### a) Active power loss

The objective of the reactive power dispatch is to minimize the active power loss in the transmission network, which can be described as follows:

$$F = PL = \sum_{k\in Nbr} g_k \left(V_i^2 + V_j^2 - 2V_iV_j\cos\theta_{ij}\right) \tag{7}$$

or

$$F = PL = \sum_{i\in Ng} P_{gi} - P_d = P_{gslack} + \sum_{i\neq slack}^{Ng} P_{gi} - P_d \tag{8}$$

where $g_k$ : is the conductance of branch between nodes i and j, Nbr: is the total number of transmission lines in power systems. $P_d$: is the total active power demand, $P_{gi}$: is the generator active power of unit i, and $P_{gsalck}$: is the generator active power of slack bus.

### b) Voltage profile improvement

For minimizing the voltage deviation in PQ buses, the objective function becomes:

$$F = PL + \omega_v \times VD \tag{9}$$

where $\omega_v$: is a weighting factor of voltage deviation.
VD is the voltage deviation given by:

$$VD = \sum_{i=1}^{Npq} |V_i - 1| \tag{10}$$

### c) Equality Constraint

The equality constraint g(x,u) of the Optimal reactive power problem is represented by the power balance equation, where the total power generation must cover the total power demand and the power losses:

$$P_G = P_D + P_L \tag{11}$$

This equation is solved by running Newton Raphson load flow method, by calculating the active power of slack bus to determine active power loss.

### d) Inequality Constraints

The inequality constraints h(x,u) reflect the limits on components in the power system as well as the limits created to ensure system security. Upper and lower bounds on the active power of slack bus, and reactive power of generators:

$$P_{gslack}^{min} \leq P_{gslack} \leq P_{gslack}^{max} \tag{12}$$

$$Q_{gi}^{min} \leq Q_{gi} \leq Q_{gi}^{max}, i \in N_g \tag{13}$$

Upper and lower bounds on the bus voltage magnitudes:

$$V_i^{min} \leq V_i \leq V_i^{max}, i \in N \tag{14}$$

Upper and lower bounds on the transformers tap ratios:

$$T_i^{min} \leq T_i \leq T_i^{max}, i \in N_T \tag{15}$$

Upper and lower bounds on the compensators reactive powers:

$$Q_c^{min} \leq Q_c \leq Q_C^{max}, i \in N_C \tag{16}$$

Where N is the total number of buses, $N_T$ is the total number of Transformers; $N_c$ is the total number of shunt reactive compensators.

## IV. Kidney Search (KS) Algorithm

Kidney search (KS) algorithm is one of the population-based techniques of feature selection. As recommended by its name, it replicates various processes from the system of a biological kidney. Following are the four main elements of kidney procedures that are referenced during the imitation. 1. Filtration: movement of water and solutes from the blood to the tubules. 2. Reabsorption: transport of valuable solutes and water from the tubules to the blood. 3. Secretion: transfer of additional constituents that are destructive from the bloodstream to the tubule. 4. Excretion: moving waste products from the above processes through the urine. In KS initial phase [21], an arbitrary populace of potential solutions is formed while the objective function is computed for each of the solutions. In every iteration, there is a generation of other potential solutions through a movement toward the current optimal solution. Thus, through the application of filtration operator, there is a filtration of potential solutions with high intensity toward the filtered blood (FB) with others being transferred to waste (W). The reabsorption, secretion, and excretion methods of the

Global Journal of Researches in Engineering ( F ) Volume XVII Issue V Version I Year 2017

human kidney procedure are replicated here during the search procedure to check various conditions entrenched to the algorithm. When a potential solution is transferred to W, there is an allowance by the algorithm to have a chance of improving a solution to get an opportunity of moving it into FB. When the chance is not well exploited, the solution is expelled from W, and a potential solution is moved into W. Conversely, when a potential solution is moved into FB after filtration and has a poor quality in comparison to the worst solution contained by FB, the solution is excreted. On the other hand, if the solution proves to be preferable compared to the worst, the worst solution contained in FB is secreted. Lastly, the different solutions contained in FB are ranked, and an update is done on the optimal solution and the filtration rate. FB and W, are later combined. Solutions in KS population represent solutes in a human kidney. For KS, there is a generation of a new solution through shifting of the solution from previous recapitulation process to the current optimal solution. The formula of the movement is as follows:

$$Z_{i+1} = Z_i + rand(Z_{best} - Z_i) \qquad (17)$$

In Equation 17, Z denotes the solution in KS population comparable to a solute in a natural kidney. $Z_i$ is a solution involved in the it h iteration. Rand value is an arbitrary value between zero and another number while $Z_{best}$ is the current solution based on the preceding iterations. The equation can produce a good diversity of solutions based on a current and optimal solution. Moreover, relocating the solutions to the optimal solution strengthens the local conjunction competence of an algorithm.

Filtering of the solutions is done with a filtration rate computed using a filtration function during iterations. Calculation of the filtration rate ($l_r$) is done using the following formula:

$$l_r = \beta \times \frac{\sum_{i=1}^{s} f(y_i)}{s} \qquad (18)$$

$\beta$ is a constant value between 0 and 1 and is attuned in advance. s represents the size of the population. $f(y_i)$ represents an objective function of solution y at ith iteration. It is evident in the above formula that the filtration rate, $l_r$ for iterations depends on the objective function value of solutions in that population. The equation represents a ratio of each solution determined by $\beta$ . When $\beta$ equals to zero, $l_r$ will equal to zero, meaning that the process of filtration for that algorithm will not take place. When the value of $\beta$ is set at 1, the average value for objective functions equals to the value of $l_r$. There are different rates of filtration to help in the merging of the algorithm. During iterations, objective function values get closer to the global optimal solution and the filtration rate is thus computed using the solutions. This provides the algorithm with improved solutions with exaggerated exploration procedure. Reabsorption operator can be defined as the process of giving a solution which is being moved to W and a chance to be included in FB. Any solution that is moved into W can be allocated to FB if after the operator accountable for the movement & (Eq.17) is applied. It meets the rates of filtration and qualifies to be allotted into FB. Ideally, this mimics the reabsorption process of solutes in the kidney of a human being. In exploration, reabsorption is important one. A secretion is a form of operator for those solutions which have been progressed to FB. When a solution that has the opportunity to be moved to FB but does not prove to be improved in comparison to FB worst solution, secretion takes place, and the solution is moved to W; else the solution vestiges in FB while the worst solution assigned in FB is excreted and moved into W. Secretion of solutions into W takes place if the solutions fail to satisfy the filtration rate after several attempts to be reabsorbed as part of FB. In such a case, the solution in W is replaced with any other solution. Implanting arbitrary solutions emulates the continuous process of inserting water and solutes into the glomerular capillaries of the kidney.

Fix the population
Estimate the solution in the population
Fix the best solution $Z_{best}$ ,
Fix filtration rate, $l_r$, by equation (18)
Fix waste, W
Fix filtered blood, FB
Fix number of iteration,
Do while (iteration < $number\ of\ iterations$)
For all $Z_i$
Calculate new $Z_i$ by equation (17)
Check $Z_i$ using $l_r$
If $Z_i$ allocated to W,
Put on reabsorption and engender $Z_{new}$ by using equation (17)
If reabsorption is not satisfied ($Z_{new}$ cannot be part of FB)
Eliminate $Z_i$ from W (excretion)
Put on an arbitrary Z into W to swap $Z_i$
End if
$Z_i$ is reabsorbed
Else
If it is better than the $Z_{worst}$ $in\ FB$
$Z_{worst}$ is secreted
End if
End if
End for
Rank the $Z_s$ from FB and modernize the $Z_{best}$
Amalgamate W and FB
Modernize filtration rate $l_r$ by equation (18)
End while
Return $Z_{best}$

## V. Simulation Results

Validity of the proposed Kidney Search (KS) algorithm has been verified by testing in IEEE 30-bus, 41 branch system and it has 6 generator-bus voltage magnitudes, 4 transformer-tap settings, and 2 bus shunt reactive compensators. Bus 1 is taken as slack bus and 2, 5, 8, 11 and 13 are considered as PV generator buses and others are PQ load buses. Control variables limits are given in Table 1.

*Table 1:* Primary Variable Limits (Pu)

| Variables | Min. | Max. | category |
|---|---|---|---|
| Generator Bus | 0.95 | 1.1 | Continuous |
| Load Bus | 0.95 | 1.05 | Continuous |
| Transformer-Tap | 0.9 | 1.1 | Discrete |
| Shunt Reactive Compensator | -0.11 | 0.31 | Discrete |

In Table 2 the power limits of generators buses are listed.

*Table 2:* Generators Power Limits

| Bus | Pg | Pgmin | Pgmax | Qgmin | Qmax |
|---|---|---|---|---|---|
| 1 | 96.00 | 49 | 200 | 0 | 10 |
| 2 | 79.00 | 18 | 79 | -40 | 50 |
| 5 | 49.00 | 14 | 49 | -40 | 40 |
| 8 | 21.00 | 11 | 31 | -10 | 40 |
| 11 | 21.00 | 11 | 28 | -6 | 24 |
| 13 | 21.00 | 11 | 39 | -6 | 24 |

Table 3 shows the proposed Kidney Search (KS) algorithm successfully kept the control variables within limits.Table 4 narrates about the performance of the proposed Kidney Search (KS) algorithm. Fig 1 shows about the voltage deviations during the iterations and Table 5 list out the overall comparison of the results of optimal solution obtained by various methods.

*Table 3:* After optimization values of control variables

| Control Variables | KS |
|---|---|
| V1 | 1.0401 |
| V2 | 1.0405 |
| V5 | 1.0198 |
| V8 | 1.0289 |
| V11 | 1.0697 |
| V13 | 1.0499 |
| T4,12 | 0.00 |
| T6,9 | 0.01 |
| T6,10 | 0.90 |
| T28,27 | 0.91 |
| Q10 | 0.10 |
| Q24 | 0.10 |
| Real power loss | 4.2732 |
| Voltage deviation | 0.9082 |

*Table 4:* Performance of KS algorithm

| | |
|---|---|
| Iterations | 32 |
| Time taken (secs) | 9.92 |
| Real power loss | 4.2732 |

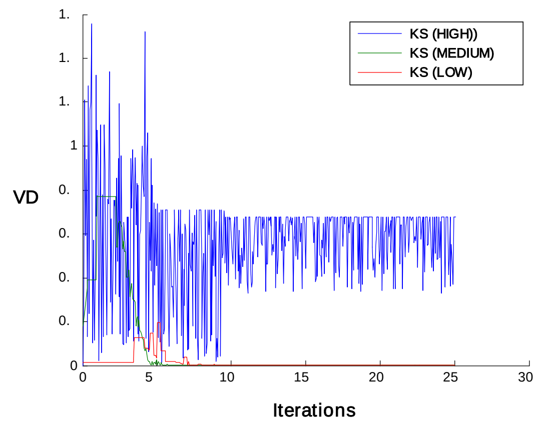


*Fig. 1:* Voltage deviation (VD) characteristics

*Table 5:* Comparison of results

| Techniques | Real power loss (MW) |
|---|---|
| SGA(Wu et al., 1998) [22] | 4.98 |
| PSO(Zhao et al., 2005) [23] | 4.9262 |
| LP(Mahadevan et al., 2010) [24] | 5.988 |
| EP(Mahadevan et al., 2010) [24] | 4.963 |
| CGA(Mahadevan et al., 2010) [24] | 4.980 |
| AGA(Mahadevan et al., 2010) [24] | 4.926 |
| CLPSO(Mahadevan et al., 2010) [24] | 4.7208 |
| HSA (Khazali et al., 2011) [25] | 4.7624 |
| BB-BC (Sakthivel et al., 2013) [26] | 4.690 |
| MCS(Tejaswini sharma et al.,2016) [27] | 4.87231 |
| Proposed KS | 4.2732 |

## VI. Conclusion

Kidney Search (KS) algorithm has been successfully applied for solving reactive power problem. In the proposed Kidney Search (KS) algorithm solutions are rated based on the average value of the objective function of the solutions in a particular population in a particular round. Proposed Kidney Search (KS) algorithm has been tested in standard IEEE 30 bus system and simulation results reveal about the improved performance of the proposed Kidney Search (KS) algorithm in plummeting the real power loss when compared to other stated standard algorithms.

## References Références Referencias

1. O. Alsac and B. Scott, “Optimal load flow with steady state security”, IEEE Transaction. PAS-1973, pp. 745-751.
2. Lee K Y ,Paru Y M , Oritz J L –A united approach to optimal real and reactive power dispatch, IEEE

Transactions on power Apparatus and systems 1985: PAS-104 : 1147-1153
3. A.Monticelli, M.V.F Pereira ,and S. Granville, "Security constrained optimal power flow with post contingency corrective rescheduling", IEEE Transactions on Power Systems :PWRS-2, No. 1, pp.175-182.,1987.
4. Deeb N, Shahidehpur S.M ,Linear reactive power optimization in a large power network using the decomposition approach. IEEE Transactions on power system 1990: 5(2) : 428-435
5. E. Hobson,'Network consrained reactive power control using linear programming, 'IEEE Transactions on power systems PAS -99 (4), pp 868=877, 1980
6. K.Y Lee, Y.M Park , and J.L Oritz, "Fuel –cost optimization for both real and reactive power dispatches", IEE Proc; 131C,(3), pp.85-93.
7. M.K. Mangoli, and K.Y. Lee, "Optimal real and reactive power control using linear programming", Electr.Power Syst.Res, Vol.26, pp.1-10,1993.
8. C.A. Canizares , A.C.Z.de Souza and V.H. Quintana, "Comparison of performance indices for detection of proximity to voltage collapse,'' vol. 11. no.3, pp.1441-1450, Aug 1996.
9. K.Anburaja, "Optimal power flow using refined genetic algorithm", Electr.Power Compon.Syst , Vol. 30, 1055-1063,2002.
10. D. Devaraj, and B. Yeganarayana, "Genetic algorithm based optimal power flow for security enhancement", IEE proc-Generation. Transmission and. Distribution; 152, 6 November 2005.
11. A. Berizzi, C. Bovo, M. Merlo, and M. Delfanti, "A ga approach to compare orpf objective functions including secondary voltage regulation," Electric Power Systems Research, vol. 84, no. 1, pp. 187 – 194, 2012.
12. C.-F. Yang, G. G. Lai, C.-H. Lee, C.-T. Su, and G. W. Chang, "Optimal setting of reactive compensation devices with an improved voltage stability index for voltage stability enhancement," International Journal of Electrical Power and Energy Systems, vol. 37, no. 1, pp. 50 – 57, 2012.
13. P. Roy, S. Ghoshal, and S. Thakur, "Optimal var control for improvements in voltage profiles and for real power loss minimization using biogeography based optimization," International Journal of Electrical Power and Energy Systems, vol. 43, no. 1, pp. 830 – 838, 2012.
14. B. Venkatesh, G. Sadasivam, and M. Khan, "A new optimal reactive power scheduling method for loss minimization and voltage stability margin maximization using successive multi-objective fuzzy lp technique," IEEE Transactions on Power Systems, vol. 15, no. 2, pp. 844 – 851, may 2000.
15. W. Yan, S. Lu, and D. Yu, "A novel optimal reactive power dispatch method based on an improved hybrid evolutionary programming technique," IEEE Transactions on Power Systems, vol. 19, no. 2, pp. 913 – 918, may 2004.
16. W. Yan, F. Liu, C. Chung, and K. Wong, "A hybrid genetic algorithminterior point method for optimal reactive power flow," IEEE Transactions on Power Systems, vol. 21, no. 3, pp. 1163 –1169, aug. 2006.
17. J. Yu, W. Yan, W. Li, C. Chung, and K. Wong, "An unfixed piecewiseoptimal reactive power-flow model and its algorithm for ac-dc systems," IEEE Transactions on Power Systems, vol. 23, no. 1, pp. 170 –176, feb. 2008.
18. F. Capitanescu, "Assessing reactive power reserves with respect to operating constraints and voltage stability," IEEE Transactions on Power Systems, vol. 26, no. 4, pp. 2224–2234, nov. 2011.
19. Z. Hu, X. Wang, and G. Taylor, "Stochastic optimal reactive power dispatch: Formulation and solution method," International Journal of Electrical Power and Energy Systems, vol. 32, no. 6, pp. 615 – 621, 2010.
20. A. Kargarian, M. Raoofat, and M. Mohammadi, "Probabilistic reactive power procurement in hybrid electricity markets with uncertain loads," Electric Power Systems Research, vol. 82, no. 1, pp. 68 – 80, 2012.
21. Jaddi, N.S., J. Alvankarian, and S. Abdullah, "Kidney-inspired algorithm for optimization problems", Communications in Nonlinear Science and Numerical Simulation, 2017. 42: p. 358-369.
22. Wu.Q.H, Y.J.Cao, and J.Y.Wen, (1998), "Optimal reactive power dispatch using an adaptive genetic algorithm", Int.J.Elect.Power Energy Syst. Vol 20. Pp. 563-569.
23. Zhao.B, C.X.Guo, and Y.J.CAO, (2005), "Multiagent-based particle swarm optimization approach for optimal reactive power dispatch",IEEE Trans. Power Syst. Vol. 20, no. 2, pp. 1070-1078.
24. Mahadevan.K, Kannan P.S,(2010) "Comprehensive Learning Particle Swarm Optimization for Reactive Power Dispatch", Applied Soft Computing, Vol. 10, No. 2, pp. 641–52.
25. Khazali.A.H,M.Kalantar,(2011),"Optimal Reactive Power Dispatch based on Harmony Search Algorithm", Electrical Power and Energy Systems, Vol. 33, No. 3, pp. 684–692.
26. Sakthivel. S, M. Gayathri, V. Manimozhi, (2013), "A Nature Inspired Optimization Algorithm for Reactive Power Control in a Power System", International Journal of Recent Technology and Engineering, pp29-33Vol.2, Issue-1.
27. Tejaswini Sharma,Laxmi Srivastava,Shishir Dixit (2016). "Modified Cuckoo Search Algorithm For Optimal Reactive Power Dispatch", Proceedings of 38 th IRF International Conference,pp4-8. 20th March, 2016, Chennai, India, ISBN: 978-93-85973-76-5.

Global Journals Inc. (US) Guidelines Handbook 2017

www.GlobalJournals.org

# Fellows

## FELLOW OF ASSOCIATION OF RESEARCH SOCIETY IN ENGINEERING (FARSE)

Global Journals Incorporate (USA) is accredited by Open Association of Research Society (OARS), U.S.A and in turn, awards “FARSE ” title to individuals. The 'FARSE' title is accorded to a selected professional after the approval of the Editor-in-Chief /Editorial Board Members/Dean.

- The “FARSE” is a dignified title which is accorded to a person’s name viz. Dr. John E. Hall, Ph.D., FARSE or William Walldroff, M.S., FARSE.

FARSE accrediting is an honor. It authenticates your research activities. After recognition as FARSE, you can add 'FARSE' title with your name as you use this recognition as additional suffix to your status. This will definitely enhance and add more value and repute to your name. You may use it on your professional Counseling Materials such as CV, Resume, and Visiting Card etc.

*The following benefits can be availed by you only for next three years from the date of certification:*

FARSE designated members are entitled to avail a 40% discount while publishing their research papers (of a single author) with Global Journals Incorporation (USA), if the same is accepted by Editorial Board/Peer Reviewers. If you are a main author or co-author in case of multiple authors, you will be entitled to avail discount of 10%.

Once FARSE title is accorded, the Fellow is authorized to organize a symposium/seminar/conference on behalf of Global Journal Incorporation (USA).The Fellow can also participate in conference/seminar/symposium organized by another institution as representative of Global Journal. In both the cases, it is mandatory for him to discuss with us and obtain our consent.

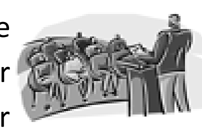

You may join as member of the Editorial Board of Global Journals Incorporation (USA) after successful completion of three years as Fellow and as Peer Reviewer. In addition, it is also desirable that you should organize seminar/symposium/conference at least once.

We shall provide you intimation regarding launching of e-version of journal of your stream time to time.This may be utilized in your library for the enrichment of knowledge of your students as well as it can also be helpful for the concerned faculty members.

The FARSE can go through standards of OARS. You can also play vital role if you have any suggestions so that proper amendment can take place to improve the same for the benefit of entire research community.

As FARSE, you will be given a renowned, secure and free professional email address with 100 GB of space e.g. johnhall@globaljournals.org. This will include Webmail, Spam Assassin, Email Forwarders,Auto-Responders, Email Delivery Route tracing, etc.

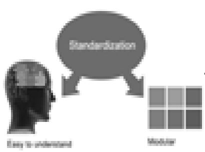


The FARSE will be eligible for a free application of standardization of their researches. Standardization of research will be subject to acceptability within stipulated norms as the next step after publishing in a journal. We shall depute a team of specialized research professionals who will render their services for elevating your researches to next higher level, which is worldwide open standardization.

The FARSE member can apply for grading and certification of standards of their educational and Institutional Degrees to Open Association of Research, Society U.S.A. Once you are designated as FARSE, you may send us a scanned copy of all of your credentials. OARS will verify, grade and certify them. This will be based on your academic records, quality of research papers published by you, and some more criteria. After certification of all your credentials by OARS, they will be published on your Fellow Profile link on website https://associationofresearch.org which will be helpful to upgrade the dignity.


The FARSE members can avail the benefits of free research podcasting in Global Research Radio with their research documents. After publishing the work, (including published elsewhere worldwide with proper authorization) you can upload your research paper with your recorded voice or you can utilize chargeable services of our professional RJs to record your paper in their voice on request.

The FARSE member also entitled to get the benefits of free research podcasting of their research documents through video clips. We can also streamline your conference videos and display your slides/ online slides and online research video clips at reasonable charges, on request.

The FARSE is eligible to earn from sales proceeds of his/her researches/reference/review Books or literature, while publishing with Global Journals. The FARSE can decide whether he/she would like to publish his/her research in a closed manner. In this case, whenever readers purchase that individual research paper for reading, maximum 60% of its profit earned as royalty by Global Journals, will be credited to his/her bank account. The entire entitled amount will be credited to his/her bank account exceeding limit of minimum fixed balance. There is no minimum time limit for collection. The FARSE member can decide its price and we can help in making the right decision.

The FARSE member is eligible to join as a paid peer reviewer at Global Journals Incorporation (USA) and can get remuneration of 15% of author fees, taken from the author of a respective paper. After reviewing 5 or more papers you can request to transfer the amount to your bank account.

## MEMBER OF ASSOCIATION OF RESEARCH SOCIETY IN ENGINEERING (MARSE)

The ' MARSE ' title is accorded to a selected professional after the approval of the Editor-in-Chief / Editorial Board Members/Dean.

The "MARSE" is a dignified ornament which is accorded to a person's name viz. Dr. John E. Hall, Ph.D., MARSE or William Walldroff, M.S., MARSE.

MARSE accrediting is an honor. It authenticates your research activities. After becoming MARSE, you can add 'MARSE' title with your name as you use this recognition as additional suffix to your status. This will definitely enhance and add more value and repute to your name. You may use it on your professional Counseling Materials such as CV, Resume, Visiting Card and Name Plate etc.

*The following benefitscan be availed by you only for next three years from the date of certification.*

MARSE designated members are entitled to avail a 25% discount while publishing their research papers (of a single author) in Global Journals Inc., if the same is accepted by our Editorial Board and Peer Reviewers. If you are a main author or co-author of a group of authors, you will get discount of 10%.

As MARSE, you will be given a renowned, secure and free professional email address with 30 GB of space e.g. johnhall@globaljournals.org. This will include Webmail, Spam Assassin, Email Forwarders,Auto-Responders, Email Delivery Route tracing, etc.


We shall provide you intimation regarding launching of e-version of journal of your stream time to time.This may be utilized in your library for the enrichment of knowledge of your students as well as it can also be helpful for the concerned faculty members.

The MARSE member can apply for approval, grading and certification of standards of their educational and Institutional Degrees to Open Association of Research, Society U.S.A.


Once you are designated as MARSE, you may send us a scanned copy of all of your credentials. OARS will verify, grade and certify them. This will be based on your academic records, quality of research papers published by you, and some more criteria.

It is mandatory to read all terms and conditions carefully.

# Auxiliary Memberships

## Institutional Fellow of Open Association of Research Society (USA)-OARS (USA)

Global Journals Incorporation (USA) is accredited by Open Association of Research Society, U.S.A (OARS) and in turn, affiliates research institutions as "Institutional Fellow of Open Association of Research Society" (IFOARS).

The "FARSC" is a dignified title which is accorded to a person's name viz. Dr. John E. Hall, Ph.D., FARSC or William Walldroff, M.S., FARSC.

The IFOARS institution is entitled to form a Board comprised of one Chairperson and three to five board members preferably from different streams. The Board will be recognized as "Institutional Board of Open Association of Research Society"-(IBOARS).

*The Institute will be entitled to following benefits:*

The IBOARS can initially review research papers of their institute and recommend them to publish with respective journal of Global Journals. It can also review the papers of other institutions after obtaining our consent. The second review will be done by peer reviewer of Global Journals Incorporation (USA)
The Board is at liberty to appoint a peer reviewer with the approval of chairperson after consulting us.
The author fees of such paper may be waived off up to 40%.

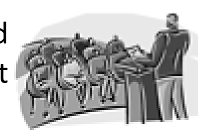

The Global Journals Incorporation (USA) at its discretion can also refer double blind peer reviewed paper at their end to the board for the verification and to get recommendation for final stage of acceptance of publication.

The IBOARS can organize symposium/seminar/conference in their country on behalf of Global Journals Incorporation (USA)-OARS (USA). The terms and conditions can be discussed separately.


The Board can also play vital role by exploring and giving valuable suggestions regarding the Standards of "Open Association of Research Society, U.S.A (OARS)" so that proper amendment can take place for the benefit of entire research community. We shall provide details of particular standard only on receipt of request from the Board.

The board members can also join us as Individual Fellow with 40% discount on total fees applicable to Individual Fellow. They will be entitled to avail all the benefits as declared. Please visit Individual Fellow-sub menu of GlobalJournals.org to have more relevant details.

We shall provide you intimation regarding launching of e-version of journal of your stream time to time. This may be utilized in your library for the enrichment of knowledge of your students as well as it can also be helpful for the concerned faculty members.

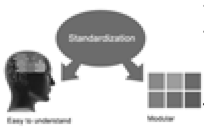


After nomination of your institution as "Institutional Fellow" and constantly functioning successfully for one year, we can consider giving recognition to your institute to function as Regional/Zonal office on our behalf.
The board can also take up the additional allied activities for betterment after our consultation.

**The following entitlements are applicable to individual Fellows:**

Open Association of Research Society, U.S.A (OARS) By-laws states that an individual Fellow may use the designations as applicable, or the corresponding initials. The Credentials of individual Fellow and Associate designations signify that the individual has gained knowledge of the fundamental concepts. One is magnanimous and proficient in an expertise course covering the professional code of conduct, and follows recognized standards of practice.


Open Association of Research Society (US)/ Global Journals Incorporation (USA), as described in Corporate Statements, are educational, research publishing and professional membership organizations. Achieving our individual Fellow or Associate status is based mainly on meeting stated educational research requirements.

Disbursement of 40% Royalty earned through Global Journals : Researcher = 50%, Peer Reviewer = 37.50%, Institution = 12.50% E.g. Out of 40%, the 20% benefit should be passed on to researcher, 15 % benefit towards remuneration should be given to a reviewer and remaining 5% is to be retained by the institution.

We shall provide print version of 12 issues of any three journals [as per your requirement] out of our 38 journals worth $ 2376 USD.

**Other:**

**The individual Fellow and Associate designations accredited by Open Association of Research Society (US) credentials signify guarantees following achievements:**

- The professional accredited with Fellow honor, is entitled to various benefits viz. name, fame, honor, regular flow of income, secured bright future, social status etc.

- In addition to above, if one is single author, then entitled to 40% discount on publishing research paper and can get 10%discount if one is co-author or main author among group of authors.
- The Fellow can organize symposium/seminar/conference on behalf of Global Journals Incorporation (USA) and he/she can also attend the same organized by other institutes on behalf of Global Journals.
- The Fellow can become member of Editorial Board Member after completing 3yrs.
- The Fellow can earn 60% of sales proceeds from the sale of reference/review books/literature/publishing of research paper.
- Fellow can also join as paid peer reviewer and earn 15% remuneration of author charges and can also get an opportunity to join as member of the Editorial Board of Global Journals Incorporation (USA)
- • This individual has learned the basic methods of applying those concepts and techniques to common challenging situations. This individual has further demonstrated an in–depth understanding of the application of suitable techniques to a particular area of research practice.

**Note :**

"

- In future, if the board feels the necessity to change any board member, the same can be done with the consent of the chairperson along with anyone board member without our approval.
- In case, the chairperson needs to be replaced then consent of 2/3rd board members are required and they are also required to jointly pass the resolution copy of which should be sent to us. In such case, it will be compulsory to obtain our approval before replacement.
- In case of "Difference of Opinion [if any]" among the Board members, our decision will be final and binding to everyone.

"

# Process of submission of Research Paper

The Area or field of specialization may or may not be of any category as mentioned in 'Scope of Journal' menu of the GlobalJournals.org website. There are 37 Research Journal categorized with Six parental Journals GJCST, GJMR, GJRE, GJMBR, GJSFR, GJHSS. For Authors should prefer the mentioned categories. There are three widely used systems UDC, DDC and LCC. The details are available as 'Knowledge Abstract' at Home page. The major advantage of this coding is that, the research work will be exposed to and shared with all over the world as we are being abstracted and indexed worldwide.

The paper should be in proper format. The format can be downloaded from first page of 'Author Guideline' Menu. The Author is expected to follow the general rules as mentioned in this menu. The paper should be written in MS-Word Format (*.DOC,*.DOCX).

The Author can submit the paper either online or offline. The authors should prefer online submission.Online Submission: There are three ways to submit your paper:

**(A) (I) First, register yourself using top right corner of Home page then Login. If you are already registered, then login using your username and password.**

**(II) Choose corresponding Journal.**

**(III) Click 'Submit Manuscript'. Fill required information and Upload the paper.**

**(B) If you are using Internet Explorer, then Direct Submission through Homepage is also available.**

**(C) If these two are not conveninet , and then email the paper directly to dean@globaljournals.org.**

Offline Submission: Author can send the typed form of paper by Post. However, online submission should be preferred.

**MANUSCRIPT STYLE INSTRUCTION** **(Must be strictly followed)**

Page Size: 8.27" X 11'"

- Left Margin: 0.65
- Right Margin: 0.65
- Top Margin: 0.75
- Bottom Margin: 0.75
- Font type of all text should be Swis 721 Lt BT.
- Paper Title should be of Font Size 24 with one Column section.
- Author Name in Font Size of 11 with one column as of Title.
- Abstract Font size of 9 Bold, “Abstract” word in Italic Bold.
- Main Text: Font size 10 with justified two columns section
- Two Column with Equal Column with of 3.38 and Gaping of .2
- First Character must be three lines Drop capped.
- Paragraph before Spacing of 1 pt and After of 0 pt.
- Line Spacing of 1 pt
- Large Images must be in One Column
- Numbering of First Main Headings (Heading 1) must be in Roman Letters, Capital Letter, and Font Size of 10.
- Numbering of Second Main Headings (Heading 2) must be in Alphabets, Italic, and Font Size of 10.

**You can use your own standard format also.**
**Author Guidelines:**

1. General,

2. Ethical Guidelines,

3. Submission of Manuscripts,

4. Manuscript’s Category,

5. Structure and Format of Manuscript,

6. After Acceptance.

**1. GENERAL**

Before submitting your research paper, one is advised to go through the details as mentioned in following heads. It will be beneficial, while peer reviewer justify your paper for publication.

**Scope**

The Global Journals Inc. (US) welcome the submission of original paper, review paper, survey article relevant to the all the streams of Philosophy and knowledge. The Global Journals Inc. (US) is parental platform for Global Journal of Computer Science and Technology, Researches in Engineering, Medical Research, Science Frontier Research, Human Social Science, Management, and Business organization. The choice of specific field can be done otherwise as following in Abstracting and Indexing Page on this Website. As the all Global

Journals Inc. (US) are being abstracted and indexed (in process) by most of the reputed organizations. Topics of only narrow interest will not be accepted unless they have wider potential or consequences.

**2. ETHICAL GUIDELINES**

Authors should follow the ethical guidelines as mentioned below for publication of research paper and research activities.

Papers are accepted on strict understanding that the material in whole or in part has not been, nor is being, considered for publication elsewhere. If the paper once accepted by Global Journals Inc. (US) and Editorial Board, will become the copyright of the Global Journals Inc. (US).

**Authorship: The authors and coauthors should have active contribution to conception design, analysis and interpretation of findings. They should critically review the contents and drafting of the paper. All should approve the final version of the paper before submission**

The Global Journals Inc. (US) follows the definition of authorship set up by the Global Academy of Research and Development. According to the Global Academy of R&D authorship, criteria must be based on:

1) Substantial contributions to conception and acquisition of data, analysis and interpretation of the findings.

2) Drafting the paper and revising it critically regarding important academic content.

3) Final approval of the version of the paper to be published.

All authors should have been credited according to their appropriate contribution in research activity and preparing paper. Contributors who do not match the criteria as authors may be mentioned under Acknowledgement.

Acknowledgements: Contributors to the research other than authors credited should be mentioned under acknowledgement. The specifications of the source of funding for the research if appropriate can be included. Suppliers of resources may be mentioned along with address.

**Appeal of Decision: The Editorial Board's decision on publication of the paper is final and cannot be appealed elsewhere.**

**Permissions: It is the author's responsibility to have prior permission if all or parts of earlier published illustrations are used in this paper.**

Please mention proper reference and appropriate acknowledgements wherever expected.

If all or parts of previously published illustrations are used, permission must be taken from the copyright holder concerned. It is the author's responsibility to take these in writing.

Approval for reproduction/modification of any information (including figures and tables) published elsewhere must be obtained by the authors/copyright holders before submission of the manuscript. Contributors (Authors) are responsible for any copyright fee involved.

**3. SUBMISSION OF MANUSCRIPTS**

Manuscripts should be uploaded via this online submission page. The online submission is most efficient method for submission of papers, as it enables rapid distribution of manuscripts and consequently speeds up the review procedure. It also enables authors to know the status of their own manuscripts by emailing us. Complete instructions for submitting a paper is available below.

Manuscript submission is a systematic procedure and little preparation is required beyond having all parts of your manuscript in a given format and a computer with an Internet connection and a Web browser. Full help and instructions are provided on-screen. As an author, you will be prompted for login and manuscript details as Field of Paper and then to upload your manuscript file(s) according to the instructions.

To avoid postal delays, all transaction is preferred by e-mail. A finished manuscript submission is confirmed by e-mail immediately and your paper enters the editorial process with no postal delays. When a conclusion is made about the publication of your paper by our Editorial Board, revisions can be submitted online with the same procedure, with an occasion to view and respond to all comments.

Complete support for both authors and co-author is provided.

**4. MANUSCRIPT'S CATEGORY**

Based on potential and nature, the manuscript can be categorized under the following heads:

Original research paper: Such papers are reports of high-level significant original research work.

Review papers: These are concise, significant but helpful and decisive topics for young researchers.

Research articles: These are handled with small investigation and applications

Research letters: The letters are small and concise comments on previously published matters.

**5.STRUCTURE AND FORMAT OF MANUSCRIPT**

The recommended size of original research paper is less than seven thousand words, review papers fewer than seven thousands words also.Preparation of research paper or how to write research paper, are major hurdle, while writing manuscript. The research articles and research letters should be fewer than three thousand words, the structure original research paper; sometime review paper should be as follows:

**Papers**: These are reports of significant research (typically less than 7000 words equivalent, including tables, figures, references), and comprise:

(a)Title should be relevant and commensurate with the theme of the paper.

(b) A brief Summary, "Abstract" (less than 150 words) containing the major results and conclusions.

(c) Up to ten keywords, that precisely identifies the paper's subject, purpose, and focus.

(d) An Introduction, giving necessary background excluding subheadings; objectives must be clearly declared.

(e) Resources and techniques with sufficient complete experimental details (wherever possible by reference) to permit repetition; sources of information must be given and numerical methods must be specified by reference, unless non-standard.

(f) Results should be presented concisely, by well-designed tables and/or figures; the same data may not be used in both; suitable statistical data should be given. All data must be obtained with attention to numerical detail in the planning stage. As reproduced design has been recognized to be important to experiments for a considerable time, the Editor has decided that any paper that appears not to have adequate numerical treatments of the data will be returned un-refereed;

(g) Discussion should cover the implications and consequences, not just recapitulating the results; conclusions should be summarizing.

(h) Brief Acknowledgements.

(i) References in the proper form.

Authors should very cautiously consider the preparation of papers to ensure that they communicate efficiently. Papers are much more likely to be accepted, if they are cautiously designed and laid out, contain few or no errors, are summarizing, and be conventional to the approach and instructions. They will in addition, be published with much less delays than those that require much technical and editorial correction.

The Editorial Board reserves the right to make literary corrections and to make suggestions to improve briefness.

It is vital, that authors take care in submitting a manuscript that is written in simple language and adheres to published guidelines.

**Format**

*Language: The language of publication is UK English. Authors, for whom English is a second language, must have their manuscript efficiently edited by an English-speaking person before submission to make sure that, the English is of high excellence. It is preferable, that manuscripts should be professionally edited.*

Standard Usage, Abbreviations, and Units: Spelling and hyphenation should be conventional to The Concise Oxford English Dictionary. Statistics and measurements should at all times be given in figures, e.g. 16 min, except for when the number begins a sentence. When the number does not refer to a unit of measurement it should be spelt in full unless, it is 160 or greater.

Abbreviations supposed to be used carefully. The abbreviated name or expression is supposed to be cited in full at first usage, followed by the conventional abbreviation in parentheses.

Metric SI units are supposed to generally be used excluding where they conflict with current practice or are confusing. For illustration, 1.4 l rather than 1.4 × 10-3 m3, or 4 mm somewhat than 4 × 10-3 m. Chemical formula and solutions must identify the form used, e.g. anhydrous or hydrated, and the concentration must be in clearly defined units. Common species names should be followed by underlines at the first mention. For following use the generic name should be constricted to a single letter, if it is clear.

**Structure**

All manuscripts submitted to Global Journals Inc. (US), ought to include:

Title: The title page must carry an instructive title that reflects the content, a running title (less than 45 characters together with spaces), names of the authors and co-authors, and the place(s) wherever the work was carried out. The full postal address in addition with the e-mail address of related author must be given. Up to eleven keywords or very brief phrases have to be given to help data retrieval, mining and indexing.

*Abstract, used in Original Papers and Reviews:*

Optimizing Abstract for Search Engines

Many researchers searching for information online will use search engines such as Google, Yahoo or similar. By optimizing your paper for search engines, you will amplify the chance of someone finding it. This in turn will make it more likely to be viewed and/or cited in a further work. Global Journals Inc. (US) have compiled these guidelines to facilitate you to maximize the web-friendliness of the most public part of your paper.

Key Words

A major linchpin in research work for the writing research paper is the keyword search, which one will employ to find both library and Internet resources.

One must be persistent and creative in using keywords. An effective keyword search requires a strategy and planning a list of possible keywords and phrases to try.

Search engines for most searches, use Boolean searching, which is somewhat different from Internet searches. The Boolean search uses "operators," words (and, or, not, and near) that enable you to expand or narrow your affords. Tips for research paper while preparing research paper are very helpful guideline of research paper.

Choice of key words is first tool of tips to write research paper. Research paper writing is an art.A few tips for deciding as strategically as possible about keyword search:

- One should start brainstorming lists of possible keywords before even begin searching. Think about the most important concepts related to research work. Ask, "What words would a source have to include to be truly valuable in research paper?" Then consider synonyms for the important words.
- It may take the discovery of only one relevant paper to let steer in the right keyword direction because in most databases, the keywords under which a research paper is abstracted are listed with the paper.
- One should avoid outdated words.

Keywords are the key that opens a door to research work sources. Keyword searching is an art in which researcher's skills are bound to improve with experience and time.

Numerical Methods: Numerical methods used should be clear and, where appropriate, supported by references.

*Acknowledgements: Please make these as concise as possible.*

References

References follow the Harvard scheme of referencing. References in the text should cite the authors' names followed by the time of their publication, unless there are three or more authors when simply the first author's name is quoted followed by et al. unpublished work has to only be cited where necessary, and only in the text. Copies of references in press in other journals have to be supplied with submitted typescripts. It is necessary that all citations and references be carefully checked before submission, as mistakes or omissions will cause delays.

References to information on the World Wide Web can be given, but only if the information is available without charge to readers on an official site. Wikipedia and Similar websites are not allowed where anyone can change the information. Authors will be asked to make available electronic copies of the cited information for inclusion on the Global Journals Inc. (US) homepage at the judgment of the Editorial Board.

The Editorial Board and Global Journals Inc. (US) recommend that, citation of online-published papers and other material should be done via a DOI (digital object identifier). If an author cites anything, which does not have a DOI, they run the risk of the cited material not being noticeable.

The Editorial Board and Global Journals Inc. (US) recommend the use of a tool such as Reference Manager for reference management and formatting.

Tables, Figures and Figure Legends

*Tables: Tables should be few in number, cautiously designed, uncrowned, and include only essential data. Each must have an Arabic number, e.g. Table 4, a self-explanatory caption and be on a separate sheet. Vertical lines should not be used.*

*Figures: Figures are supposed to be submitted as separate files. Always take in a citation in the text for each figure using Arabic numbers, e.g. Fig. 4. Artwork must be submitted online in electronic form by e-mailing them.*

Preparation of Electronic Figures for Publication

Even though low quality images are sufficient for review purposes, print publication requires high quality images to prevent the final product being blurred or fuzzy. Submit (or e-mail) EPS (line art) or TIFF (halftone/photographs) files only. MS PowerPoint and Word Graphics are unsuitable for printed pictures. Do not use pixel-oriented software. Scans (TIFF only) should have a resolution of at least 350 dpi (halftone) or 700 to 1100 dpi (line drawings) in relation to the imitation size. Please give the data for figures in black and white or submit a Color Work Agreement Form. EPS files must be saved with fonts embedded (and with a TIFF preview, if possible).

For scanned images, the scanning resolution (at final image size) ought to be as follows to ensure good reproduction: line art: >650 dpi; halftones (including gel photographs) : >350 dpi; figures containing both halftone and line images: >650 dpi.

*Figure Legends: Self-explanatory legends of all figures should be incorporated separately under the heading 'Legends to Figures'. In the full-text online edition of the journal, figure legends may possibly be truncated in abbreviated links to the full screen version. Therefore, the first 100 characters of any legend should notify the reader, about the key aspects of the figure.*

**6. AFTER ACCEPTANCE**

Upon approval of a paper for publication, the manuscript will be forwarded to the dean, who is responsible for the publication of the Global Journals Inc. (US).

**6.1 Proof Corrections**

The corresponding author will receive an e-mail alert containing a link to a website or will be attached. A working e-mail address must therefore be provided for the related author.

Acrobat Reader will be required in order to read this file. This software can be downloaded

(Free of charge) from the following website:

www.adobe.com/products/acrobat/readstep2.html. This will facilitate the file to be opened, read on screen, and printed out in order for any corrections to be added. Further instructions will be sent with the proof.

Proofs must be returned to the dean at dean@globaljournals.org within three days of receipt.

As changes to proofs are costly, we inquire that you only correct typesetting errors. All illustrations are retained by the publisher. Please note that the authors are responsible for all statements made in their work, including changes made by the copy editor.

**6.2 Early View of Global Journals Inc. (US) (Publication Prior to Print)**

The Global Journals Inc. (US) are enclosed by our publishing's Early View service. Early View articles are complete full-text articles sent in advance of their publication. Early View articles are absolute and final. They have been completely reviewed, revised and edited for publication, and the authors' final corrections have been incorporated. Because they are in final form, no changes can be made after sending them. The nature of Early View articles means that they do not yet have volume, issue or page numbers, so Early View articles cannot be cited in the conventional way.

**6.3 Author Services**

Online production tracking is available for your article through Author Services. Author Services enables authors to track their article - once it has been accepted - through the production process to publication online and in print. Authors can check the status of their articles online and choose to receive automated e-mails at key stages of production. The authors will receive an e-mail with a unique link that enables them to register and have their article automatically added to the system. Please ensure that a complete e-mail address is provided when submitting the manuscript.

**6.4 Author Material Archive Policy**

Please note that if not specifically requested, publisher will dispose off hardcopy & electronic information submitted, after the two months of publication. If you require the return of any information submitted, please inform the Editorial Board or dean as soon as possible.

**6.5 Offprint and Extra Copies**

A PDF offprint of the online-published article will be provided free of charge to the related author, and may be distributed according to the Publisher's terms and conditions. Additional paper offprint may be ordered by emailing us at: editor@globaljournals.org .

You must strictly follow above Author Guidelines before submitting your paper or else we will not at all be responsible for any corrections in future in any of the way.

Before start writing a good quality Computer Science Research Paper, let us first understand what is Computer Science Research Paper? So, Computer Science Research Paper is the paper which is written by professionals or scientists who are associated to Computer Science and Information Technology, or doing research study in these areas. If you are novel to this field then you can consult about this field from your supervisor or guide.

## TECHNIQUES FOR WRITING A GOOD QUALITY RESEARCH PAPER:

**1. Choosing the topic:** In most cases, the topic is searched by the interest of author but it can be also suggested by the guides. You can have several topics and then you can judge that in which topic or subject you are finding yourself most comfortable. This can be done by asking several questions to yourself, like Will I be able to carry our search in this area? Will I find all necessary recourses to accomplish the search? Will I be able to find all information in this field area? If the answer of these types of questions will be "Yes" then you can choose that topic. In most of the cases, you may have to conduct the surveys and have to visit several places because this field is related to Computer Science and Information Technology. Also, you may have to do a lot of work to find all rise and falls regarding the various data of that subject. Sometimes, detailed information plays a vital role, instead of short information.

**2. Evaluators are human:** First thing to remember that evaluators are also human being. They are not only meant for rejecting a paper. They are here to evaluate your paper. So, present your Best.

**3. Think Like Evaluators:** If you are in a confusion or getting demotivated that your paper will be accepted by evaluators or not, then think and try to evaluate your paper like an Evaluator. Try to understand that what an evaluator wants in your research paper and automatically you will have your answer.

**4. Make blueprints of paper:** The outline is the plan or framework that will help you to arrange your thoughts. It will make your paper logical. But remember that all points of your outline must be related to the topic you have chosen.

**5. Ask your Guides:** If you are having any difficulty in your research, then do not hesitate to share your difficulty to your guide (if you have any). They will surely help you out and resolve your doubts. If you can't clarify what exactly you require for your work then ask the supervisor to help you with the alternative. He might also provide you the list of essential readings.

**6. Use of computer is recommended:** As you are doing research in the field of Computer Science, then this point is quite obvious.

**7. Use right software:** Always use good quality software packages. If you are not capable to judge good software then you can lose quality of your paper unknowingly. There are various software programs available to help you, which you can get through Internet.

**8. Use the Internet for help:** An excellent start for your paper can be by using the Google. It is an excellent search engine, where you can have your doubts resolved. You may also read some answers for the frequent question how to write my research paper or find model research paper. From the internet library you can download books. If you have all required books make important reading selecting and analyzing the specified information. Then put together research paper sketch out.

**9. Use and get big pictures:** Always use encyclopedias, Wikipedia to get pictures so that you can go into the depth.

**10. Bookmarks are useful:** When you read any book or magazine, you generally use bookmarks, right! It is a good habit, which helps to not to lose your continuity. You should always use bookmarks while searching on Internet also, which will make your search easier.

**11. Revise what you wrote:** When you write anything, always read it, summarize it and then finalize it.

**12. Make all efforts:** Make all efforts to mention what you are going to write in your paper. That means always have a good start. Try to mention everything in introduction, that what is the need of a particular research paper. Polish your work by good skill of writing and always give an evaluator, what he wants.

**13. Have backups:** When you are going to do any important thing like making research paper, you should always have backup copies of it either in your computer or in paper. This will help you to not to lose any of your important.

**14. Produce good diagrams of your own:** Always try to include good charts or diagrams in your paper to improve quality. Using several and unnecessary diagrams will degrade the quality of your paper by creating "hotchpotch." So always, try to make and include those diagrams, which are made by your own to improve readability and understandability of your paper.

**15. Use of direct quotes:** When you do research relevant to literature, history or current affairs then use of quotes become essential but if study is relevant to science then use of quotes is not preferable.

**16. Use proper verb tense:** Use proper verb tenses in your paper. Use past tense, to present those events that happened. Use present tense to indicate events that are going on. Use future tense to indicate future happening events. Use of improper and wrong tenses will confuse the evaluator. Avoid the sentences that are incomplete.

**17. Never use online paper:** If you are getting any paper on Internet, then never use it as your research paper because it might be possible that evaluator has already seen it or maybe it is outdated version.

**18. Pick a good study spot:** To do your research studies always try to pick a spot, which is quiet. Every spot is not for studies. Spot that suits you choose it and proceed further.

**19. Know what you know:** Always try to know, what you know by making objectives. Else, you will be confused and cannot achieve your target.

**20. Use good quality grammar:** Always use a good quality grammar and use words that will throw positive impact on evaluator. Use of good quality grammar does not mean to use tough words, that for each word the evaluator has to go through dictionary. Do not start sentence with a conjunction. Do not fragment sentences. Eliminate one-word sentences. Ignore passive voice. Do not ever use a big word when a diminutive one would suffice. Verbs have to be in agreement with their subjects. Prepositions are not expressions to finish sentences with. It is incorrect to ever divide an infinitive. Avoid clichés like the disease. Also, always shun irritating alliteration. Use language that is simple and straight forward. put together a neat summary.

**21. Arrangement of information:** Each section of the main body should start with an opening sentence and there should be a changeover at the end of the section. Give only valid and powerful arguments to your topic. You may also maintain your arguments with records.

**22. Never start in last minute:** Always start at right time and give enough time to research work. Leaving everything to the last minute will degrade your paper and spoil your work.

**23. Multitasking in research is not good:** Doing several things at the same time proves bad habit in case of research activity. Research is an area, where everything has a particular time slot. Divide your research work in parts and do particular part in particular time slot.

**24. Never copy others' work:** Never copy others' work and give it your name because if evaluator has seen it anywhere you will be in trouble.

**25. Take proper rest and food:** No matter how many hours you spend for your research activity, if you are not taking care of your health then all your efforts will be in vain. For a quality research, study is must, and this can be done by taking proper rest and food.

**26. Go for seminars:** Attend seminars if the topic is relevant to your research area. Utilize all your resources.

**27. Refresh your mind after intervals:** Try to give rest to your mind by listening to soft music or by sleeping in intervals. This will also improve your memory.

**28. Make colleagues:** Always try to make colleagues. No matter how sharper or intelligent you are, if you make colleagues you can have several ideas, which will be helpful for your research.

**29. Think technically:** Always think technically. If anything happens, then search its reasons, its benefits, and demerits.

**30. Think and then print:** When you will go to print your paper, notice that tables are not be split, headings are not detached from their descriptions, and page sequence is maintained.

**31. Adding unnecessary information:** Do not add unnecessary information, like, I have used MS Excel to draw graph. Do not add irrelevant and inappropriate material. These all will create superfluous. Foreign terminology and phrases are not apropos. One should NEVER take a broad view. Analogy in script is like feathers on a snake. Not at all use a large word when a very small one would be sufficient. Use words properly, regardless of how others use them. Remove quotations. Puns are for kids, not grunt readers. Amplification is a billion times of inferior quality than sarcasm.

**32. Never oversimplify everything:** To add material in your research paper, never go for oversimplification. This will definitely irritate the evaluator. Be more or less specific. Also too, by no means, ever use rhythmic redundancies. Contractions aren't essential and shouldn't be there used. Comparisons are as terrible as clichés. Give up ampersands and abbreviations, and so on. Remove commas, that are, not necessary. Parenthetical words however should be together with this in commas. Understatement is all the time the complete best way to put onward earth-shaking thoughts. Give a detailed literary review.

**33. Report concluded results:** Use concluded results. From raw data, filter the results and then conclude your studies based on measurements and observations taken. Significant figures and appropriate number of decimal places should be used. Parenthetical remarks are prohibitive. Proofread carefully at final stage. In the end give outline to your arguments. Spot out perspectives of further study of this subject. Justify your conclusion by at the bottom of them with sufficient justifications and examples.

**34. After conclusion:** Once you have concluded your research, the next most important step is to present your findings. Presentation is extremely important as it is the definite medium though which your research is going to be in print to the rest of the crowd. Care should be taken to categorize your thoughts well and present them in a logical and neat manner. A good quality research paper format is essential because it serves to highlight your research paper and bring to light all necessary aspects in your research.

## Informal Guidelines of Research Paper Writing

**Key points to remember:**

- Submit all work in its final form.
- Write your paper in the form, which is presented in the guidelines using the template.
- Please note the criterion for grading the final paper by peer-reviewers.

**Final Points:**

A purpose of organizing a research paper is to let people to interpret your effort selectively. The journal requires the following sections, submitted in the order listed, each section to start on a new page.

The introduction will be compiled from reference matter and will reflect the design processes or outline of basis that direct you to make study. As you will carry out the process of study, the method and process section will be constructed as like that. The result segment will show related statistics in nearly sequential order and will direct the reviewers next to the similar intellectual paths throughout the data that you took to carry out your study. The discussion section will provide understanding of the data and projections as to the implication of the results. The use of good quality references all through the paper will give the effort trustworthiness by representing an alertness of prior workings.

Writing a research paper is not an easy job no matter how trouble-free the actual research or concept. Practice, excellent preparation, and controlled record keeping are the only means to make straightforward the progression.

**General style:**

Specific editorial column necessities for compliance of a manuscript will always take over from directions in these general guidelines.

To make a paper clear

· Adhere to recommended page limits

Mistakes to evade

- Insertion a title at the foot of a page with the subsequent text on the next page
- Separating a table/chart or figure - impound each figure/table to a single page
- Submitting a manuscript with pages out of sequence

In every sections of your document

· Use standard writing style including articles ("a", "the," etc.)

· Keep on paying attention on the research topic of the paper

· Use paragraphs to split each significant point (excluding for the abstract)

· Align the primary line of each section

· Present your points in sound order

· Use present tense to report well accepted

· Use past tense to describe specific results

· Shun familiar wording, don't address the reviewer directly, and don't use slang, slang language, or superlatives

· Shun use of extra pictures - include only those figures essential to presenting results

**Title Page:**

Choose a revealing title. It should be short. It should not have non-standard acronyms or abbreviations. It should not exceed two printed lines. It should include the name(s) and address (es) of all authors.

**Abstract:**

The summary should be two hundred words or less. It should briefly and clearly explain the key findings reported in the manuscript--must have precise statistics. It should not have abnormal acronyms or abbreviations. It should be logical in itself. Shun citing references at this point.

An abstract is a brief distinct paragraph summary of finished work or work in development. In a minute or less a reviewer can be taught the foundation behind the study, common approach to the problem, relevant results, and significant conclusions or new questions.

Write your summary when your paper is completed because how can you write the summary of anything which is not yet written? Wealth of terminology is very essential in abstract. Yet, use comprehensive sentences and do not let go readability for briefness. You can maintain it succinct by phrasing sentences so that they provide more than lone rationale. The author can at this moment go straight to shortening the outcome. Sum up the study, with the subsequent elements in any summary. Try to maintain the initial two items to no more than one ruling each.

- Reason of the study - theory, overall issue, purpose
- Fundamental goal
- To the point depiction of the research
- Consequences, including definite statistics - if the consequences are quantitative in nature, account quantitative data; results of any numerical analysis should be reported
- Significant conclusions or questions that track from the research(es)

Approach:

- Single section, and succinct
- As a outline of job done, it is always written in past tense
- A conceptual should situate on its own, and not submit to any other part of the paper such as a form or table
- Center on shortening results - bound background information to a verdict or two, if completely necessary
- What you account in an conceptual must be regular with what you reported in the manuscript
- Exact spelling, clearness of sentences and phrases, and appropriate reporting of quantities (proper units, important statistics) are just as significant in an abstract as they are anywhere else

**Introduction:**

The **Introduction** should "introduce" the manuscript. The reviewer should be presented with sufficient background information to be capable to comprehend and calculate the purpose of your study without having to submit to other works. The basis for the study should be offered. Give most important references but shun difficult to make a comprehensive appraisal of the topic. In the introduction, describe the problem visibly. If the problem is not acknowledged in a logical, reasonable way, the reviewer will have no attention in your result. Speak in common terms about techniques used to explain the problem, if needed, but do not present any particulars about the protocols here. Following approach can create a valuable beginning:

- Explain the value (significance) of the study
- Shield the model - why did you employ this particular system or method? What is its compensation? You strength remark on its appropriateness from a abstract point of vision as well as point out sensible reasons for using it.
- Present a justification. Status your particular theory (es) or aim(s), and describe the logic that led you to choose them.
- Very for a short time explain the tentative propose and how it skilled the declared objectives.

Approach:

- Use past tense except for when referring to recognized facts. After all, the manuscript will be submitted after the entire job is done.
- Sort out your thoughts; manufacture one key point with every section. If you make the four points listed above, you will need a least of four paragraphs.

- Present surroundings information only as desirable in order hold up a situation. The reviewer does not desire to read the whole thing you know about a topic.
- Shape the theory/purpose specifically - do not take a broad view.
- As always, give awareness to spelling, simplicity and correctness of sentences and phrases.

**Procedures (Methods and Materials):**

This part is supposed to be the easiest to carve if you have good skills. A sound written Procedures segment allows a capable scientist to replacement your results. Present precise information about your supplies. The suppliers and clarity of reagents can be helpful bits of information. Present methods in sequential order but linked methodologies can be grouped as a segment. Be concise when relating the protocols. Attempt for the least amount of information that would permit another capable scientist to spare your outcome but be cautious that vital information is integrated. The use of subheadings is suggested and ought to be synchronized with the results section. When a technique is used that has been well described in another object, mention the specific item describing a way but draw the basic principle while stating the situation. The purpose is to text all particular resources and broad procedures, so that another person may use some or all of the methods in one more study or referee the scientific value of your work. It is not to be a step by step report of the whole thing you did, nor is a methods section a set of orders.

Materials:

- Explain materials individually only if the study is so complex that it saves liberty this way.
- Embrace particular materials, and any tools or provisions that are not frequently found in laboratories.
- Do not take in frequently found.
- If use of a definite type of tools.
- Materials may be reported in a part section or else they may be recognized along with your measures.

Methods:

- Report the method (not particulars of each process that engaged the same methodology)
- Describe the method entirely
- To be succinct, present methods under headings dedicated to specific dealings or groups of measures
- Simplify - details how procedures were completed not how they were exclusively performed on a particular day.
- If well known procedures were used, account the procedure by name, possibly with reference, and that's all.

Approach:

- It is embarrassed or not possible to use vigorous voice when documenting methods with no using first person, which would focus the reviewer's interest on the researcher rather than the job. As a result when script up the methods most authors use third person passive voice.
- Use standard style in this and in every other part of the paper - avoid familiar lists, and use full sentences.

What to keep away from

- Resources and methods are not a set of information.
- Skip all descriptive information and surroundings - save it for the argument.
- Leave out information that is immaterial to a third party.

**Results:**

The principle of a results segment is to present and demonstrate your conclusion. Create this part a entirely objective details of the outcome, and save all understanding for the discussion.

The page length of this segment is set by the sum and types of data to be reported. Carry on to be to the point, by means of statistics and tables, if suitable, to present consequences most efficiently.You must obviously differentiate material that would usually be incorporated in a study editorial from any unprocessed data or additional appendix matter that would not be available. In fact, such matter should not be submitted at all except requested by the instructor.

Content

- Sum up your conclusion in text and demonstrate them, if suitable, with figures and tables.
- In manuscript, explain each of your consequences, point the reader to remarks that are most appropriate.
- Present a background, such as by describing the question that was addressed by creation an exacting study.
- Explain results of control experiments and comprise remarks that are not accessible in a prescribed figure or table, if appropriate.
- Examine your data, then prepare the analyzed (transformed) data in the form of a figure (graph), table, or in manuscript form.

What to stay away from

- Do not discuss or infer your outcome, report surroundings information, or try to explain anything.
- Not at all, take in raw data or intermediate calculations in a research manuscript.
- Do not present the similar data more than once.
- Manuscript should complement any figures or tables, not duplicate the identical information.
- Never confuse figures with tables - there is a difference.

Approach

- As forever, use past tense when you submit to your results, and put the whole thing in a reasonable order.
- Put figures and tables, appropriately numbered, in order at the end of the report
- If you desire, you may place your figures and tables properly within the text of your results part.

Figures and tables

- If you put figures and tables at the end of the details, make certain that they are visibly distinguished from any attach appendix materials, such as raw facts
- Despite of position, each figure must be numbered one after the other and complete with subtitle
- In spite of position, each table must be titled, numbered one after the other and complete with heading
- All figure and table must be adequately complete that it could situate on its own, divide from text

**Discussion:**

The Discussion is expected the trickiest segment to write and describe. A lot of papers submitted for journal are discarded based on problems with the Discussion. There is no head of state for how long a argument should be. Position your understanding of the outcome visibly to lead the reviewer through your conclusions, and then finish the paper with a summing up of the implication of the study. The purpose here is to offer an understanding of your results and hold up for all of your conclusions, using facts from your research and generally accepted information, if suitable. The implication of result should be visibly described. Infer your data in the conversation in suitable depth. This means that when you clarify an observable fact you must explain mechanisms that may account for the observation. If your results vary from your prospect, make clear why that may have happened. If your results agree, then explain the theory that the proof supported. It is never suitable to just state that the data approved with prospect, and let it drop at that.

- Make a decision if each premise is supported, discarded, or if you cannot make a conclusion with assurance. Do not just dismiss a study or part of a study as "uncertain."
- Research papers are not acknowledged if the work is imperfect. Draw what conclusions you can based upon the results that you have, and take care of the study as a finished work
- You may propose future guidelines, such as how the experiment might be personalized to accomplish a new idea.
- Give details all of your remarks as much as possible, focus on mechanisms.
- Make a decision if the tentative design sufficiently addressed the theory, and whether or not it was correctly restricted.
- Try to present substitute explanations if sensible alternatives be present.
- One research will not counter an overall question, so maintain the large picture in mind, where do you go next? The best studies unlock new avenues of study. What questions remain?
- Recommendations for detailed papers will offer supplementary suggestions.

Approach:

- When you refer to information, differentiate data generated by your own studies from available information
- Submit to work done by specific persons (including you) in past tense.
- Submit to generally acknowledged facts and main beliefs in present tense.

Please carefully note down following rules and regulation before submitting your Research Paper to Global Journals Inc. (US):

**Segment Draft and Final Research Paper:** You have to strictly follow the template of research paper. If it is not done your paper may get rejected.

- The **major constraint** is that you must independently make all content, tables, graphs, and facts that are offered in the paper. You must write each part of the paper wholly on your own. The Peer-reviewers need to identify your own perceptive of the concepts in your own terms. NEVER extract straight from any foundation, and never rephrase someone else's analysis.
- Do not give permission to anyone else to "PROOFREAD" your manuscript.
- Methods to avoid Plagiarism is applied by us on every paper, if found guilty, you will be blacklisted by all of our collaborated research groups, your institution will be informed for this and strict legal actions will be taken immediately.)
- To guard yourself and others from possible illegal use please do not permit anyone right to use to your paper and files.

## Criterion for Grading a Research Paper (Compilation) by Global Journals Inc. (US)

**Please note that following table is only a Grading of "Paper Compilation" and not on "Performed/Stated Research" whose grading solely depends on Individual Assigned Peer Reviewer and Editorial Board Member. These can be available only on request and after decision of Paper. This report will be the property of Global Journals Inc. (US).**

| Topics | Grades | | |
|---|---|---|---|
| | **A-B** | **C-D** | **E-F** |
| ***Abstract*** | Clear and concise with appropriate content, Correct format. 200 words or below | Unclear summary and no specific data, Incorrect form<br><br>Above 200 words | No specific data with ambiguous information<br><br>Above 250 words |
| ***Introduction*** | Containing all background details with clear goal and appropriate details, flow specification, no grammar and spelling mistake, well organized sentence and paragraph, reference cited | Unclear and confusing data, appropriate format, grammar and spelling errors with unorganized matter | Out of place depth and content, hazy format |
| ***Methods and Procedures*** | Clear and to the point with well arranged paragraph, precision and accuracy of facts and figures, well organized subheads | Difficult to comprehend with embarrassed text, too much explanation but completed | Incorrect and unorganized structure with hazy meaning |
| ***Result*** | Well organized, Clear and specific, Correct units with precision, correct data, well structuring of paragraph, no grammar and spelling mistake | Complete and embarrassed text, difficult to comprehend | Irregular format with wrong facts and figures |
| ***Discussion*** | Well organized, meaningful specification, sound conclusion, logical and concise explanation, highly structured paragraph reference cited | Wordy, unclear conclusion, spurious | Conclusion is not cited, unorganized, difficult to comprehend |
| ***References*** | Complete and correct format, well organized | Beside the point, Incomplete | Wrong format and structuring |

# Index

## A

Asynchronous · 4
Attenuation · 4

## C

Chaotic · 35, 50
Clamping · 16
Collision · 53, 57

## D

Damping · 1
Datum · 55, 56, 59

## H

Heuristic · 18, 26, 35, 60
Hyperbolic · 48, 50

## O

Optoelectronic · 50, 51

## P

Photovoltaic · 36, 46
Plummeting · IV

## R

Reciprocating · 53
Reinvigorates · 48
Reiterations · 60
Roulette · 18

## S

Spikes · 9, 10, 14, 15
Surveillance · 50

save our planet

# Global Journal of Researches in Engineering

Visit us on the Web at www.GlobalJournals.org | www.EngineeringResearch.org
or email us at helpdesk@globaljournals.org

ISSN 9755861